PNNL-15540

Hydroacoustic Evaluation of Juvenile Salmonid Passage at The Dalles Dam Sluiceway, 2005

GE Johnson
F Khan
JB Hedgepeth
RP Mueller
CL Rakowski
MC Richmond
JA Serkowski
JR Skalski

FINAL REPORT
May 2006

Prepared for the U.S. Army Corps of Engineers
Portland District, Portland, Oregon
Under a Related Services Agreement
with the U.S. Department of Energy
Contract DE-AC05-76RL01830

Pacific Northwest National Laboratory
Operated by Battelle for the U.S. Department of Energy

PACIFIC NORTHWEST NATIONAL LABORATORY
operated by
BATTELLE
for the
UNITED STATES DEPARTMENT OF ENERGY
under Contract DE-AC05-76RL01830

Printed in the United States of America
Available to DOE and DOE contractors from the
Office of Scientific and Technical Information,
P.O. Box 62, Oak Ridge, TN 37831-0062;
ph: (865) 576-8401
fax: (865) 576-5728
email: reports@adonis.osti.gov

Available to the public from the National Technical Information Service,
U.S. Department of Commerce, 5285 Port Royal Rd., Springfield, VA 22161
ph: (800) 553-6847
fax: (703) 605-6900
email: orders@ntis.fedworld.gov
online ordering: http://www.ntis.gov/ordering.htm

This document was printed on recycled paper.
(9/2003)

PNNL-15540

Hydroacoustic Evaluation of Juvenile Salmonid Passage at The Dalles Dam Sluiceway, 2005

GE Johnson
F Khan
JB Hedgepeth[a]
RP Mueller
CL Rakowski
MC Richmond
JA Serkowski
JR Skalski[b]

FINAL REPORT
May 2006

Prepared for the U.S. Army Corps of Engineers
Portland District, Portland, Oregon
Under a Related Services Agreement
with the U.S. Department of Energy
Contract DE-AC05-76RL01830

Pacific Northwest National Laboratory
P.O. Box 999
Richland, Washington 99352

[a] Tenera Environmental, LLC, San Luis Obispo, California
[b] University of Washington, Seattle, Washington

Summary

The U.S. Army Corps of Engineers Portland District engaged the Pacific Northwest National Laboratory to evaluate fish passage at The Dalles Dam (TDA) powerhouse in 2005. The goal of the study was to provide information on smolt passage that will inform decisions on long-term measures and operations to enhance sluiceway passage and reduce turbine passage to improve smolt survival at the dam. The study addressed one of the main components of the Juvenile Survival Program at The Dalles Dam: Surface Flow Bypass.

The study objectives (see below) were met using a combination of hydroacoustic and hydraulic data. The study incorporated fixed-location hydroacoustic methods across the entire powerhouse, with especially intense sampling using multiple split-beam transducers at all sluiceway portals. We did not sample fish passage at the spillway in 2005. In the sluiceway nearfield, we used an acoustic camera to track fish movements. The fish data were interpreted with hydraulic data from a computational fluid dynamics (CFD) model. Fish passage data were collected in the framework of an "experiment" using a randomized block design (3-day treatments; two treatments) to compare two sluiceway operational configurations: Sluice 2+5 and Sluice 2+19 (six gates open for each configuration). The 90-day 2005 study was divided into two seasonal periods: spring (April 18 to June 4) and summer (June 5 to July 16).

During the 2005 study, daily outflow at TDA ranged from 117 to 287 thousand cubic feet per second (kcfs). Mean daily outflow was 205 kcfs in spring and 181 kcfs in summer. Outflow peaked in early June. Total project outflow was 76% of the 10-year average for the spring period and 71% of the 10-year average for the summer period. Daily powerhouse discharge averaged 136 kcfs in spring and 114 kcfs in summer. Spill for fish protection commenced on April 11 and was bulked in Bays 1-6. Daily spill flow during our study ranged from 45 to 81 kcfs, with a mean of 69 kcfs (34% of total project) in spring and 66 kcfs (37% of total project) in summer. Daily sluice flow was about 4.5 kcfs, depending on forebay elevation. In spring and summer, mean sluice discharge was about 3.3% and 3.8% of total powerhouse discharge, respectively.

Our study encompassed the majority of the migration period for yearling (stream-type) Chinook (*Oncorhyncus tshawytscha*), coho (*O. kisutch*), and sockeye (*O. nerka*) salmon as well as steelhead (*O. mykiss*) trout and subyearling (ocean-type) Chinook salmon. During the spring study period, species composition was: yearling Chinook salmon (61%); steelhead (24%); sockeye (4%); coho (8%), and subyearling Chinook salmon (3%). Passage of yearling fish peaked in mid to late May. During the summer study period, subyearling Chinook salmon comprised 96% of the outmigration with the remainder being yearling salmonids. Passage of subyearling Chinook salmon peaked at the end of June.

The main findings, summarized by objective, were as follows:

1. Estimate fish passage run timing and vertical, horizontal, and diel fish distributions at the powerhouse.

- There were peaks in run timing during both spring and summer. The study encompassed the majority of the spring and summer outmigrations.
- The vertical distribution of fish at the powerhouse turbine intakes was skewed toward the intake ceiling. Vertical distribution was deeper during summer than spring. Fish were deeper during night than day in spring, whereas the opposite was true for summer.

- At the powerhouse, the horizontal distribution showed fish passage was highest at Sluice (SL) 2 and Main Unit (MU) 8 during spring. During summer, passage at the powerhouse was highest at SL 2 and 5 and MU 8. The horizontal distribution of passage was not skewed to the east during summer, as observed in previous studies.
- Not including the sluice routes, fish passage per unit flow was highest at MU 21 during both seasons. Fish passage per unit flow in turbines was higher in summer than spring, and it was higher at the middle and eastern than western areas of the powerhouse in 2005.
- The diel distribution of passage was more variable during summer than spring. Generally, during spring and summer, passage at the powerhouse turbine intakes peaked at dusk while sluiceway passage was somewhat higher during day than night with no prominent peaks.

2. *Estimate sluiceway passage efficiency[a] and effectiveness (relative to total powerhouse passage) on a seasonal and daily basis.*

- The following table shows the seasonal passage efficiency and effectiveness metrics with 95% confidence intervals at The Dalles Dam as estimated with hydroacoustics during 2005.

	Spring (4/18-6/4)	Summer (6/5-7/16)
Sluice Efficiency re: powerhouse	0.333 ± 0.14	0.217 ± 0.008
Sluice Effectiveness re: powerhouse	10.17 ± 0.43	5.72 ± 0.20

- Daily sluiceway efficiency and effectiveness estimates were variable with a decreasing trend from April to July.

3. *Analyze the effect of sluiceway skimmer gate operation on fish passage into the sluiceway. Treatments included open sluice gates at Sluice 2+5 (SL 2-1, 2-2, 2-3, 5-1, 5-2, 5-3) and Sluice 2+19 (SL 2-1, 2-2, 2-3, 19-1, 19-2, 19-3).*

- SL 2+5 had significantly higher sluiceway efficiency than SL 2+19 in both spring ($P<0.10$) and summer ($P<0.05$):

	Spring (4/18-6/4)	Summer (6/5-7/16)
SL 2+5	0.367 ± 0.023	0.262 ± 0.012
SL 2+19	0.304 ± 0.016	0.169 ± 0.009

- For a given location, sluiceway efficiency was higher at SL 2 and SL 5 than SL 19 during both spring and summer (95% confidence intervals were within approximately 5% of the estimate):

[a] By definition, "efficiency" is the proportion of fish passing a given route and "effectiveness" is the fish:flow ratio (proportion fish divided by proportion water through a particular route).

	Spring (4/18-6/4)	Summer (6/5-7/16)
SL 2	0.916	0.622
SL 5	0.674	0.876
SL 19	0.462	0.442

4. *Describe sluiceway nearfield fish movements and interpret these data using hydraulic data.*

- The sluiceway zone of influence is the region immediately upstream of a sluice entrance where juvenile salmonids have a high probability (> 90%) of ultimately moving into the sluiceway. Data from the tracking effort using the acoustic camera in the sluiceway nearfield showed the zone of influence was highest at 17 ft during spring, night at SL 2.
- Generally, fish movement probabilities into the sluice entrances were higher during night than day and higher at SL 2 than SL 19.
- The predominate fish movement at SL 2 and SL 19 was to the west, not into the sluiceway, except for spring, night at SL 2.

5. *Provide recommendations for sluiceway operations and long-term measures to enhance sluiceway passage and reduce turbine passage.*

- The sluice should be operated 24 h/d from April until November.
- Open six rather than three sluice gates to take advantage of the maximum hydraulic capacity of the sluiceway.
- Open the three gates above the western-most operating main turbine unit and the three gates at MU 8 where turbine passage rates are relatively high.
- Operate the turbine units below open sluice gates as a standard fish operations procedure.
- Develop hydraulic and entrance enhancements to the sluiceway to tap the potential of The Dalles Dam sluiceway to be highly efficient and effective at passing juvenile salmonids, including:
    - Form an extensive surface flow bypass flow net (surface bypass discharge greater than ~7% of total project discharge) at both the west and east ends of the dam.
    - Create a gradual increase in water velocity approaching the surface flow bypass (ideally, acceleration < 1 m/s per meter).
    - Make water velocities at an entrance high enough (> 3 m/s) to entrain the subject juvenile fishes, e.g., 10,000 cfs or so.
    - Adapt the shape and orientation of the surface entrance(s) to fit site-specific features, i.e., test a Removable Sluiceway Weir.
- The Dalles Dam sluiceway has the potential to be highly efficient and effective at passing juvenile salmonids in the vicinity of the powerhouse. We recommend tapping this potential with enhancements to the sluiceway.

Preface

This research was conducted under the auspices of the U.S. Army Corps of Engineers, Northwestern Division's Anadromous Fish Evaluation Program (AFEP) to implement the Congressionally appropriated Columbia River Fish Mitigation Project. The research pertains to AFEP study code SBE-P-00-017. It is related to and complements surface flow bypass research at other dams in the Federal Columbia River Power System (study codes SBE-W-96-1, SBE-W-96-2, SBE-P-00-6, and SBE-P-00-13). This study was funded by the Portland District, U.S. Army Corps of Engineers under a contract with the Pacific Northwest National Laboratory (PNNL), operated by Battelle for the U.S. Department of Energy. Subcontractors to PNNL included Tenera Environmental and the University of Washington.

Acknowledgments

We earnestly acknowledge contributions to this study by:

- U.S. Army Corps of Engineers fisheries biologists: Bob Cordie, Bernard Klatte, Mike Langeslay, and Miro Zyndol
- U.S. Army Corps of Engineers personnel –Sue Fox, Dick Harrison, Don Hibbs, Paul Ocker, Norm Tolonen, and Art Kunigel and the structural crew
- Battelle staff – Kyle Bouchard, Dennis Dauble, Eric Fischer, Al Garcia, Terri Gilbride, James Hughes, Kathy Lavender, Gene Ploskey, Kathi Ruiz, Mark Weiland, and Shon Zimmerman
- Schlosser Machine Shop - Vincent Schlosser
- Honald Crane Services – Bob Austin and Mike Honald
- University of Washington, Applied Physics Laboratory – Ed Belcher and Bill Hanot
- University of Washington, Columbia Basin Research – Cindy Helfrich and Jim Lady.

Contents

Figures

Tables

1.0 Introduction

Development of long-term measures to protect juvenile salmon at The Dalles Dam (Figure 1.1) is a high priority in the endeavor to increase salmon smolt survival through the Federal Columbia River Power System (FCRPS) (National Marine Fisheries Service 2000). Juvenile salmon pass The Dalles Dam (TDA) through one of three routes: turbines, spillway, or sluiceway. In 2005, the US Army Corps of Engineers (COE) Portland District contracted Pacific Northwest National Laboratory (PNNL) to evaluate fish passage via the turbine and sluiceway routes using hydroacoustics. The goal of the study was to provide information on smolt passage at The Dalles Dam to inform decisions on long-term measures and operations to enhance sluiceway passage and to reduce turbine passage in order to improve smolt survival at the dam.

1.1 Background

The multi-faceted strategy to improve smolt survival at The Dalles Dam involves all three types of passage routes there. At the turbines, intake occlusions were tested in 2001 and 2002 to determine if blocking the upper half of the turbine intakes at the trash racks might significantly reduce turbine entrainment. Results indicated that the occlusions were generally not effective at reducing turbine passage (Johnson et al. 2003; Hausmann et al. 2004). At The Dalles spillway, survival of downstream migrants is typically lower than at other projects on the lower Columbia River (Ploskey et al. 2001a). In an effort to improve survival of spilled fish, a wall dividing the spillway between Bays 6 and 7 was installed prior to the 2004 juvenile salmonid migration season and a bulk spill pattern at Bays 1-6 was implemented in 2004 and 2005. Other spillway improvements, such as vortex suppression at Bay 6, are ongoing. For the forebay, bioengineering is underway to design a floating wall to divert juvenile salmonids from the powerhouse to the spillway. This effort is applying results from forebay distribution and migration pathway studies by Cash et al. (2005) and Faber et al. (2005). At the sluiceway, an alternate means of operating the entrance gates is being investigated to provide additional protection for juvenile salmonids at the TDA powerhouse.

The sluiceway at The Dalles Dam is a functional surface flow outlet.[a] Current sluiceway operations were essentially established from mark-recapture studies using sluiceway fyke nets in the late 1970s and early 1980s (Nichols 1979 and 1980; Nichols and Ransom 1981 and 1982). In 1971, Michimoto (1971) recommended, “full-time operation of the ice-trash sluiceway at The Dalles dam with maximum flow.” In 1978, Nichols (1979) found that the sluice gates at the west end of the powerhouse had higher yearling salmon passage rates than did gates in the middle. In 1979, Nichols (1980) reported sub-yearling passage was significantly higher at Units 17 and 18 than at Units 1 and 2, but in 1980 Nichols and Ransom (1981) reported no significant difference. Nichols (1980) recommended that the sluiceway be operated 24 hours per day (h/d) because noticeable numbers of smolts used the sluiceway at night, although highest passage was during daylight hours. Based on these data, fisheries managers recommended that the sluice gates above Main Unit 1 be open 24 h/d to pass juvenile salmonids during spring and summer. The Dalles Dam sluiceway has been operated this way for the last 24 years.

[a] A surface flow outlet at a hydropower dam is any portal where water flows from the forebay over the dam structure to the river downstream of the dam.

Figure 1.1. The Dalles Dam. Flow is from right to left. The Powerhouse has 22 turbine units (main units) numbered from west to east (left to right in photograph)

However, fish approach and horizontal distribution data from 1997-2002, the fyke net data for sub-yearlings (Nichols 1980), and new hydraulic calculations of sluiceway inflows raised the need to confirm that a west end sluice operation is optimal for both spring and summer emigrants. For example, in 1997 researchers using radio telemetry first detected about 60% of the steelhead and 56% of the yearling Chinook salmon entering the forebay off the eastern end of the powerhouse (Hensleigh et al. 1999). This pattern was consistent with other radio telemetry studies at The Dalles Dam (Sheer et al. 1997; Holmberg et al. 1997; Hansel et al. 2000; Beeman et al. 2004; Hansel et al. 2005). Recent hydroacoustic studies have shown that the distribution of fish passage at the powerhouse was uniform or skewed toward the west end in spring but skewed toward the east end in summer (Ploskey et al. 2001b; Moursund et al. 2001; Moursund et al. 2002; Johnson et al. 2003). Furthermore, Nichols (1980) found higher passage for marked subyearling salmon at the east end sluice (SL 17 and 18) than the west end (SL 1 and 2), although in a repeat study Nichols and Ransom (1981) reported no significant difference between east and west sluice passage. In 2003, engineers determined that the sluiceway at The Dalles Dam is at less than maximum hydraulic capacity when only the three chain gates above Main Unit 1 are open. That is, additional gates can be opened before the maximum hydraulic capacity of the sluiceway channel is reached (~4,500 cfs). Collectively, the biological and engineering studies provided an impetus for renewed sluiceway operations research. In 2004, sluiceway efficiency for the standard operation of three open gates at SL1 was significantly ($P<0.05$) less than that for six open gates at SL 1 and SL 18 (Johnson et al. 2005), but the optimum location for open gates was still unclear. In 2005, the hydroacoustic study at The Dalles Dam was driven by the need to optimize sluiceway operations for juvenile salmonid passage to support the Surface Flow Bypass component of the Juvenile Survival Program.

1.2 Goal and Objectives

This study provides information on juvenile salmonid passage at The Dalles Dam that can be used by the Corps of Engineers and fisheries resource managers to make decisions on long-term measures to enhance sluiceway passage. The main goal of this study is to reduce turbine passage in order to increase smolt survival rates at the dam. The 90-d study was divided into spring (April 18 to June 4) and summer (June 5 to July 16) periods. The objectives of the study were as follows:

1. *Estimate fish passage run timing and vertical, horizontal, and diel fish distributions at the powerhouse.*

   Fish distribution is fundamental to a fish passage evaluation. Distribution data are also used to aid design of project operations and structures intended to increase juvenile salmonid survival.

2. *Estimate sluice passage efficiency*[a] *and effectiveness on a seasonal and daily basis.*

   Efficiency and effectiveness estimates from hydroacoustics are used to summarize fish passage for the run-at-large during the spring and summer migration seasons. Because similar methods have been applied in the last six years at The Dalles Dam, the metrics can be compared across years. This provides fisheries resource managers with data on trends and patterns in fish passage to make decisions on project operations and fish protection design efforts.

3. *Analyze the effect of sluiceway skimmer gate operation on fish passage into the sluiceway. Treatments will include open sluice (SL) gates at Sluice 2+5 (SL 2-1, 2-2, 2-3, 5-1, 5-2, 5-3) and Sluice 2+19 (SL 2-1, 2-2, 2-3, 19-1, 19-2, 19-3) regions of the powerhouse.*

   This study compared fish passage under two gate configurations to establish the sluiceway configuration that was most efficient at passing juvenile salmonids.

4. *Describe sluiceway nearfield fish movements and interpret these data using hydraulic data.*

   Previous studies used fish movement data to determine the zone of influence for the sluiceway flow net (Hedgepeth et al. 2002a, 2002b; Johnson et al. 2004). Given the hydraulic tools now available and advanced imaging sonar methods (acoustic camera) to track fish in the nearfield of the sluiceway (< 30 ft), this effort improved understanding of fish behavior for the purpose of designing methods to enhance sluiceway passage.

5. *Provide recommendations for sluiceway operations and long-term measures to enhance sluiceway passage and reduce turbine passage.*

   It was important to discuss and interpret the collective information from this study and others as it pertains to short- and long-term smolt protection measures at The Dalles Dam.

---

[a] By definition, "efficiency" is the proportion of fish passing a given route and "effectiveness" is the fish/flow ratio (proportion of fish divided by proportion of water through a particular route).

1.3 Report Content

This report has seven sections and two appendices. Following the introduction in Section 1, the study site description is in Section 2. Section 3 contains the study methods. Section 4 has the results. Section 5 provides a discussion of the results. Section 6 contains recommendations. Section 7 lists the literature cited. Appendix A contains a synopsis of the statistical methods. Appendix B presents the results of an exploratory analysis of the relationships between load following and fish passage.

2.0 Study Site Description

2.1 General

The Dalles Dam (Figure 1.1) is located at river mile 192. It is the second closest dam to the Pacific Ocean in the Federal Columbia River Power System. Full pool elevation is rated at 160 ft above mean sea level (MSL) and minimum operating pool elevation is 155 ft. The thalweg intersects the dam at the eastern end of the powerhouse and, although there are deep areas immediately in front of the powerhouse (Figure 2.1), much of the forebay is relatively shallow (< 65 ft deep).

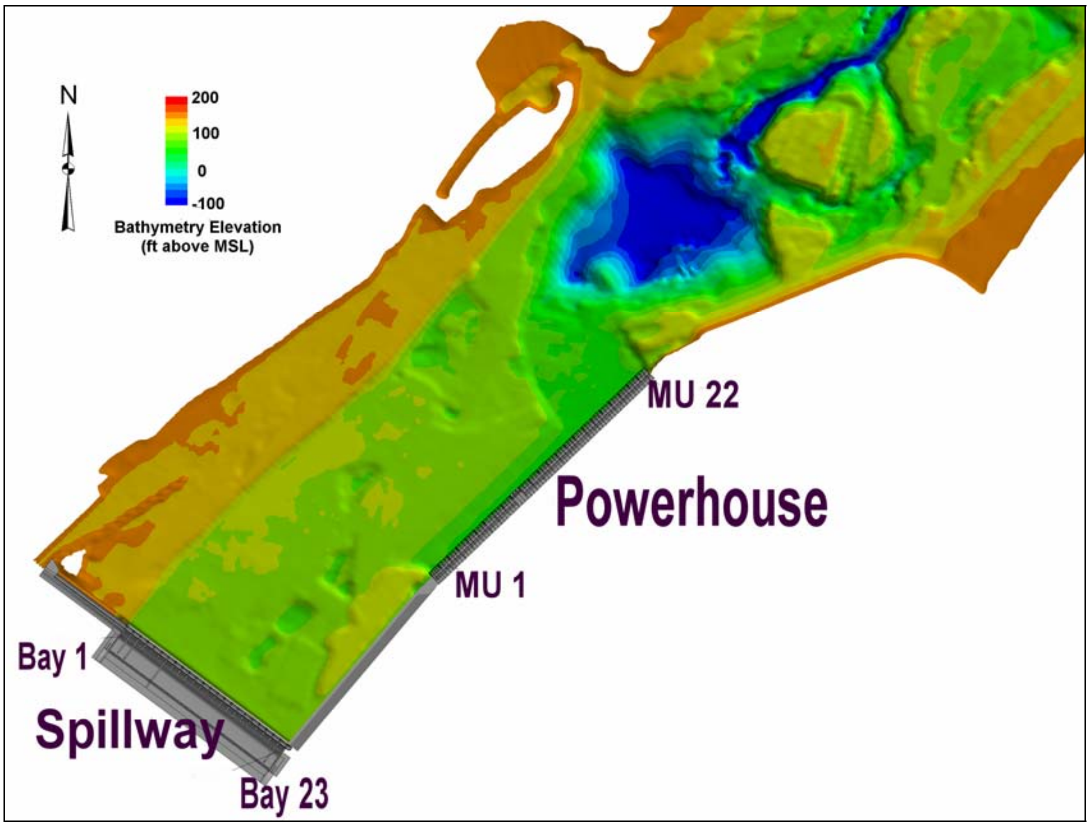

Figure 2.1. Plan View of The Dalles Dam Showing Forebay Bathymetry

The Dalles Dam has a 2,090-ft-long powerhouse with 22 turbine units (called “Main Units” or MU), a total generating capacity of 1,800 MW, and total powerhouse hydraulic capacity of 330 kcfs. The powerhouse also has two small turbine units at the west end that provide attraction flow to the fish ladder for upstream migrant adult salmonids; these are called the Fish Units. The face of the powerhouse is 11.3° off vertical. The turbine intake ceiling intersects the trash racks at elevation 141 ft. The 1,380-ft-long spillway is comprised of 23 bays with radial gates 50 ft wide. The spillway was modified during winter 2003-2004 to include a training wall that divides the stilling basin between Bays 6 and 7. Spill patterns were designed to place the bulk of spill discharge through Bays 1-6 during the 2005 spill period.

2.2 Sluiceway

The ice and trash sluiceway is a channel that extends the entire length of the forebay side of the powerhouse. The sluiceway has three 20-ft wide entrance gates positioned over each of the 22 turbine units. Water enters the sluiceway channel from the forebay when gates are moved off the sill at elevation 151 ft. A maximum of six sluice gates can be opened at any time before reaching the hydraulic capacity of the channel (~4,500 cfs). Flow into the sluiceway is dependent on forebay elevation and the number and location of open gates. For example, given a forebay elevation equal to 158.4 ft (above mean sea level) and two sluice gate operating conditions (see above), flows over the individual weir gates range from 561 to 1059 cfs with the highest flows at the west end nearest the sluiceway channel outlet (Tables 2.1 and 2.2). Overall, sluiceway discharge (~4,500 cfs) is a relatively small proportion of total project discharge (~2%).

During 2005, alternative sluiceway operation configurations were evaluated. Before 2004, typically only the three sluice gates at MU 1 were opened to pass juvenile salmonids. These gates are designated SL 1. However, as mentioned above, engineers determined that the sluiceway at The Dalles Dam is at less than maximum hydraulic capacity when only three sluice gates are open, making it possible hydraulically to open additional gates. In 2005, Main Unit 1 was off-line the entire study; therefore, the western-most sluice entrance above MU 2 was used. Previous data (e.g., Nichols 1980) showed that three sluice gates at the west end of TDA are preferred for passing juvenile salmonids. During 2005, we were interested in determining whether three additional gates in the middle passed more fish than three more gates in the eastern part of the dam. Thus, the two sluiceway treatments (gate openings) we tested were as follows:

- Sluice 2+5 = 2-1, 2-2, 2-3, 5-1, 5-2, 5-3
- Sluice 2+19 = 2-1, 2-2, 2-3, 19-1, 19-2, 19-3.

Table 2.1. Hydraulic Calculations for the Sluiceway at The Dalles Dam, Example for Sluice 1. Data provided by CENWP-Hydraulics.

West Only Unit 1 Sluice Gates Open				
Reservoir Level = 158.4 ft; Open Weir Elevation = 151.0 ft; Manning's Roughness = 0.014				
		West	East	Total
Sluice(s) Open		SL 1	none	1
No. Gates		3	0	3
Total Sluiceway Discharge = 3138 cfs				
Unit No. (order from d/s)	Weir No. (order from d/s)	Q-weir flow over weir (cfs)	WS water level in channel (ft)	Ave. Velocity over weirs
1	1	1059	146.6	7.2
1	2	1051	150.7	7.1
1	3	1029	152.0	7.0
Total		3138		7.1

Table 2.2. Hydraulic Calculations for the Sluiceway at The Dalles Dam, Example for Sluice 1&18. Data provided by CENWP-Hydraulics.

West + East Units 1 & 18 Sluice Gates Open				
Reservoir Level = 158.4 ft; Open Weir Elevation = 151.0 ft; Manning's Roughness = 0.014				
		West	East	Total
Sluices Open		SL 1	SL 18	2
No. Gates		3	3	6
Total Sluiceway Discharge = 4451 cfs				
Summary Weir Data				
Unit No. (order from d/s)	Weir No. (order from d/s)	Q-weir flow over weir (CFS)	WS water level in channel (ft)	Ave. Velocity over weirs
1	1	1014	149.7	6.8
1	2	876	154.0	5.9
1	3	765	155.6	5.2
18	4	645	156.7	4.4
18	5	589	157.2	4.0
18	6	561	157.4	3.8
Total		4451		5.0

3.0 Methods

The methods section includes descriptions of the experimental design, hydroacoustic techniques, and hydraulic approaches.

3.1 Experimental Design

The hydroacoustic evaluation of the smolt run at large at The Dalles Dam in 2005 was divided into the spring (48 d, April 18 to June 4) and summer (42 d, June 5 to July 16) study periods. The seasonal periods were established by examining the 5-year record of smolt passage indices from John Day Dam, the next dam upstream.

The two treatments in the sluiceway study (Sluice 2+5 and Sluice 2+19) were sampled according to a randomized block design (Table 3.1). Each treatment lasted 3 days producing 6-day blocks. The total study period consisted of 8 blocks during spring and 7 blocks during summer. A treatment period began at 0800 h, with approximately 45 min required to change from one treatment to the other.

We obtained fish passage and nearfield fish movement data using fixed-location hydroacoustics and acoustic imaging, respectively. We obtained hydraulic data for this study from a computational fluid dynamics (CFD) model. In addition, hydraulic calculations for the sluiceway (presented in Table 2.1) were provided by the CENWP-Hydraulics Branch.

3.2 Fixed-Location Hydroacoustics

The fixed-location hydroacoustic technique was employed to accomplish Objectives 1 and 2 of this study. This technique, conceived by Carlson et al. (1981) for single-beam acoustic systems, is described by Thorne and Johnson (1993). In addition to single-beam, split-beam technology is now an important element of fixed-location hydroacoustics. The split-beam technique is explained by MacLennan and Simmonds (1992). The methods used in 2005 were similar to those employed in the 2001, 2002, and 2004 hydroacoustic studies at The Dalles Dam (Moursund et al. 2002; Johnson et al. 2003; Johnson et al. 2005).

The general approach was to deploy a combination of single-beam and split-beam transducers to sample fish and apply the acoustic screen model to estimate fish passage rates and distributions. Split-beam transducers provided data to determine weighting factors, assess assumptions of the model, and determine the magnitude of any biases. Split-beam transducer deployments at each type of passage route were used to estimate the average backscattering cross section, direction of travel, and speed of fish for detectability modeling to determine effective transducer beamwidths. Single and split-beam transducers were deployed to sample fish passage at the sluiceway and turbines. Transducer sampling volumes were positioned to minimize both ambiguity in ultimate fish passage routes and the potential for multiple detections of the same fish.

Table 3.1. Randomized Block Sampling Design for Sluice Treatments at the Dalles Dam, 2005

Spring			Summer		
Block	Date	Configuration	Block	Date	Configuration
1	18-Apr	SL 2+5	9	5-Jun	SL 2+5
	19-Apr	SL 2+5		6-Jun	SL 2+5
	20-Apr	SL 2+5		7-Jun	SL 2+5
	21-Apr	SL 2+19		8-Jun	SL 2+19
	22-Apr	SL 2+19		9-Jun	SL 2+19
	23-Apr	SL 2+19		10-Jun	SL 2+19
2	24-Apr	SL 2+19	10	11-Jun	SL 2+5
	25-Apr	SL 2+19		12-Jun	SL 2+5
	26-Apr	SL 2+19		13-Jun	SL 2+5
	27-Apr	SL 2+5		14-Jun	SL 2+19
	28-Apr	SL 2+5		15-Jun	SL 2+19
	29-Apr	SL 2+5		16-Jun	SL 2+19
3	30-Apr	SL 2+19	11	17-Jun	SL 2+5
	1-May	SL 2+19		18-Jun	SL 2+5
	2-May	SL 2+19		19-Jun	SL 2+5
	3-May	SL 2+5		20-Jun	SL 2+19
	4-May	SL 2+5		21-Jun	SL 2+19
	5-May	SL 2+5		22-Jun	SL 2+19
4	6-May	SL 2+5	12	23-Jun	SL 2+19
	7-May	SL 2+5		24-Jun	SL 2+19
	8-May	SL 2+5		25-Jun	SL 2+19
	9-May	SL 2+19		25-Jun	SL 2+5
	10-May	SL 2+19		27-Jun	SL 2+5
	11-May	SL 2+19		28-Jun	SL 2+5
5	12-May	SL 2+5	13	29-Jun	SL 2+5
	13-May	SL 2+5		30-Jun	SL 2+5
	14-May	SL 2+5		1-Jul	SL 2+5
	15-May	SL 2+19		2-Jul	SL 2+19
	16-May	SL 2+19		3-Jul	SL 2+19
	17-May	SL 2+19		4-Jul	SL 2+19
6	18-May	SL 2+5	14	5-Jul	SL 2+5
	19-May	SL 2+5		6-Jul	SL 2+5
	20-May	SL 2+5		7-Jul	SL 2+5
	21-May	SL 2+19		8-Jul	SL 2+19
	22-May	SL 2+19		9-Jul	SL 2+19
	23-May	SL 2+19		10-Jul	SL 2+19
7	24-May	SL 2+19	15	11-Jul	SL 2+19
	25-May	SL 2+19		12-Jul	SL 2+19
	26-May	SL 2+19		13-Jul	SL 2+19
	27-May	SL 2+5		14-Jul	SL 2+5
	28-May	SL 2+5		15-Jul	SL 2+5
	29-May	SL 2+5		16-Jul	SL 2+5
8	30-May	SL 2+19			
	31-May	SL 2+19			
	1-Jun	SL 2+19			
	2-Jun	SL 2+5			
	3-Jun	SL 2+5			
	4-Jun	SL 2+5			

3.2.1 Hydroacoustic Systems

Data collection involved three Precision Acoustic Systems (PAS) single-beam and four split-beam PAS hydroacoustic systems. All systems operated at 420 kHz. The data collection systems consisted of either Harp-1B (single beam) or Harp-SB (split beam) Data Acquisition/Signal Processing Software installed on a personal computer controlling a PAS-103 Multi-Mode Scientific Sounder. The PAS-103 Sounders controlled transducers deployed in main turbine units, fish units, and sluiceway entrances. A total of 34 transducers, 21 single-beam and 13 split-beam, were deployed at the turbines and sluiceway (Table 3.2). All systems used a -56 dB (re: 1 µpa at 1 m) voltage output threshold.

Table 3.2. Sample Locations and Spatial Sampling Intensity at The Dalles Dam in 2005

Area	Intensity by Unit	Intensity by Portal	Number of Transducers	Sample Locations
Fish Units	2 of 2	1 of 2	2	FU 1-2, 2-2
Main Units 1-22	19 of 22[(a)]	1 of 3	19	MU 2-1[(b)], 2-3, 5-1, 6-3, 7-1, 8-1, 9-3, 10-2, 11-3, 12-2, 13-1, 14-2, 15-1, 16-1, 17-2, 18-2, 19-3, 20-2, 21-1, 22-1
Sluiceway	3 of 3	3 of 3	12[(c)]	SL 2-1, 2-2, 2-3, 5-1, 5-2, 5-3, 19-1, 19-2, 19-3
Spillway[(d)]	n/a	n/a	n/a	n/a

(a) MU 1, 3, and 4 were not sampled because they were off-line for maintenance.
(b) The transducer in MU 2-1 stopped working on June 2, 2005, and was not replaced because a nearby location, MU 2-3, was being sampled with a split-beam transducer.
(c) Four transducers were deployed at each of the three open sluices (SL 2, 5, and 19).
The spillway was not sampled in 2005.

3.2.2 Transducer Locations and Orientations

Single-beam transducers (6°) were installed at all turbine unit sampling locations (Figure 3.1). The intakes sampled at a given turbine unit and the horizontal placement (west, middle, or east) of the transducers in that intake were randomly chosen. At all turbine intake sampling locations, with the exception of the fish units, divers installed transducers on the bottom of the second to the last trash rack at elevation 74 ft and aimed the transducers downstream and upward toward the intake ceiling at a 23° angle to the plane of the trash rack (Figure 3.2).

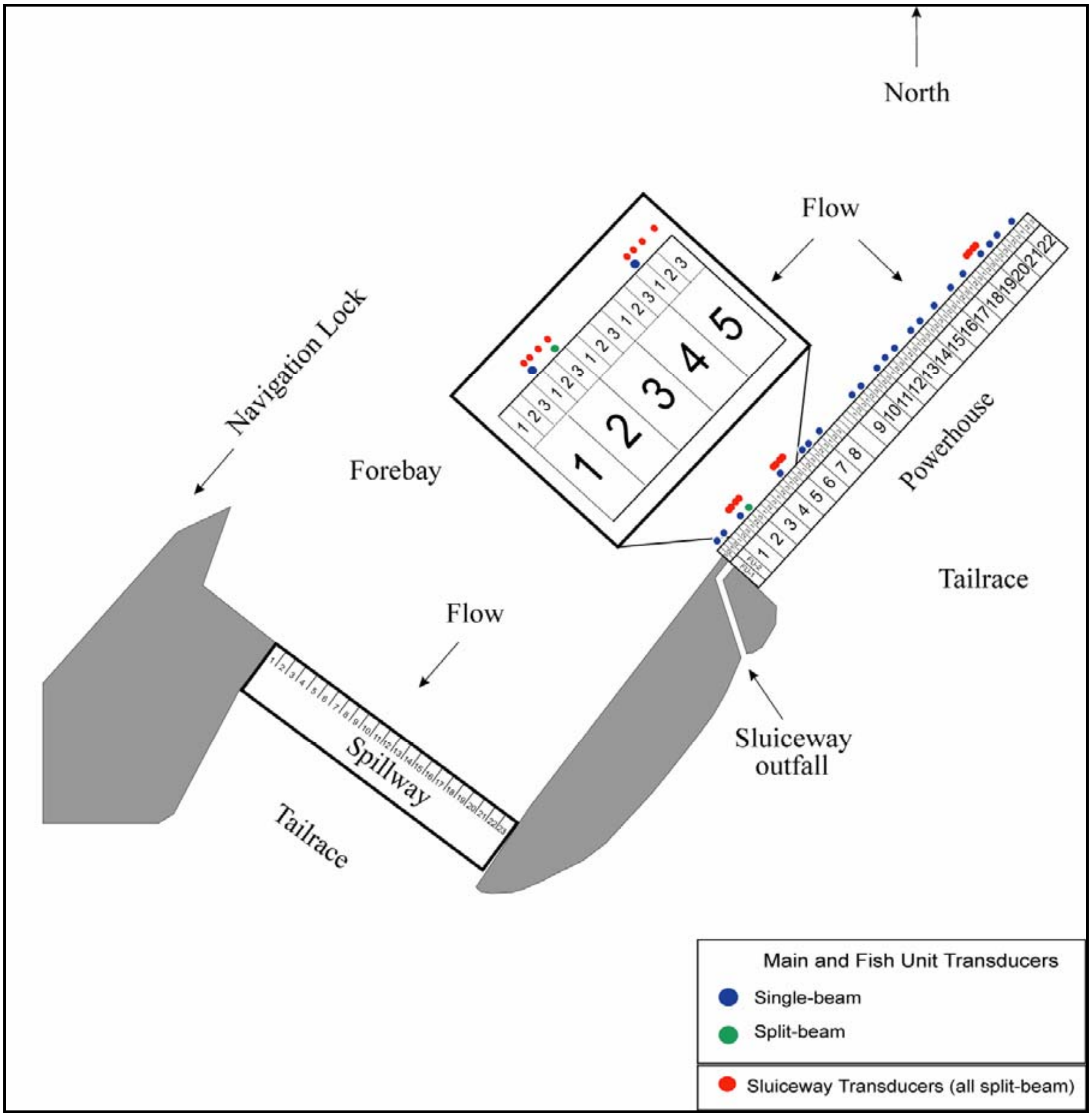

Figure 3.1. Plan View Showing Transducer Locations at The Dalles Dam, 2005

Transducers in the fish units were installed on the top trash rack at elevation 135 ft, aimed downstream and downward at a 15° angle to the plane of the trash rack (Figure 3.3). At the fish units, penetration dives were required for transducer installation because the spacing of the vertical bars of the trash racks was not wide enough to allow the transducer and mount assembly to be mounted from the forebay. Divers took a transducer attached to a mount and telemetry cable to the inside of the top trash rack. A diver then bolted the mount assembly to a horizontal bar of the trash rack at elevation 135 ft and aimed the transducer downstream toward the intake floor.

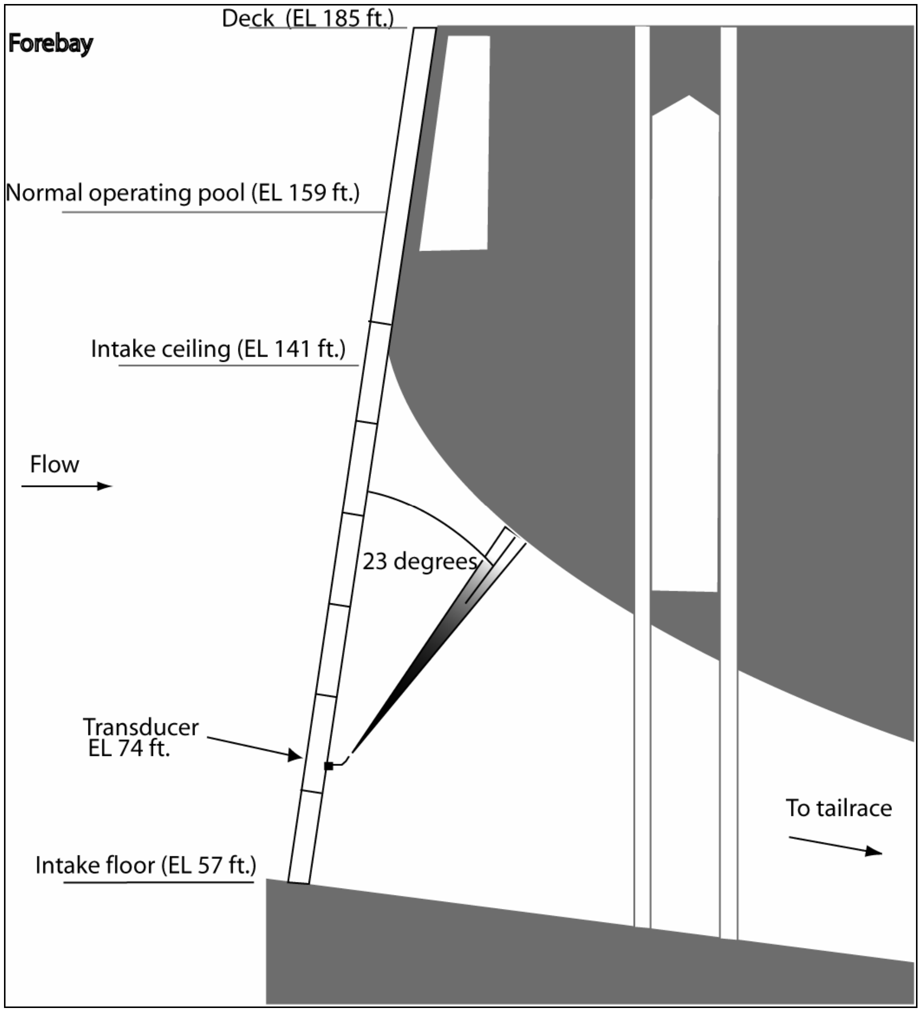

Figure 3.2. Cross-Sectional View of a Main Unit Transducer Deployment

Sluiceway transducers (6° split-beam) were installed at each of the three sluice gates of SL 2, 5, and 19 (Table 3.2). Transducers were attached to mounts, which were then affixed to either steel I-beams installed on the front of the pier noses or on the "J" extensions of the occlusion plates of MU 1 at elevation 153 ft (Figures 3.4 and 3.5). Each sluice entrance was monitored by a transducer aimed horizontally and back at a 60° angle to the plane of the sill across the sluiceway entrance (Figures 3.6 and 3.7).

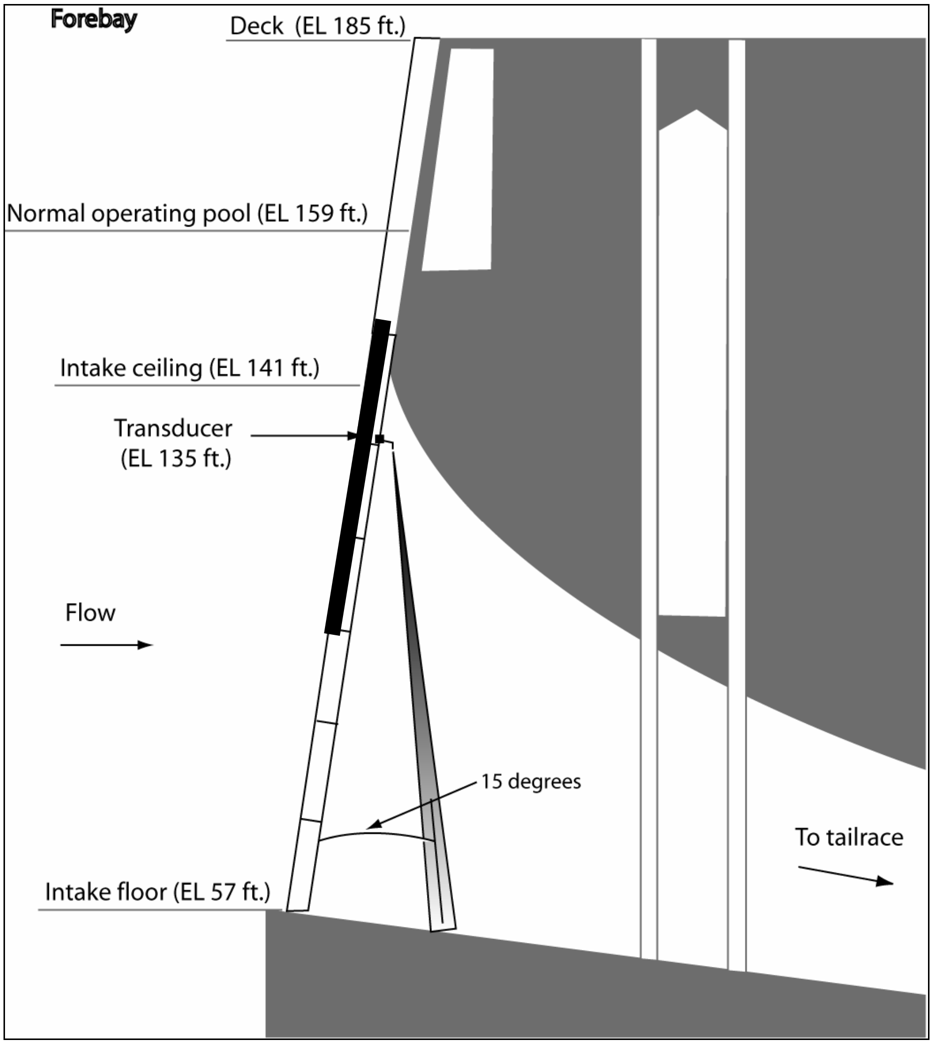

Figure 3.3. Cross-Sectional View of a Fish Unit Transducer Deployment. The solid line on the upper half of the traskracks depicts the occlusion plate (solid black bar) that is still in place from the 2002 tests at the fish units.

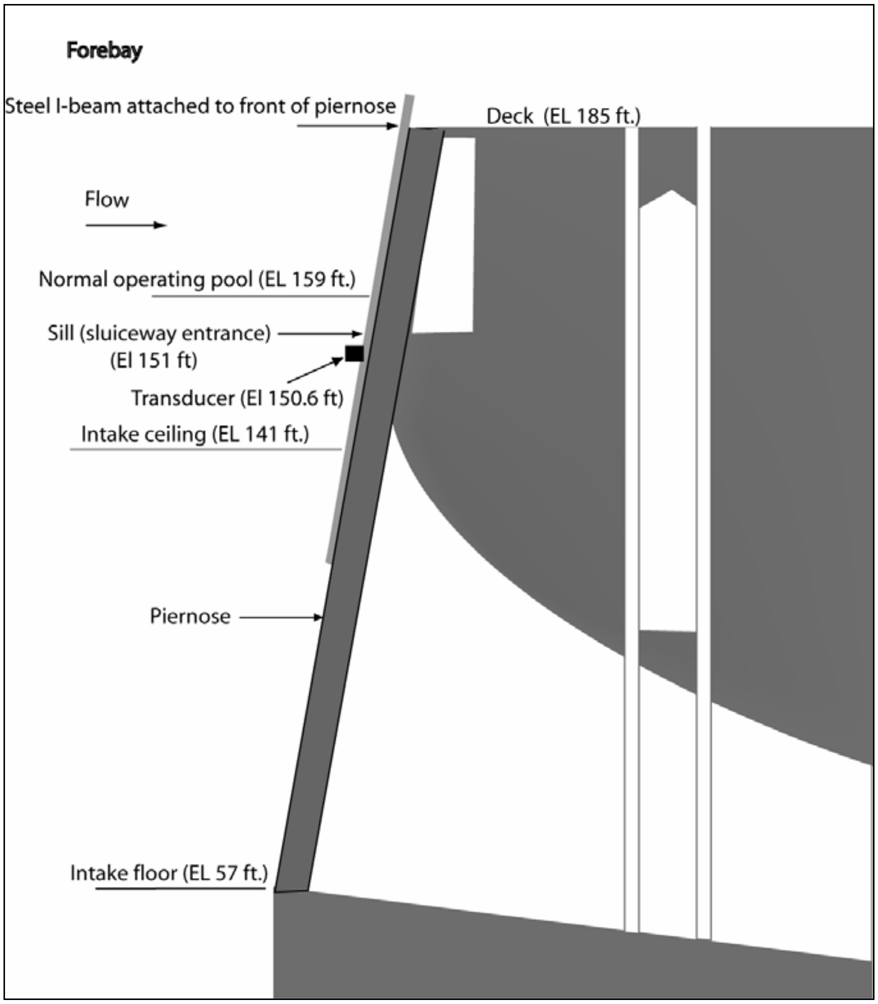

Figure 3.4. Deployment for a Side-Looking Sluiceway Transducer Mounted on a Steel I-Beam Attached to the Front of a Pier Nose

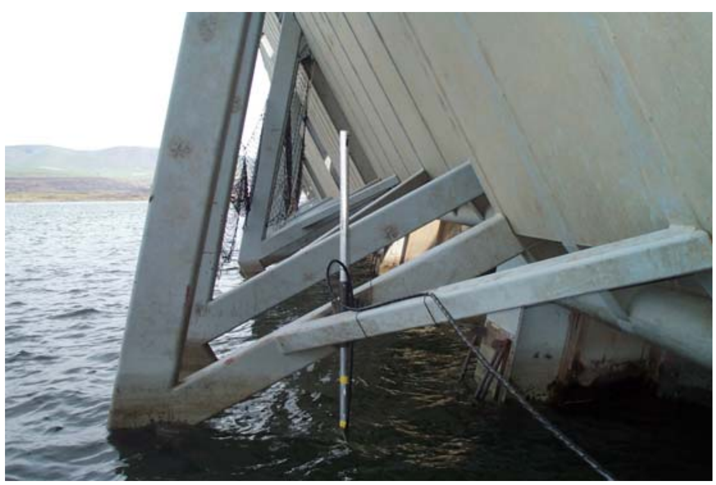

Figure 3.5. Deployment for a Side-Looking Sluiceway Transducer Mounted on "J" Occlusion Extension (SL 2)

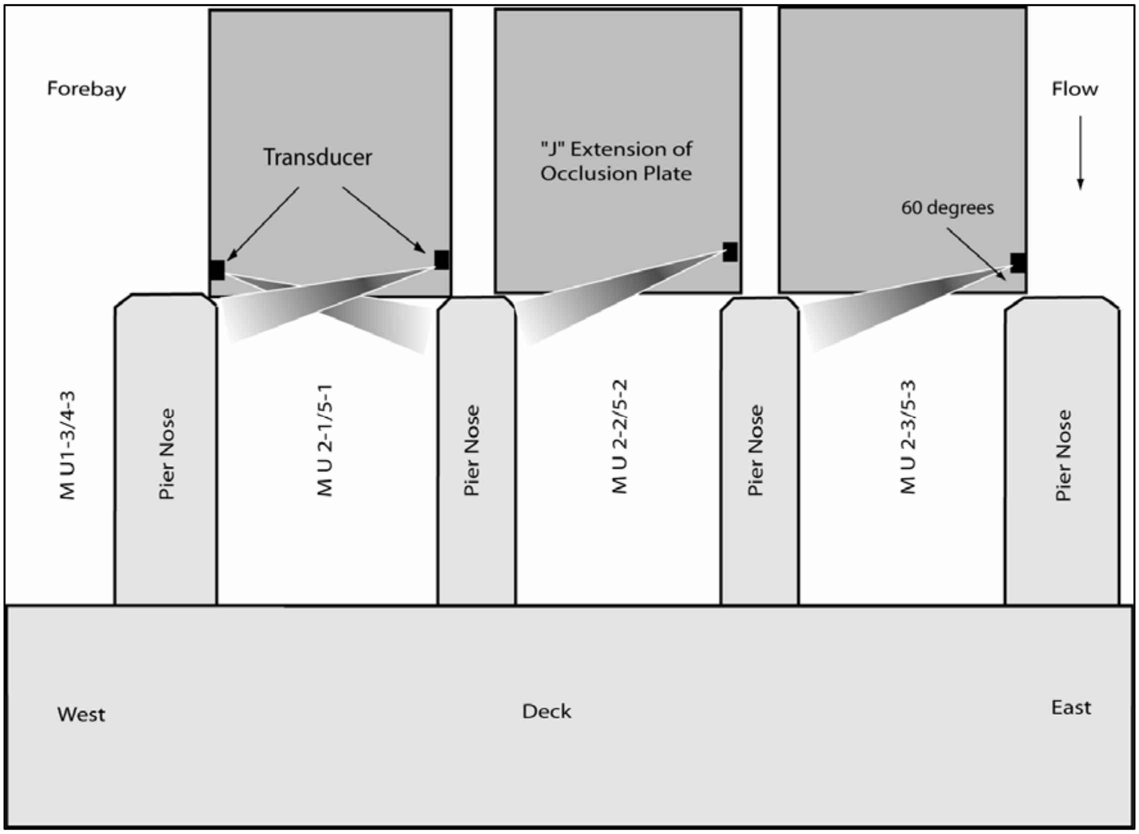

Figure 3.6. Top View of Transducer Deployment for SL 2 and SL 5. Shaded area to the top is J-Block structure which was always out of the water. Flow is from top to bottom.

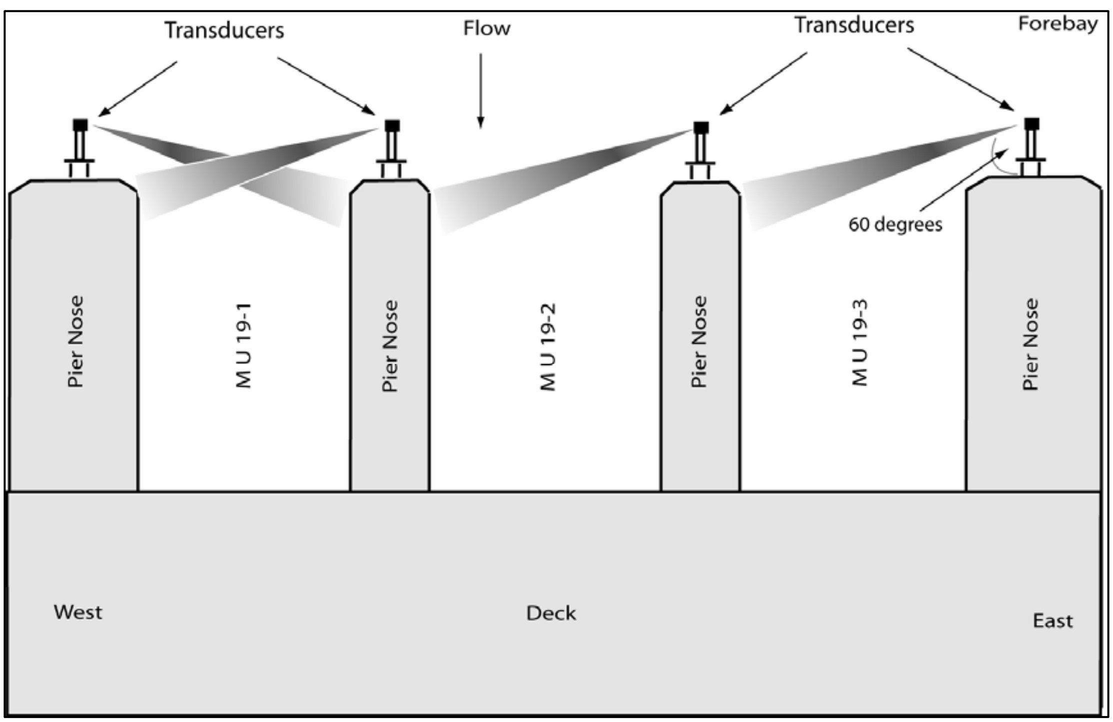

Figure 3.7. Top View of Transducer Deployment for SL 19. Flow is from top to bottom.

3.2.3 Sampling Design

The echo sounder transmission rate was 16 pps (pings per sec) at the turbine intakes and 30 pps at the sluiceway. Systematic samples, i.e., same order among sampling locations each hour, were collected at 1-min intervals 24 h/d. Each location was sampled 8 to 15 times per hour depending on the number of transducers connected to the particular echo sounder.

3.2.4 Data Processing and Reduction

After the acoustic echo data were collected and archived, they were processed to extract fish tracks. At this stage in the analysis, we were careful to set the tracking parameters to include all fish at the expense of including spurious tracks. Next, to separate acceptable from unacceptable tracks, we filtered using fish track characteristics such as slope and pulse width. This data processing and reduction process was similar to that used by Johnson et al. (2005).

3.2.5 Data Analysis

The process to estimate passage rates from filtered tracked fish is explained in detail in Appendix A. Briefly, each fish track that survived the filtering process was weighted spatially to account for the sample width of the acoustic beam at the target's mid-range relative to the width of the passage route. The sum of these weighted fish was then extrapolated temporally by the hourly sampling fraction (60/total hourly sample time per location). The variances associated with each passage rate estimate were likely underestimates because between-intake variability in passage within a given turbine unit could not be accounted for because of sampling limitations. Ninety-five percent confidence intervals (*CI*) were calculated as follows:

$$CI = \pm 1.96 * \sqrt{Variance}$$

The passage rate data were used to estimate various performance metrics, including fish passage efficiency, spillway efficiency and effectiveness, sluiceway efficiency and effectiveness, and sluiceway passage. Equations for each estimator are contained in Appendix A.

3.2.5.1 Statistical Analysis

To statistically compare the Sluice 2+5 and 2+19 treatments, sluiceway efficiency and sluiceway passage were used as response variables in a two-way (block and treatment) analysis of variance (ANOVA). For the purposes of this study, separate analyses for day and night periods were performed for each metric. (Day was defined as 0600-2000 h in spring and 0600-2100 h in summer.) The sluiceway passage data and the sluice efficiency data were transformed using the natural logarithm or arcsin functions, respectively. Two-tailed statistical tests were employed because the main concern was whether the difference observed in the response variable between the two treatments was significant. See Appendix A for more details, including the ANOVA model.

We used regression methods to explore the relationships between load following and fish passage at the TDA powerhouse. The independent variables were hourly differences in turbine discharge. The dependent variables were turbine and sluiceway passage, as well as sluiceway efficiency. See Appendix B for more details of the regression analysis of load following and fish passage.

3.3 Acoustic Imaging

To assess fish movements in the nearfield (< 10 m) in front of the sluiceway, a Dual Frequency Identification Sonar (DIDSON) was deployed. The DIDSON bridges the gap between conventional scientific fisheries sonar, which can detect acoustic targets at long ranges but cannot record the shapes of targets, and optical systems, which can record images of fish but are limited at low light levels or when turbidity is high. The DIDSON has a high resolution and fast frame rate enabling it to substitute for optical systems in turbid or dark water. This device, for example, was successfully applied at TDA in previous research on predator distributions relative to the J-occlusion plates (Johnson et al. 2003), and during a similar study to determine sluiceway entrainment zones at TDA in 2004 (Johnson et al. 2005). Figure 3.8 shows an example image of juvenile salmonids observed using the DIDSON.

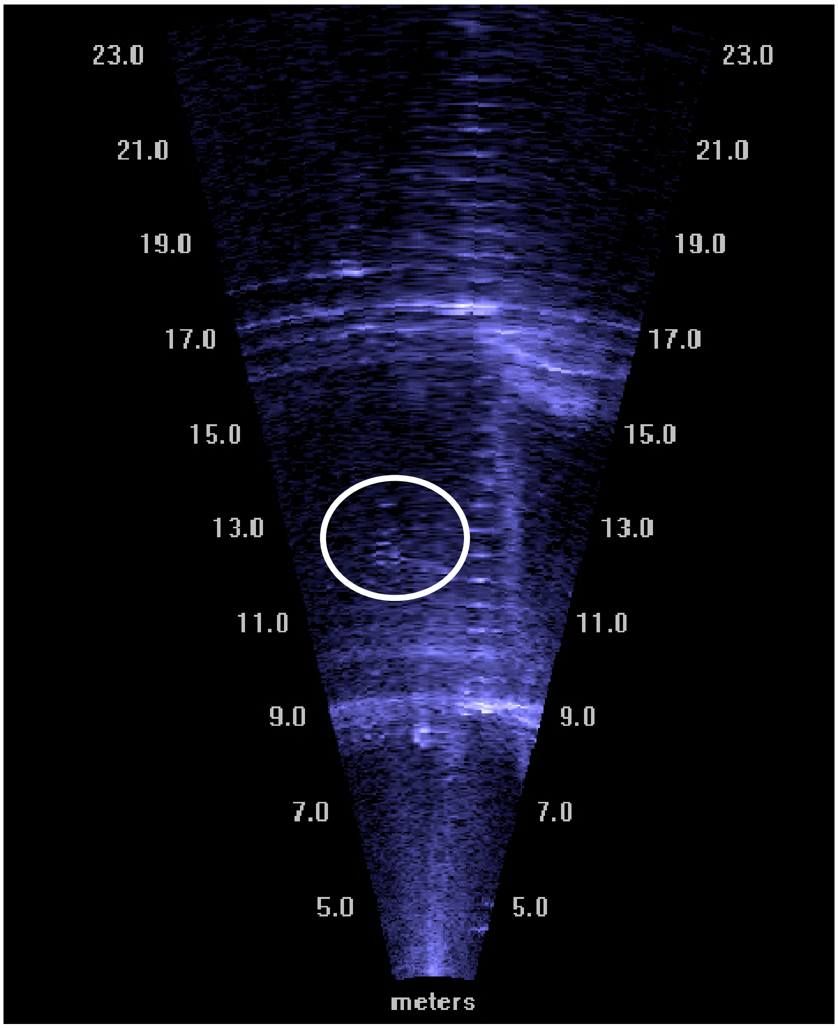

Figure 3.8. Screen capture from the DIDSON Display. The image shows a school of juvenile salmonids at the 11 to 13 m range in the middle portion of the sonar.

3.3.1 Sampling Locations and Schedule

The DIDSON was used to sample fish movement at two locations: pier nose MU 1/2 for SL 2 and pier nose MU 18/19 for SL 19 (Table 3.3). The DIDSON was mounted to a pan and tilt rotator (Remote Ocean Systems PT -10). The rotator was programmed to sample four zones near the sluiceway openings at sluiceway entrances SL-2-1, 2-2, 19-1, and 19-2. The DIDSON was used in the low frequency mode with a frame rate of 7 frames per sec. The elevation at which the DIDSON was deployed was 6 ft below the normal operating pool. For the spring period, the average forebay elevation was 158.1 ft and during the summer period the average elevation was 157.9 ft.

Table 3.3. DIDSON Sampling Schedule, 2005. A sampling day started at 0800 h and lasted for 24 h.

Date	DIDSON Location	Date	DIDSON Location
May 5	SL 2	June 20	SL 2
May 9	SL 2	June 24	SL 2
May 10	SL 2	June 25	SL 2
May 11	SL 2	June 26	SL 2
May 12	SL 2	July 2	SL 19
May 21	SL 2	July 3	SL 19
May 22	SL 2	July 4	SL 19
May 23	SL 2	July 5	SL 19
May 24	SL 2 and 19	July 8	SL 19
May 25	SL 19	July 9	SL 19
May 26	SL 19	July 10	SL 19
May 27	SL 19	July 11	SL 19 and 2
June 8	SL 19	July 12	SL 2
June 9	SL19	July 13	SL 2
		July 14	SL 2

3.3.2 Deployment and Aiming Angles

We mounted the DIDSON to an aluminum trolley and lowered it down a steel 4-inch-wide I-beam attached to the dam at each sampling location. For SL2, the beam was welded to the J-plate guide frame at the pier nose between MU 1 and 2. For SL 19, the I-beam was secured with anchor bolts to the concrete pier between MU 18 and 19. The trolley was raised and lowered using an electric winch at SL 2 and a manual winch and davit at SL 19 (Figure 3.9). A pan and tilt rotator Remote Ocean Systems (ROS) PT-10 was fastened to the trolley and the DIDSON was then fastened to the rotator (Figure 3.10). The rotator was programmed to search four zones at both sampling locations. In the low frequency mode, the DIDSON had a maximum range of 65 ft. The aiming positions (in degrees) from the rotator were also incorporated into the DIDSON output files using a serial Data Acquisition (DAQ) Module connected to a second computer. This allowed the feedback from the rotator's pan angles to be associated with each DIDSON image. The tilt position (vertical dimension) was set at 5 degrees down and was not changed during the entire sampling period.

Figure 3.9. Electric Hoist and Davit System Used to Deploy the DIDSON

Figure 3.10. DIDSON Mounted to Pan and Tilt Rotator and Trolley

3.3.3 Sampling Zones

Data collection consisted of sampling four 30^{o} pie-shaped horizontal zones in the surface layer along the face of the dam at SL 2 and SL 19 (Figure 3.11). Using the programmable rotator, the zones were sampled from Zone 1 to Zone 4 sequentially for 10 min each. All electronic data were stored to external hard-drives.

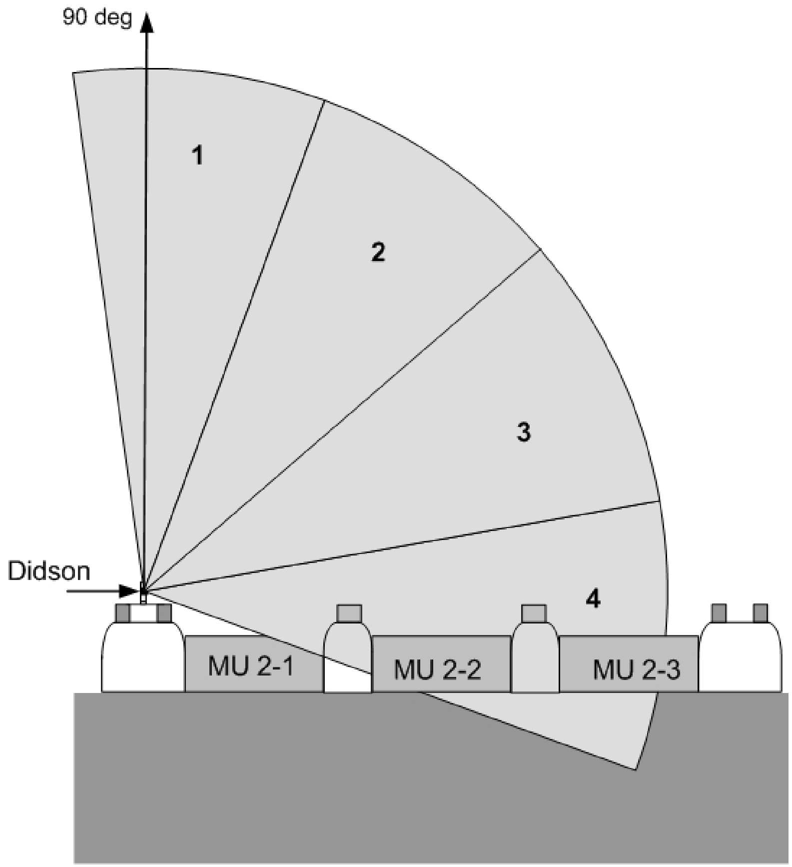

Figure 3.11. Plan View Showing the DIDSON Sampling Zones at SL 2. Sampling zones were similar for SL 19. The light gray shading represents the approximate coverage area of the four sampling zones.

3.3.4 Data Processing

An automated tracking program was developed in 2005 to process over 500 GB of electronic DIDSON data acquired during 2005. The DIDSON autotracking software was developed to facilitate tracking of fish in DIDSON images because manual processing is a slow and tedious process. A Visual Basic manual tracker program was written and used in 2004 (Johnson et al. 2005). With manual tracking, nearly 40 boxes might be drawn to spatially and temporally characterize a track lasting just 10 seconds. Like the manual tracker, the automated tracking software outputs ASCII text datafiles that contain spatial information. The autotracker outputs fish position by using the beam number (1 to 48 for the low-frequency setting used in 2005 of a total 29 degree composite beam) and bin number (a range analog) from fish images captured in binary files of the DIDSON system. The DIDSON autotracker output contained the following information:

- DIDSON filename
- Track number: a unique chronological number for each initiated fish track within a DIDSON file that restarts at one in each file
- Frame number: the ping code from the DIDSON file
- Date: year, month, and day
- Time: hour, minute, second to the hundredth second
- Pan angle: an external input that required decoding;

- Tilt angle: an external input (not applicable to this study);
- Range bin: distance from the DIDSON start range and output as a floating point from 1 to 512, with the autotracker using the centroid of the target pixels to display beam and range;
- Beam: the beam number of the centroid of the fish detected over 1 to 48 for low frequency or 1 to 96 for high frequency as used at The Dalles Dan in 2005;
- Start range: a coded start range for where DIDSON data collection is started (note: to decode Sound Metrics code: start_range in meters = code*0.4165 * 2.0);
- End_range: a coded start range for where DIDSON data collection ends (note: to decode Sound Metrics code: end_range in meters = pow(2,code)*5.0.);
- Number of pixels: determined from the autotracker's displayed tracked image;
- Amplitude: an 8-bit amplitude, a detected pixel group (0-255) corresponds roughly to a 100 dB range.

We used SAS software to filter noise from these text files using feedback from Sound Metric's DIDSON file viewer. The autotracker file format was slightly modified in this process but contained essentially the same information. Two text datasets of filtered fish tracks were output, one for spring 2005 and another for summer 2005.

Prior to a Markov chain analysis, a C-language program was used to convert the tracked fish files to fixed coordinate systems and for fish track visualization in Amtec Engineering's Tecplot software, while separating into location (Main Unit 2 and Main Unit 19) and day or night datasets and summary statistics. A second C-language program output a selection of the water volume's synoptic Tecplot visualization with fish tracks and for subsequent Markov-chain analysis. Part of this processing included filtering tracks to accept only those longer than 3 s.

The process of aligning the relative tracked fish data to fixed coordinates consisted of applying pan and fixed 5-degree down tilt angle corrections, DIDSON elevation corrections, and rotations and translations to two different coordinate systems. The coordinate system "Oregon State Plane North Zone" (OSPN) was used for preliminary three-dimensional visualization.

A second coordinate system, used in the Markov chain analysis, was relative to the face of the main piernose where the DIDSON was located, at its center and at elevation 158 ft. Note that this is seven ft higher than the sluiceway sill elevation of 151 ft used as a reference in Johnson et al. (2005). At Unit 2, coordinates were relative to a reference point "TDP1" with easting 1839844.0, northing 711330.743 (OSPN feet) (near the main piernose at MU 1-1). The DIDSON x- y- z-origin was measured relative to this point 84.25 ft along the deck (43.8º north of east), 94 in. out to the DIDSON at deck level, and downward at a slope of 1:5 to its operating elevation of approximately 152.0 ft, although this elevation varied over the course of the study due to redeployments. At Unit 19, coordinates were relative to a reference point "TDP10" with easting 1841000.16, northing 712440.59 (OSPN feet) (near the piernose between MU 18-2 and 18-3). Deployed on the main piernose at MU 19-1, the DIDSON x- y- z-origin was measured, relative to "TDP10", 27.1 ft along deck (43.8º north of east), 80 in. out to the DIDSON camera at deck level, and downward at a slope of 1:5 to its operating elevation of approximately 151.6 ft.

In relative coordinates, the x-axis was parallel to the powerhouse at an angle of 43.8º towards north from the easting parallel. The y-axis was perpendicular to the powerhouse at the center of the main piernose between MU 1 and MU 2 or between MU 18 and MU 19. The origin was set at the piernose face at elevation 158 ft, approximately water level. The DIDSON was located at several elevations based on river water level and deployment. DIDSON elevations required for adjusting the tracked fish coordinates were part of a computer program that computed both State Plane and dam-relative tracked fish coordinates. Output files were named "*.SPL" for Oregon State Plane North (OSPN) coordinates (NAD 27) but also containing relative coordinates and "*.DAT" for Tecplot software visualization in relative coordinates. Using the relative to DIDSON camera position of a fish (X, Y), its range (R), and the pan angle θ, a single tracked fish position relative to the pointing angle of DIDSON was computed as:

$$\left(X, Y\cos(\theta), R\sin(\theta)\right).$$

This position was then corrected by applying rotation and translation into positions in the two coordinate systems described above. The fish tracks were displayed and animated using custom software and subjected to a Markov Chain analysis.

3.3.5 Fish Tracks

To examine coverage and to determine size parameters used in the Markov chain analysis, fish tracks were visualized in Amtec Engineering's Tecplot software prior to application of Markov chain analysis. The fish tracks at MU 2 and MU 19 sluiceways are shown in Figures 3.12 to Figure 3.15. Day was defined as 0600-2000 h in spring and 0600-2100 h in summer. For the spring data, a second set of tracks was generated by dithering the primary fish tracks ± 2° randomly and uniformly, in order to "fill in" between sectors. The dithered tracks were used as input for a program to analyze fish movements in a Markov chain analysis, except for the spring data collected at MU 19 sluiceway because the coverage there was limited mainly to a single sector. A different method, used for summer fish tracks, adjusted the tracks by widening sector data 13% to fill in gaps.

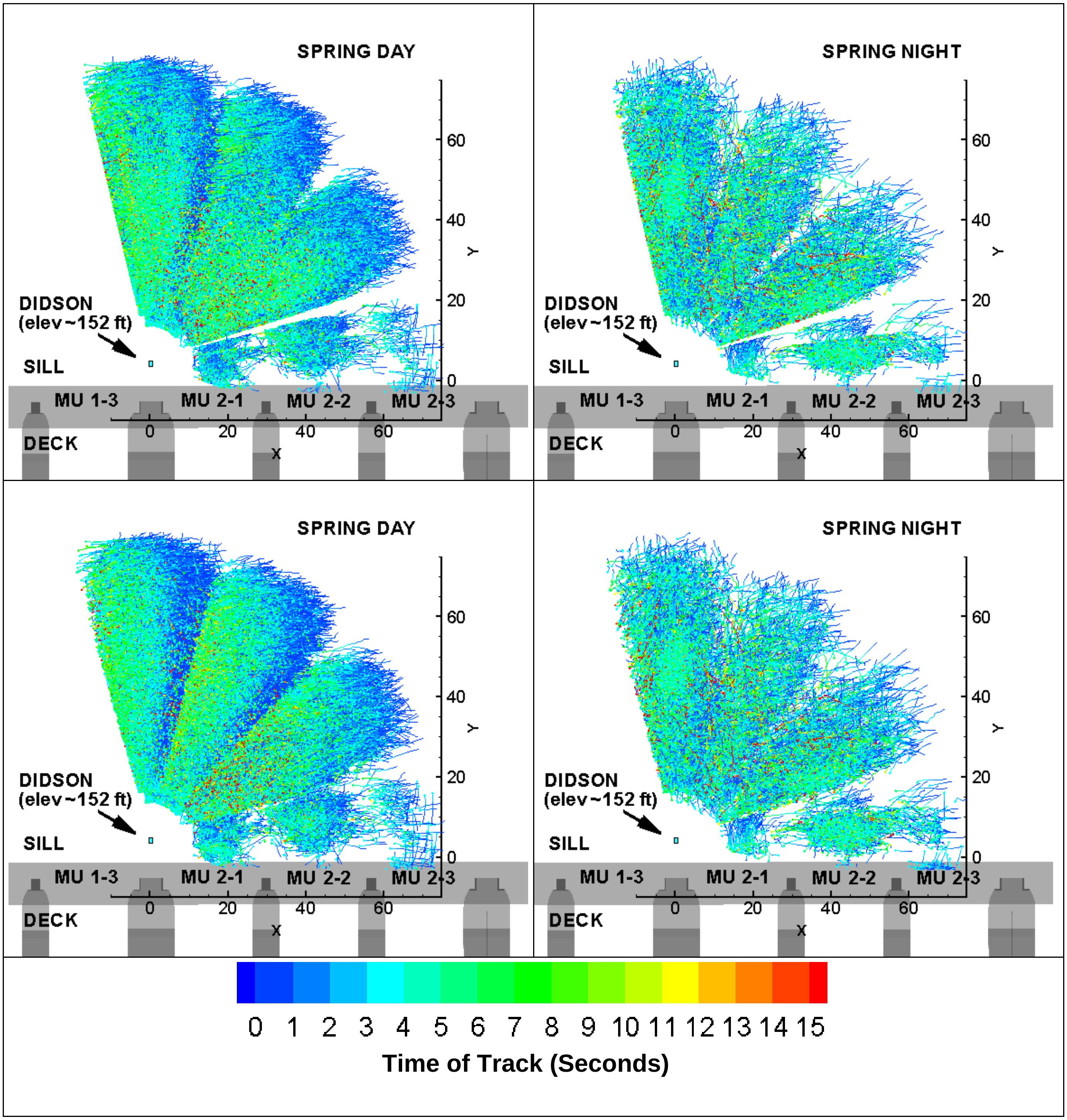

Figure 3.12. Effects of Dithering at SL 2. Upper panels portray fish tracks from the DIDSON at The Dalles Dam SL 2 for Spring 2005. Lower panels show randomly and uniformly dithered ±2.5° tracks to fill in missing data. Axes' scales are in feet. Track portions are color-coded by the seconds from the start of each fish track.

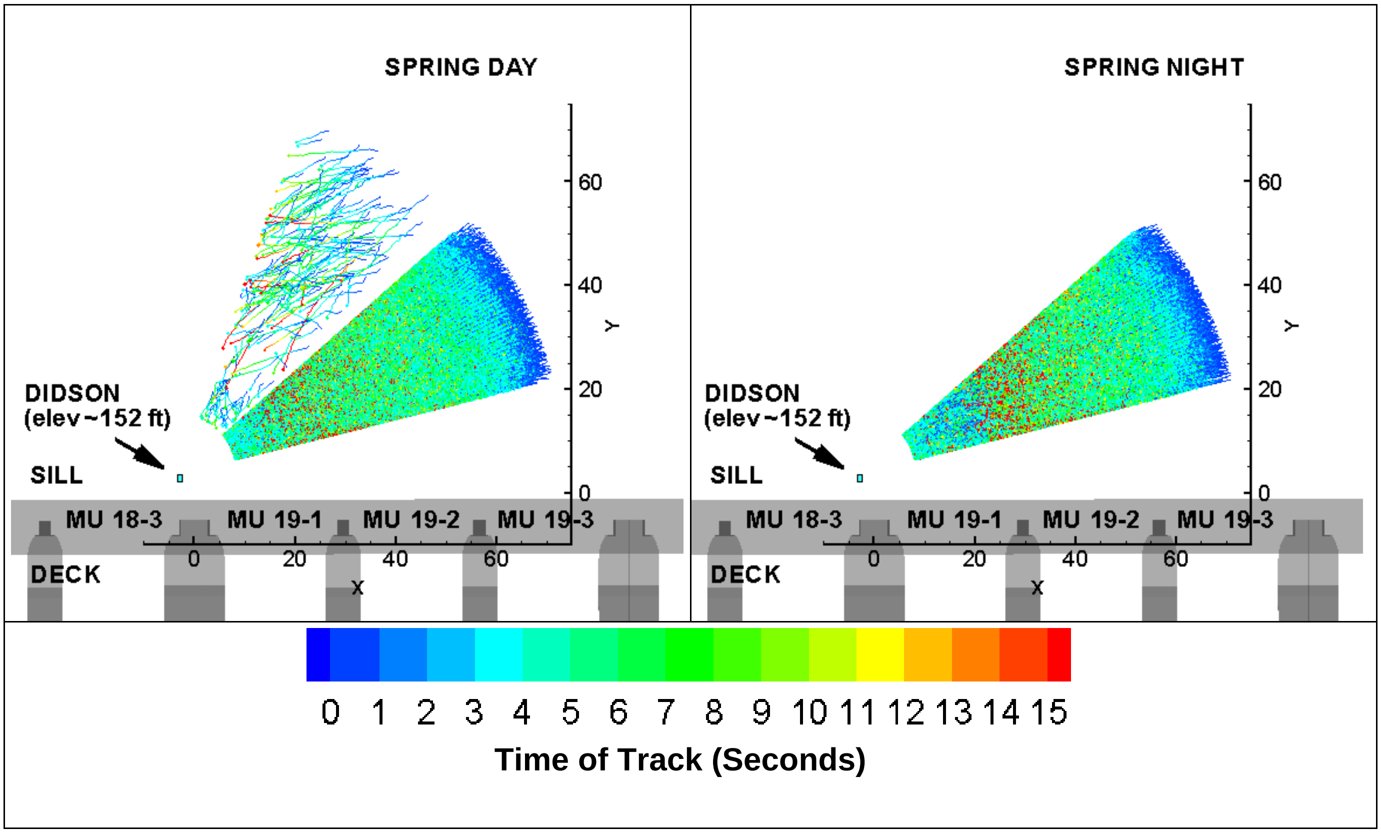

Figure 3.13. Fish Tracks from the DIDSON at The Dalles Dam at SL 19 above MU 19 for Spring 2005. Axis scales are in feet. Track portions are color-coded by the seconds from start of each fish track.

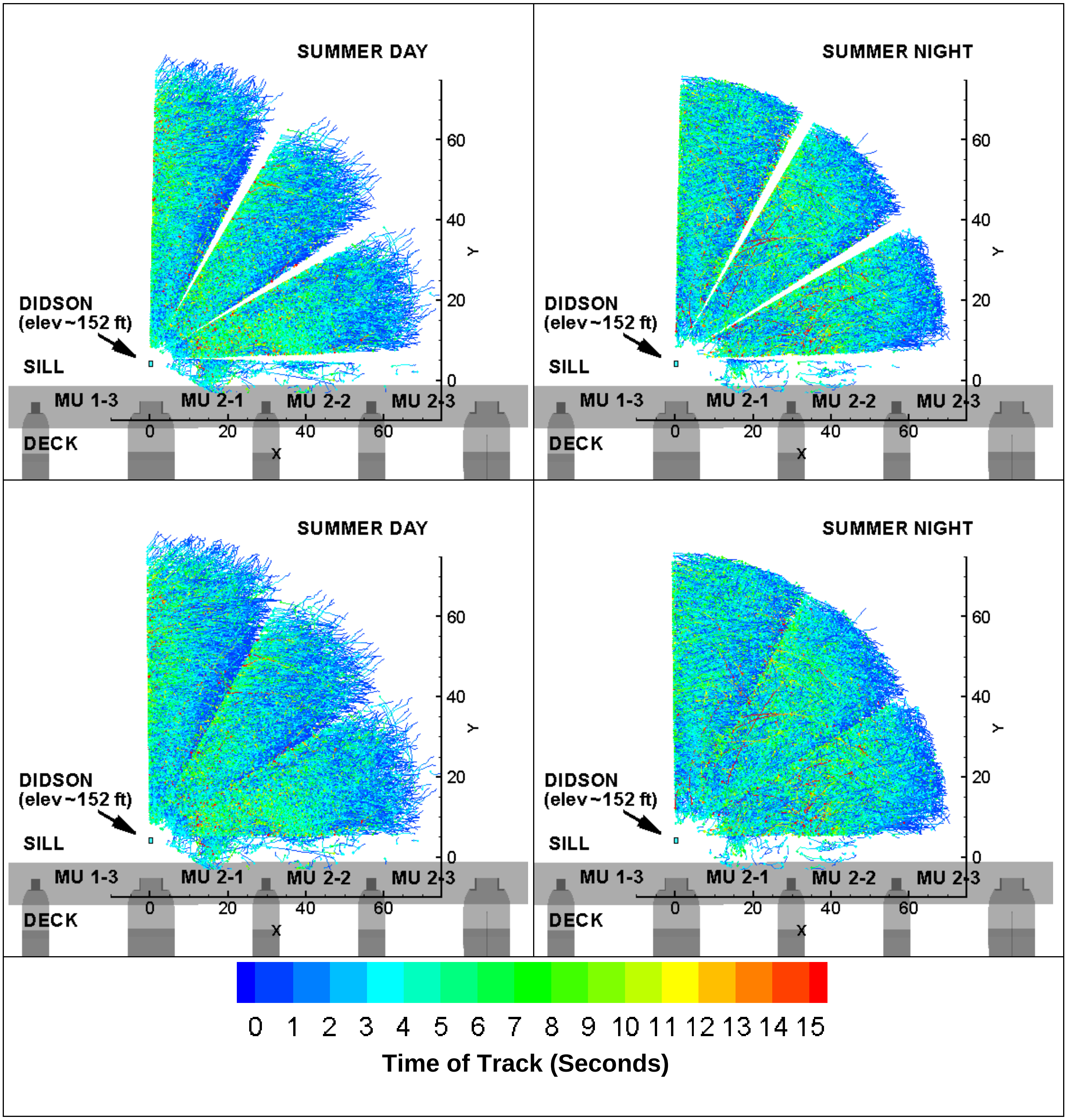

Figure 3.14. Effects of Widening at SL 2. Upper panels portray fish tracks from the DIDSON at The Dalles Dam SL 2 for Summer 2005. Lower panels show tracks adjusted by widening sector data 13% to fill in gaps. Axes' scales are in feet. Track portions are color-coded by the seconds from the start of each fish track.

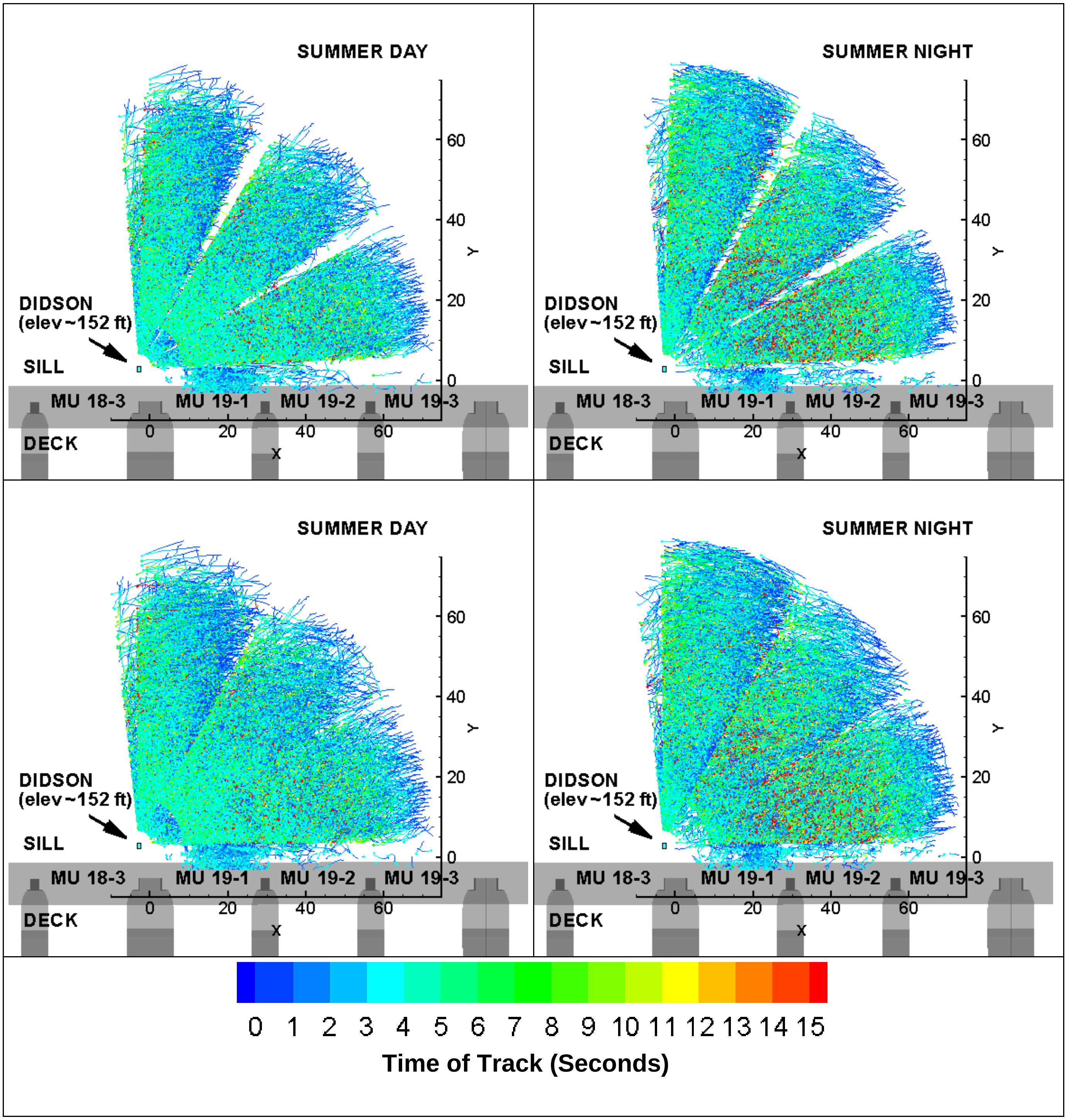

Figure 3.15. Effects of Widening at SL 19. Upper panels portray fish tracks from the DIDSON at The Dalles Dam at SL 19 above MU 19for Summer 2005. Lower panels show tracks adjusted by widening sector data 13% to fill in gaps. Axes' scales are in feet. Track portions are color-coded by the seconds from the start of each fish track.

3.3.6 Markov Chain Model Volume

The methods used to analyze fish movement were similar to those used in recent years at TDA (Johnson et al. 2005; Johnson et al. 2004). An absorbing Markov chain (Kemeny and Snell 1960) was used to capture fish movement to a particular location, the region where we considered fish were entrained into the sluiceway. A Markov chain can model continuous movement in a continuous volume when discrete time steps are chosen and volumetric cells of a sample volume are delineated over which transition movement probabilities can be calculated. The resulting Markov chain model allowed us to estimate fish movement probabilities from a given cell within the sample volume to each “absorbing” cell on the boundary of the volume.

The sample volume coordinate system (Figure 3.16) was defined as follows:

- x-dimension was parallel to the dam with northeast movement in the positive x-dimension and southwest movement in the negative x-dimension;
- y-dimension was perpendicular to the dam with movement toward the dam in the negative y-dimension and movement away from the dam in the positive y-dimension;
- z-dimension was vertical in the water column with movement upward in the positive z-dimension and movement downward in the negative z-dimension. In the following analyses there was only one cell thickness in the z-dimension, so movement was constrained to the x- and y-dimensions.

The DIDSON sample volume was roughly quarter-circular. Fish movement was sampled using the DIDSON and moving 30° between four zones (evident in fish tracks of Figure 3.12 to Figure 3.15). Each zone subtended somewhat less than 30° and as a result there was little or no overlap so that infilling was needed to provide connectedness in the Markov chain analysis. Infilling in spring at SL 2 was accomplished by dithering fish tracks using a random rotation of ±2.5°. This rotation was made at the DIDSON origin and was a uniform random addition unique to each fish track. In summer at both SL 2 and SL 19, tracks were adjusted by widening sector data 13% to provide infilling to fill in these gaps.

A rectangular volume was used to apply the Markov chain analysis (Figure 3.17) that encompassed part of the DIDSON sample volume and differed slightly between the seasons of Spring and Summer and sluiceway locations. The sample volume was chosen to encompass a sufficient number of tracked fish to estimate movement near the sluiceway. A consideration in designing the sample volume for the Markov chain analysis was to have sufficient number of fish reaching absorption cell boundaries.

The three-dimensional sample volume effectively formed a two-dimensional sample volume by allowing the z-dimension of each cell to extend to z = -20 ft relative to the surface. The x- and y-dimensions of cells were 3.0 ft (0.9144 m) on a side. We formed states (Kemeny and Snell 1960) for the Markov chain that corresponded to the location of each volumetric cell (Figure 3.17). The Markov chain sample volume was consistently 20 cells wide in the x-dimension, but varied between 22 and 23 cells out from the dam in the y-dimension, and was 1 cell deep in the z-dimension (440 to 460 total cells). In both spring and summer at both units, the rectangular volume extended 60 ft (18.3 m) across (along the dam), and was 20 ft (6.1 m) deep from the surface. At SL 2, it extended 66 ft (20.1 m) into the reservoir from the dam. In summer at SL 19, the rectangular volume extended 69 ft (21.0 m) into the reservoir from the dam.

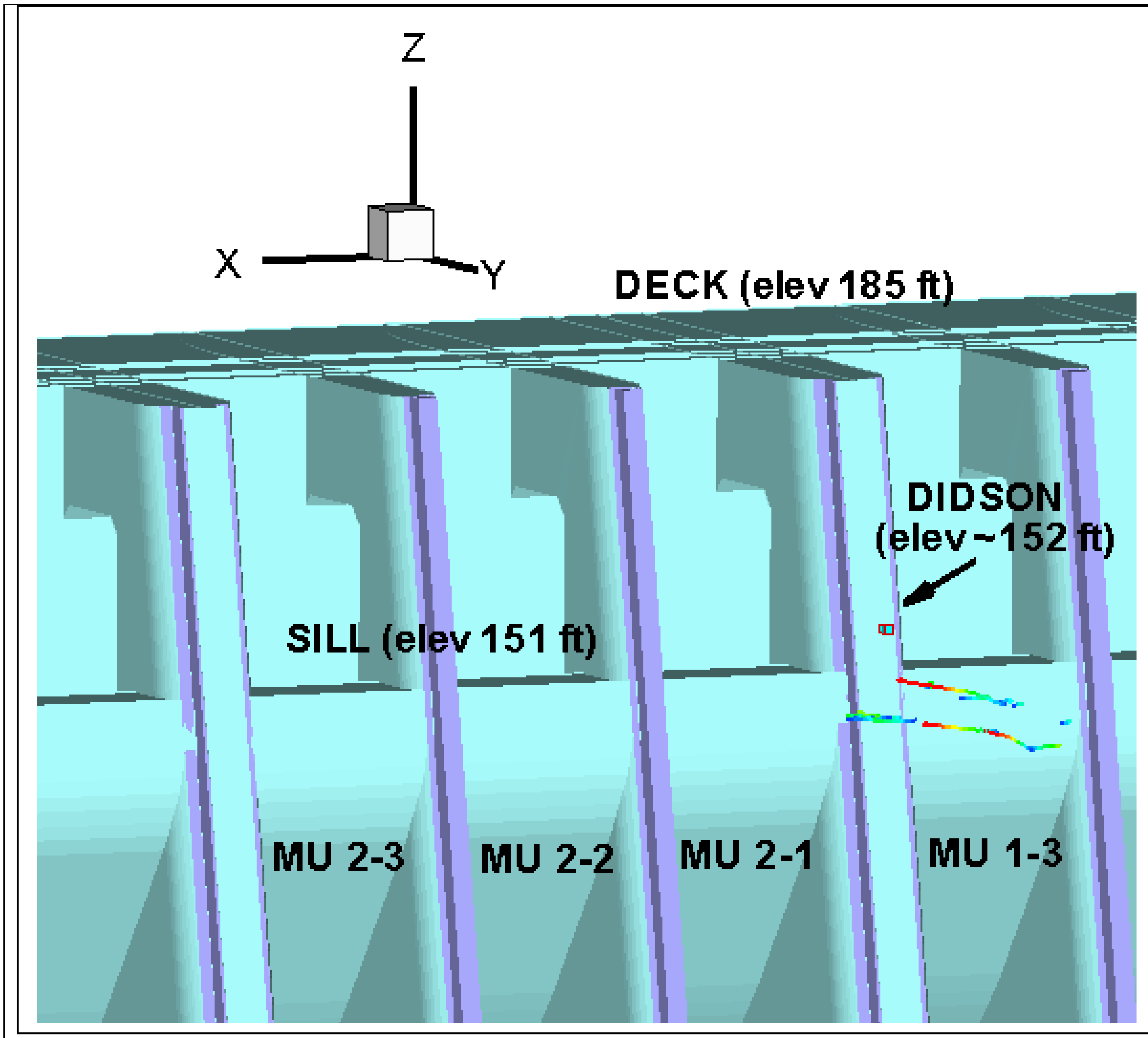

Figure 3.16. The Sample Volume Coordinate System. X-dimension was parallel to the dam with northeast movement in the positive x-dimension and southwest movement in the negative *x*-dimension; Y-dimension was perpendicular to the dam with movement toward the dam in the negative *y*-dimension and movement away from the dam in the positive *y*-dimension; Z-dimension was vertical in the water column with movement upward in the positive *z*-dimension and movement downward in the negative *z*-dimension. Sample fish tracks appearing near DIDSON are colorized by time in track (red =oldest, blue = newest).

Markov absorbing states (Kemeny and Snell 1960), called "Fates" here, were assigned on edges of the volume. Movement was not possible through the surface or bottom. Fates were calculated as probabilities of absorption into cells at a particular portion of the sample volume as follows: Sluiceway, East (true northeast), West (true southwest), and Reservoir (Figure 3.17). Movements to a boundary were observed; otherwise, the fate would be called "Stagnation." Movement fates to the faces of the sample volume are simply probabilities for movements within the sample volume.

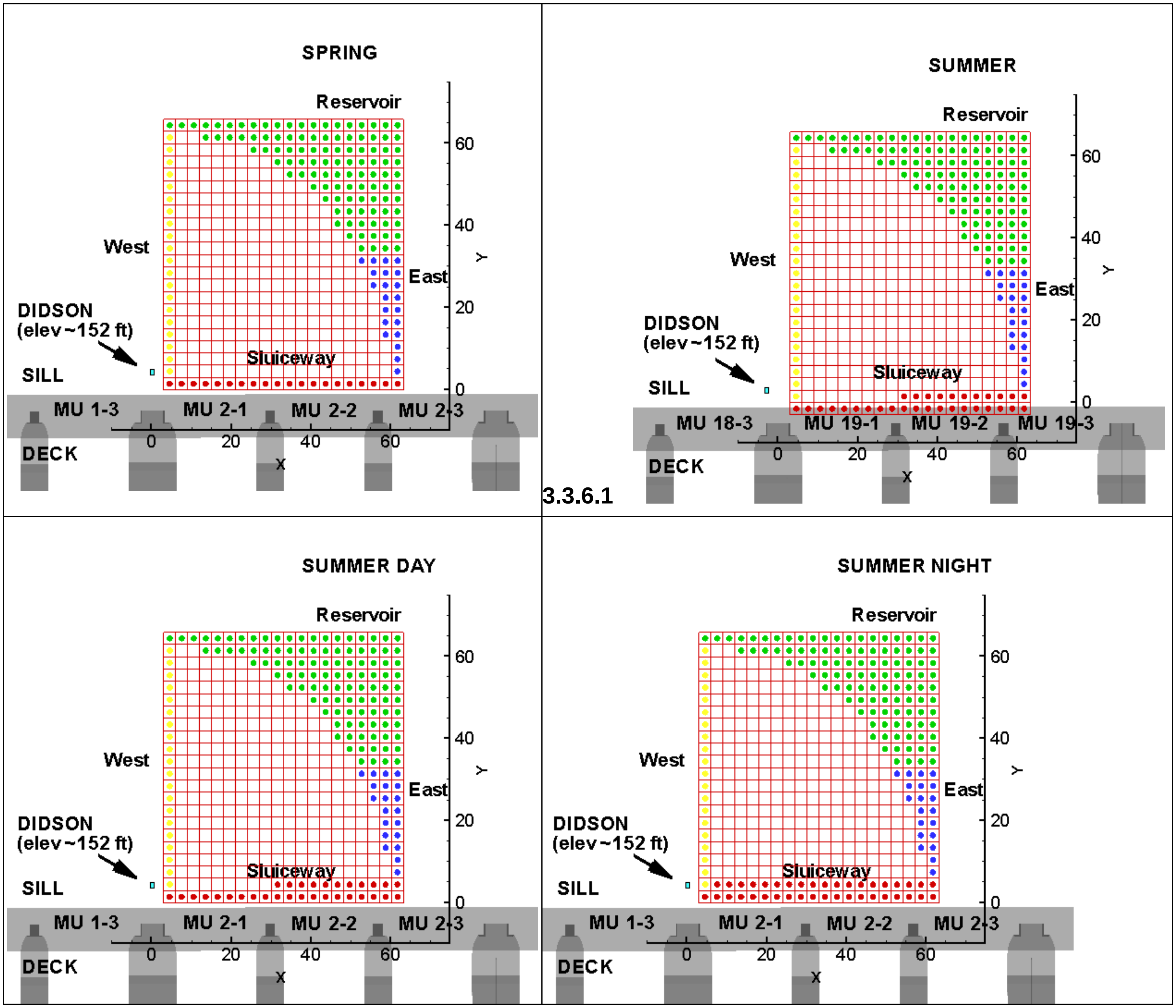

Figure 3.17. Fates Where Fish Movements Were Absorbed at Edges of the Sample Volume: Sluiceway, East, Reservoir, and West. Sluiceways are located at MU 2-1, 2-2, and 2-3 and at MU 19-1, 19-2, and 19-3. Grids, composed of 3 ft x 3 ft cells in X and Y, were used for 0.5 s fish movement observations and were centered on fish tracks for location and season. Axes shown are in feet.

Because of the allocation of absorbing states in cells that could not be reached after a track encountered the first layer boundary, the actual number of cells and states was less than the number of volumetric cells shown in Figure 3.17. For example, in spring there were 440 Markov chain volumetric cells and 101 of these were set as absorbing cells beyond the boundary absorbing cells, giving 339 cells (or states, including absorbing states). The redundant allocation was necessary to simplify the Markov chain analysis C-language computer program.

In summary, the Markov model included absorption at the faces corresponding to one of four movements: Sluiceway, East, West, and Reservoir. Of these, the Sluiceway fate was used to characterize movement into sluiceways at MU 2 and MU 19 for this study. Out of the 440 to 460 total cells, there were 254 (summer night SL 2), 262 (summer day SL 2), 272 (spring SL 2), and 280 (summer SL 19) non-absorbing cells through which fish could move in the analysis. These cells extended about 60 ft from the DIDSON. A distinction between East and Reservoir absorbing cells was made at Y=33 ft. Absorbing cells farther away than 1 cell from the non-absorbing cells are not required in a Markov chain analysis but were left for pragmatic reasons in the computation.

3.3.7 Markov Chain Analysis

For purpose of our Markov chain analysis, the data were denoted as either spring or summer based on a date division of May 30 for the end of Spring and June 1 as the beginning of Summer. Sunrise and sunset were used to differentiate day from night. Times were based on a table found at the website, http://aa.usno.navy.mil/data/, of the Astronomical Applications Department, U.S. Naval Observatory, for The Dalles, Oregon, W121º07’, N45º37’, “Rise and Set for the Sun for 2005.” Locations were at open sluiceway entrances at SL 2 and SL 19.

To determine fate probabilities, we applied a Markov chain analysis (Karlin 1968), which described smolt movement as a stochastic process. A stochastic model does not imply that the fish movements are random. Where a deterministic model describes movements as a function of covariates such as flow variables that are believed to govern fish behaviors, the movements are certain and without deviation. Instead, the Markov model describes the fish movements as a function of empirically observed transition probabilities. Taylor and Karlin (1998) noted that a Markov process $\{X^t\}$ is a stochastic process with the property that, given a value X^t, the values of X^s for $s>t$ are not influenced by the values of X^u for $u<t$. They also pointed out that transition probabilities are functions not only of the initial and final states, but also of the time of transition as well. When the one-step transition probabilities are independent of the time variable, then the Markov chain has stationary probabilities (Karlin 1968). The time of transition was set at 0.5 s and is constrained in our application by the nature of the data, specifically the size of the cells in the sample volume and the frame interval. That is, we chose a transition time small enough to characterize a fish track and (for efficiency in subsequent data manipulations) larger than the frame interval so that the probability of remaining in a cell was not large. The choice of volumetric cell size (3 ft on x- and y-sides) was based on having as many cells as possible with fish movement data given the number of samples and the velocity of fish movements.

Several assumptions were made and verified regarding connectivity in the sample volume for the Markov model. 1) There were no absorbing non-boundary cells, that is, no interior cell’s probability was equal to one. 2) Exterior cells’ probabilities were set to one as described above. 3) No interior connectivity was forced but they relied upon empirical measurements. 4) Where no movement observation from a cell was measured using the DIDSON, then the closest movement was interpolated to that cell using inverse distance squared weights. Gaps between DIDSON sectors were initially filled using dithering or sector broadening.

A C-language program was used to construct a transition matrix and apply the Markov chain analysis. The Markov transition matrix was a square matrix the size of k x k, where k was the number of distinct cells being modeled (e.g., during the spring season, k = 440). The ij^{th} element in the i^{th} row of the j^{th} column of the transition matrix was the estimated probability (p_{ij}) of moving from cell i to cell j in the next time step. These probabilities were estimated by:

$$\hat{p}_{ij} = \frac{n_{ij}}{n_i}$$

where,

n_i = number of observations of smolts in the ith cell;

n_{ij} = number of observations where a smolt in cell i moved to cell j in the next time step.

The transition probabilities for cells (3 ft x 3 ft) that bordered the edges of the sample volume (e.g., Sluiceway) were set to unity to absorb any movement that reached our defined fates. The transition matrix T was constructed using a time step of 0.5 s, using average position (i.e., $\bar{x}$, $\bar{y}$, $\bar{z}$) during each 0.5-s interval a fish was tracked. This process required that a fish be tracked for at least 1 s before the transition matrix was amended to obtain location i from the first interval and location j from the next, and so on.

After the transition matrix was formed, it was examined to find cells that were not sampled by the DIDSON. In these instances of no observation, nearby cells in Cartesian space with movement data were found and the movement patterns through those cells were interpolated to the cell with no observations using inverse distance squared weights. We limited the search radius to three cells away in order to use local data for interpolation. Of the six Markov chain analyses (SL 2 spring and summer, SL 19 summer, day and night) there were only two cells in spring Day at SL 2 and eight cells in spring night that required this interpolation.

The transition matrix T for one time step was used to estimate the transition probabilities for two or more time steps as T^t where t = the number of time steps. Matrix T^t is the transition matrix for t time steps and the transition probabilities $p_{ij}^{(t)}$ express the probability of moving from cell i to cell j in t time steps. The size of t was sufficiently large so that the tracked fish revealed an absorption state or became stagnant. The t-step transition probabilities to absorbing cells were visualized using Amtec Engineering's Tecplot software by contouring the sums of each state's (each representing an x, y, z cell) probabilities over the absorbing surfaces previously described.

3.4 Computational Fluid Dynamics Model

A CFD model of The Dalles Dam forebay was used to simulate the hydrodynamics for various operational scenarios. The model runs were integrated with biological studies of the effect of sluiceway operations on the passage of juvenile salmonids. The computational mesh used for these simulations was created for the CENWP by ENSR (Redmond, WA) and PNNL (Richland, WA). For this study, the mesh was rotated and translated onto the State Plane feet, Oregon North geographic coordinate system. The TDA forebay CFD model included three intakes for each of the turbine units, individual spill bays, sluiceway inflows, and the station service flows. The model was composed of 803,000 fluid cells and a total of 1,090,821 cells. All simulations used STAR-CD, a commercial

CFD solver. A given model run took about 3.5 hours to run on a 2.2-GHz dual processor Linux desktop with 4 GB of memory.

The CFD model was applied to four scenarios representing spring and summer 2005 flows with Sluice 2+5 and Sluice 2+19 configurations each season (Table 3.4). We selected the time periods, obtained mean total discharges for the spillway and turbines, and then made a spreadsheet and allocated the discharges by location according to the patterns from the dam operations analysis.

Table 3.4. Scenarios for CFD Modeling. Forebay elevation is in feet and discharge (Q) is in cfs.

	Spring		Summer	
Case	1	2	3	4
Sluice Configuration	SL 2+5	SL 2+19	SL 2+5	SL 2+19
Forebay Elevation	158.3	158.3	158.3	158.3
Sluice Q	4,643	4,580	4,643	4,580
Turbine Q	134,000	134,000	114,000	114,000
Spill Q	69,000	69,000	56,400	56,400
Total Project Q	207,643	207,580	175,043	174,980

4.0 Results

We organized the results from the hydroacoustic study at The Dalles Dam in 2005 into three parts: environmental conditions, fish passage evaluation, and sluiceway evaluation.

4.1 Environmental Conditions

This section contains a description of the environmental conditions during the study in 2005, including smolt migration characteristics, river discharge, and hydraulic conditions.

4.1.1 Smolt Migration Characteristics

Juvenile salmonid monitoring is not conducted at The Dalles Dam. Data on smolt migration characteristics there are based on the Smolt Monitoring Program's (SMP) sampling at John Day Dam and information on hatchery releases in the Deschutes River drainage. John Day Dam is the nearest upstream dam with smolt monitoring facilities. It is generally representative of species composition and run timing at The Dalles Dam because the travel time from John Day Dam to The Dalles Dam is about 1 d based on radio telemetry data (J. Beeman, USGS-BRD, pers. comm.). There is only one significant tributary between the two dams, the Deschutes River. This tributary has a juvenile salmonid migration that includes approximately 1 million hatchery yearling Chinook salmon. Overall at The Dalles Dam, yearling Chinook salmon and steelhead dominate the downstream migration during spring, while subyearling Chinook salmon dominate the run during summer.

Our study encompassed the majority of the migration period for yearling (stream-type) Chinook (*Oncorhyncus tshawytscha*), coho (*O. kisutch*), and sockeye (*O. nerka*) salmon as well as steelhead (*O. mykiss*) and subyearling (ocean-type) Chinook salmon (Figure 4.1). Passage of yearling fish peaked in mid- to late May (Figure 4.1). Passage of subyearling Chinook salmon, the most abundant salmonid fish migrating downstream through John Day Dam, peaked at the end of June. During the spring study period (April 18 to June 4), species composition was:

- yearling Chinook salmon (61%)
- steelhead (24%)
- coho (8%)
- sockeye (4%)
- subyearling Chinook salmon (3%).

During the summer study period (June 5 to July 16), subyearling Chinook salmon comprised 96% of the outmigration.

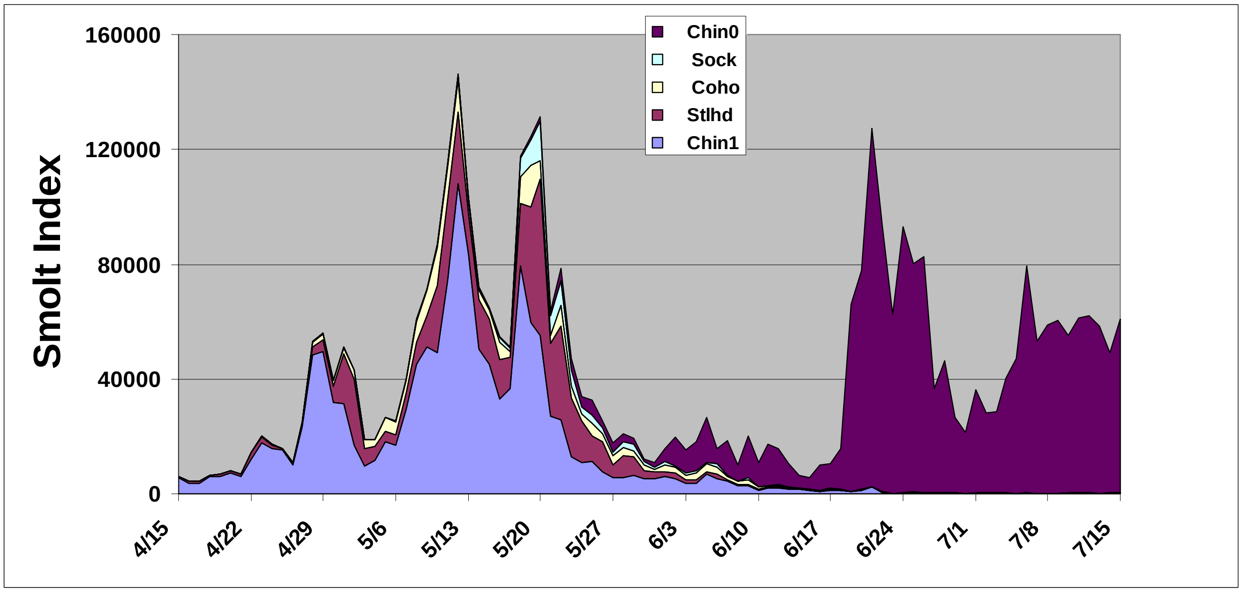

Figure 4.1. Smolt Monitoring Program (SMP) Passage Index for April 18 – July 16, 2005, from John Day Dam. Designations in the legend are for subyearling Chinook salmon (Chinook 0), yearling Chinook salmon (Chinook 1), coho salmon (Coho), sockeye salmon (hatchery and wild), and steelhead. Data were obtained from DART (http://www.cqs.washington.edu/dart/dart.html), accessed in October 2005.

4.1.2 River Discharge, Forebay Elevation, Temperature, and Turbidity

During the study (April 18 through July 16), daily outflow at TDA ranged from 117 to 287 kcfs (Figure 4.2). Mean daily outflow was 205 kcfs in spring (April 18 to June 4) and 181 kcfs in summer (June 5 to July 16). Outflow peaked in mid-May (Figure 4.2). During the 2005 study, total project outflow was 76% of the average for the previous 10 years for spring and 71% of the 10-year average for summer. Daily powerhouse discharge averaged 136 kcfs in spring and 114 kcfs in summer. Spill for fish protection commenced on April 11. Daily spill flow during our study ranged from 45 to 81 kcfs, with a mean of 69 kcfs (34% of total) in spring and 66 kcfs (37% of total) in summer. Daily sluice flow was about 4.4 kcfs, depending on forebay elevation. In spring and summer, mean sluice discharge was 3.3% and 3.8% of total powerhouse discharge, respectively.

Power peaking occurred during daytime and evening (Figure 4.3). As noted above, MU 1, 3, and 4 were off-line during the entire study. Main Units 15 and 16 were off-line most of the study.

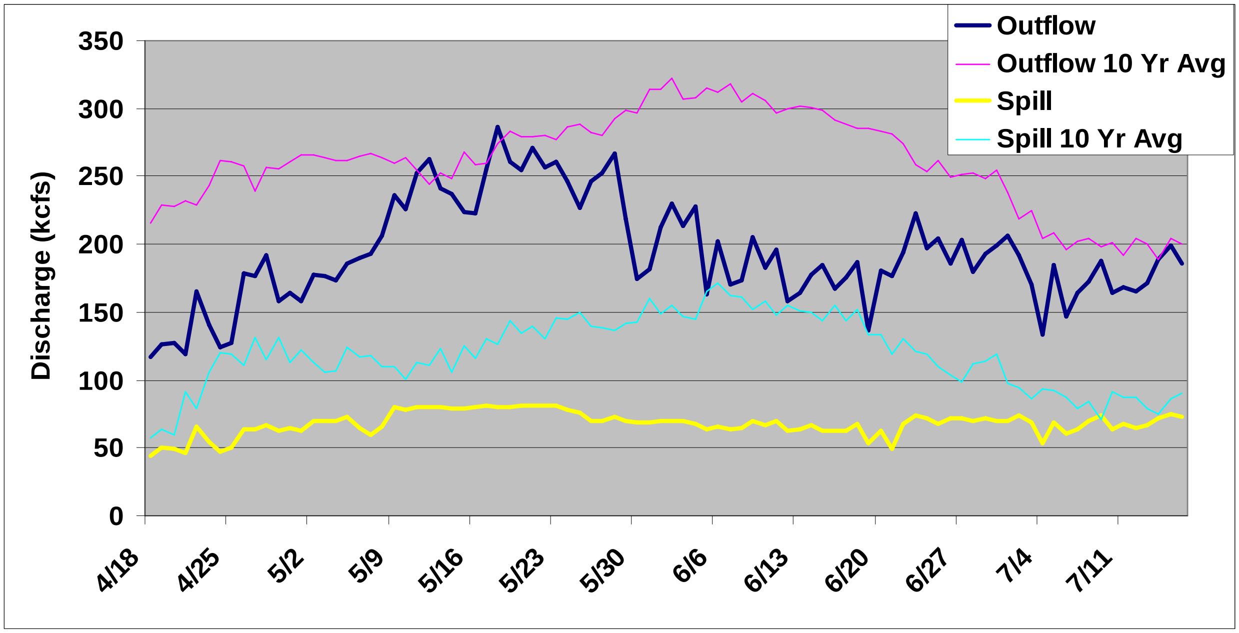

Figure 4.2. Daily Total Outflow and Spill for 2005 and the 10-yr Average (kcfs). Data were obtained from DART (http://www.cqs.washington.edu/dart/dart.html), accessed October 2005.

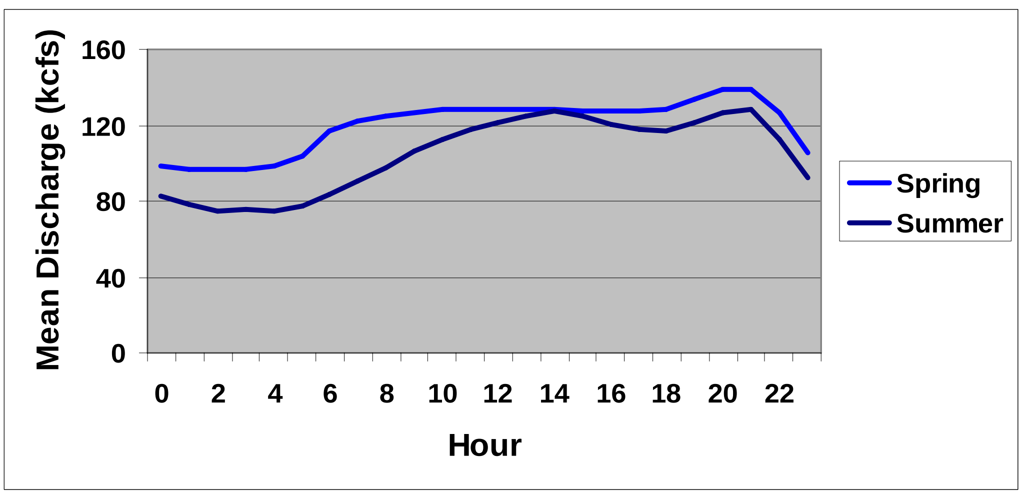

Figure 4.3. Diel Distribution of Turbine Discharge for Spring (4/18-6/4) and Summer (6/5-7/16) 2005

Mean daily forebay elevation during the study ranged from 157.5 ft to 159.1 ft (Figure 4.4). Mean forebay elevation was 158.4 ft in spring and 158.0 ft in summer.

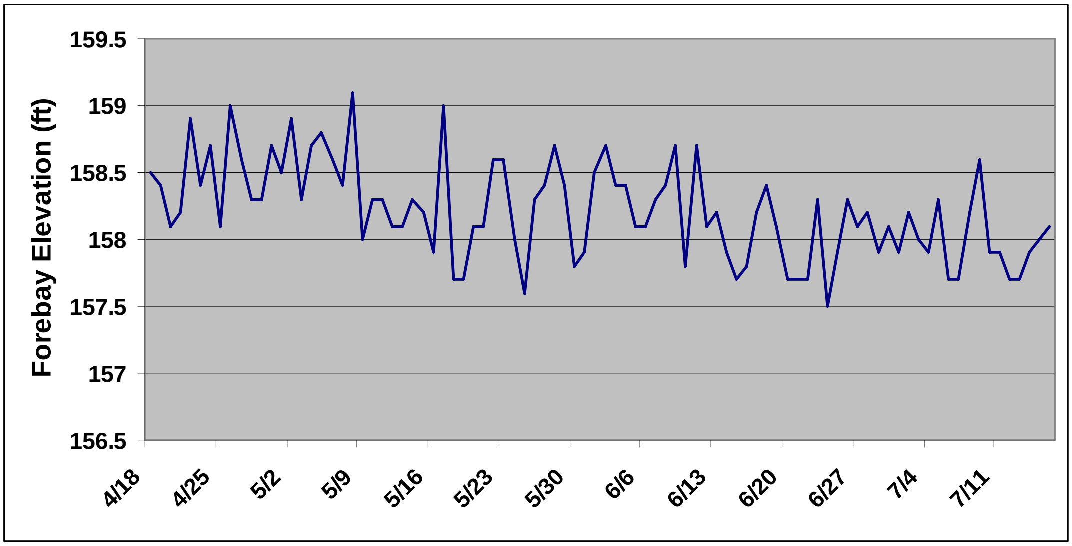

Figure 4.4. Mean Daily Forebay Elevation. Data were obtained from DART (http://www.cqs.washington.edu/dart/dart.html) in October 2005.

Water temperature generally increased as the study progressed (Figure 4.5). It ranged from 9.4°C to 20.2°C and was 0.7°C warmer than the 10-year average in spring and 0.8°C warmer in summer.

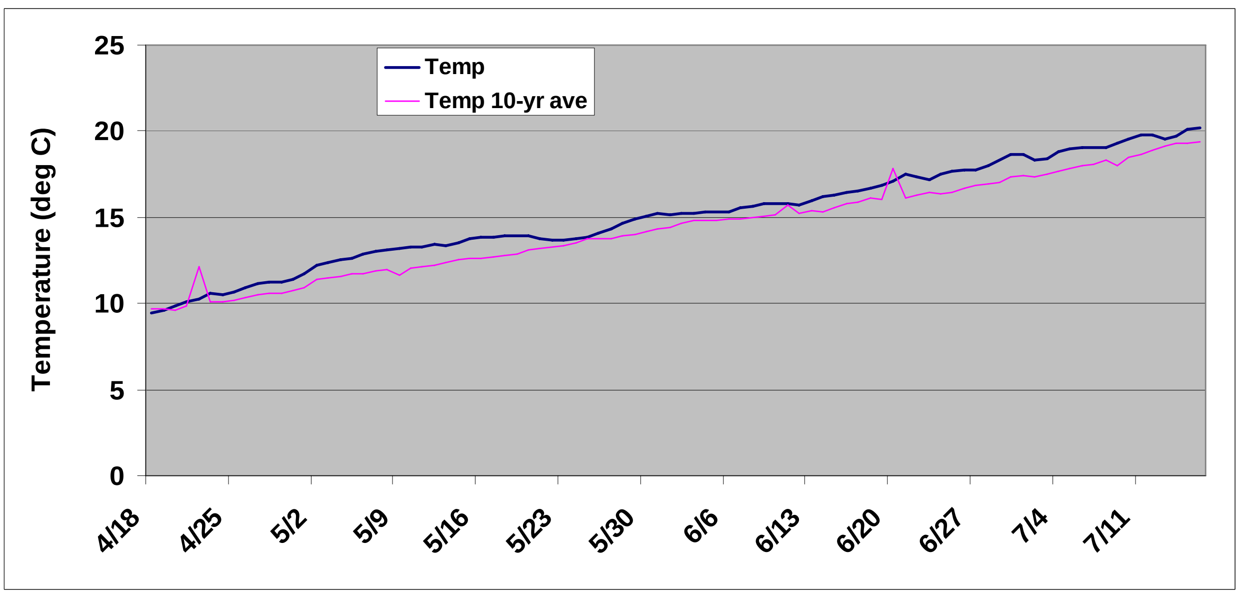

Figure 4.5. Mean Daily Temperature for April 18 – July 16, 2005, at TDA. Data were obtained from DART (http://www.cqs.washington.edu/dart/dart.html) in October 2005.

4.1.3 Hydraulic Conditions, Forebay CFD

All four discharge cases we modeled (Table 3.4) produced similar patterns at the scale of a turbine unit reported in this section (Figure 4.6). Therefore, we offer Case 1 as an example. Flow approached a sluice entrance at an oblique angle relative to the powerhouse, becoming more perpendicular to the dam the closer it got (Figure 4.7). In cross-section, flow was horizontal (parallel to the surface) until it was near the dam where it went up to the sluice or down to the turbine intake (Figure 4.8). Flow into the sluiceway had gradual acceleration until it was over the sill, then water accelerated rapidly into the sluice channel (Figures 4.7 and 4.8). The CFD modeling revealed that nearfield forebay velocities were generally less than 2 feet per second (fps), except near sluiceway entrances (Figures 4.7 and 4.9).

Velocities in the forebay of SL 2 and SL 5 were similar, except within 15 ft of the dam (Figures 4.9 and 4.10). Flow upward into the sluice entrance was stronger at SL 2 than SL 5, while flow downward to the turbine intake was stronger at SL 5 than SL 2 (Figure 4.10). A similar pattern was evident when we compared SL 2 and SL 19.

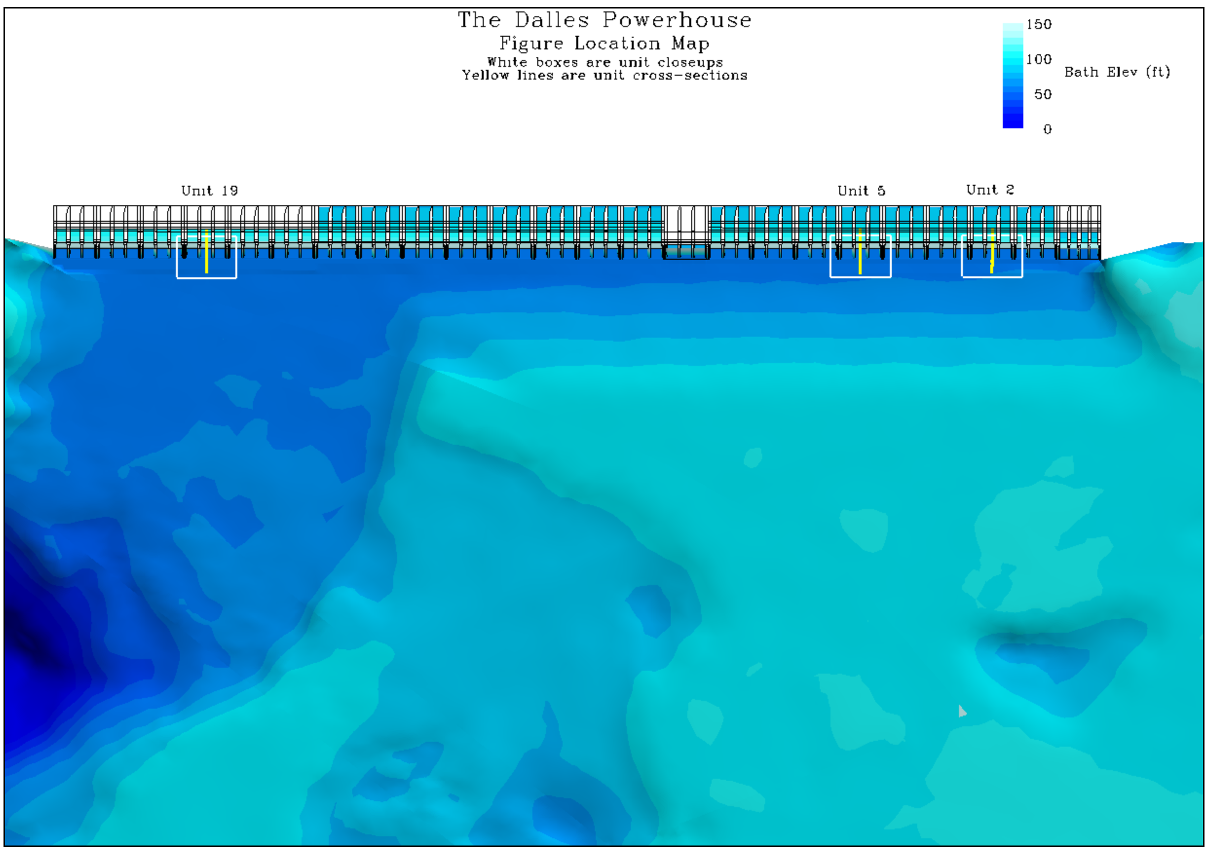

Figure 4.6. Figure Location Map with Forebay Bathymetry for CFD Graphics. White boxes depict unit close-ups (Figures 4.7 and 4.9) and yellow lines represent cross-sections (Figures 4.8 and 4.10).

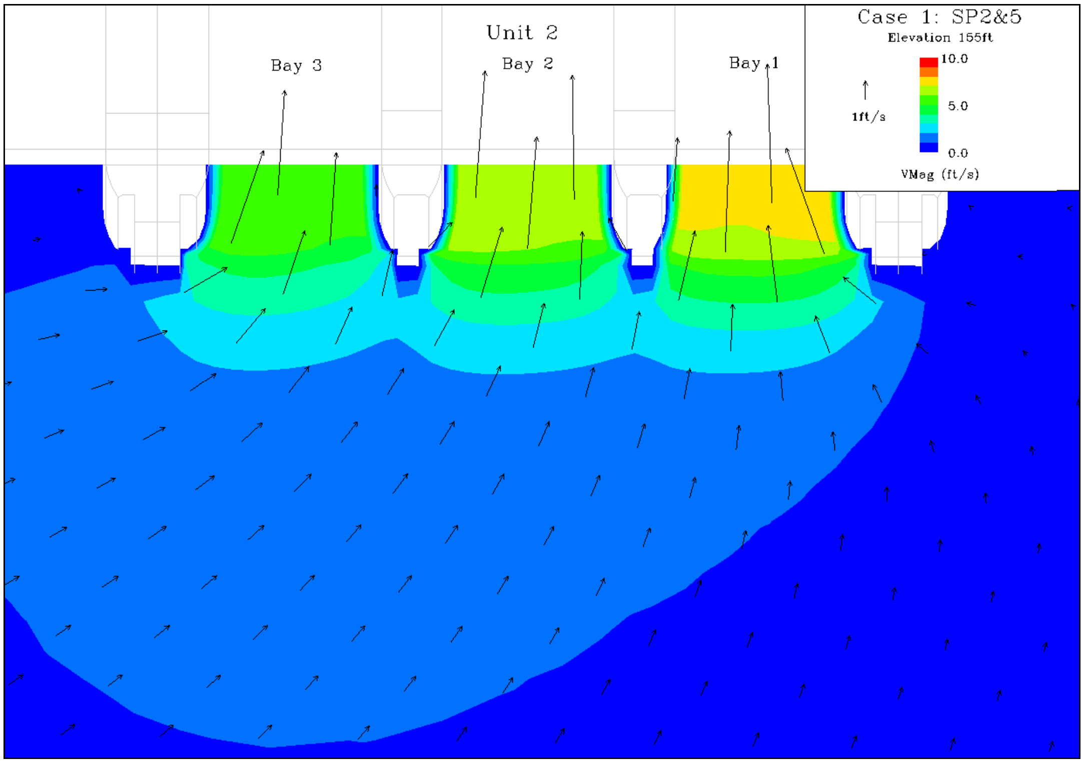

Figure 4.7. Plan View of Water Velocities at SL 2. Data are from elevation 155 ft for Case 1 (Table 3.4).

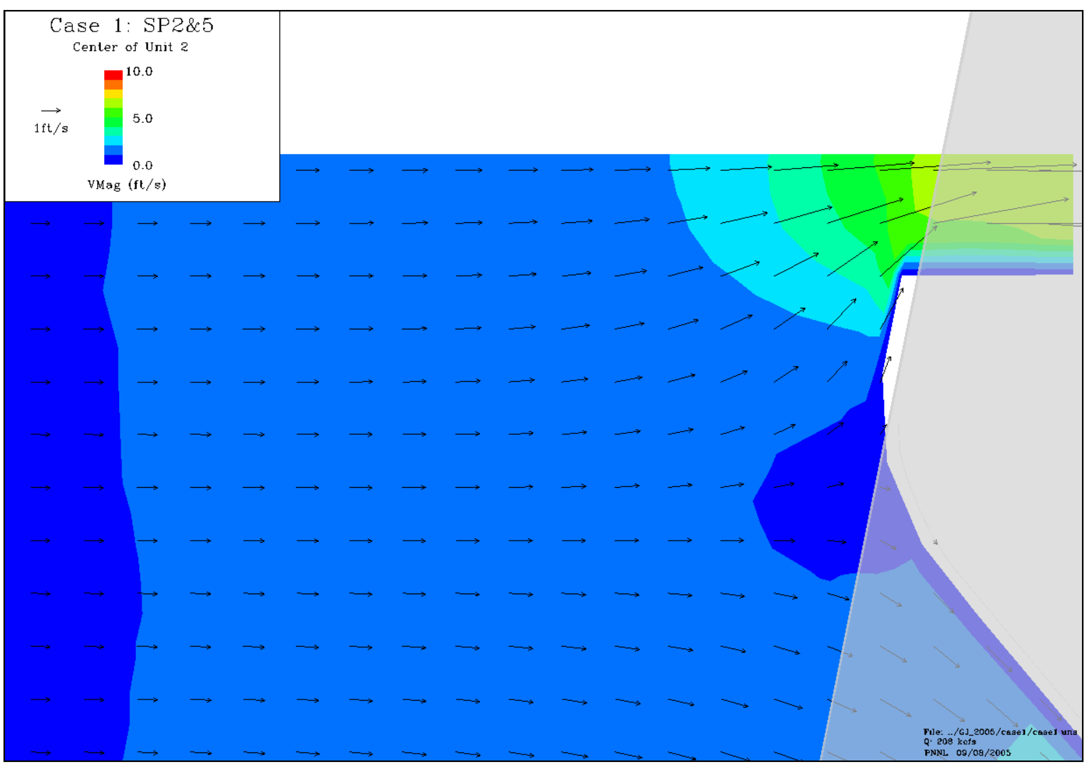

Figure 4.8. Cross-Sectional View of Water Velocities at SL 2. Data are from the centerline of SL 2-2 for Case 1 (Table 3.4).

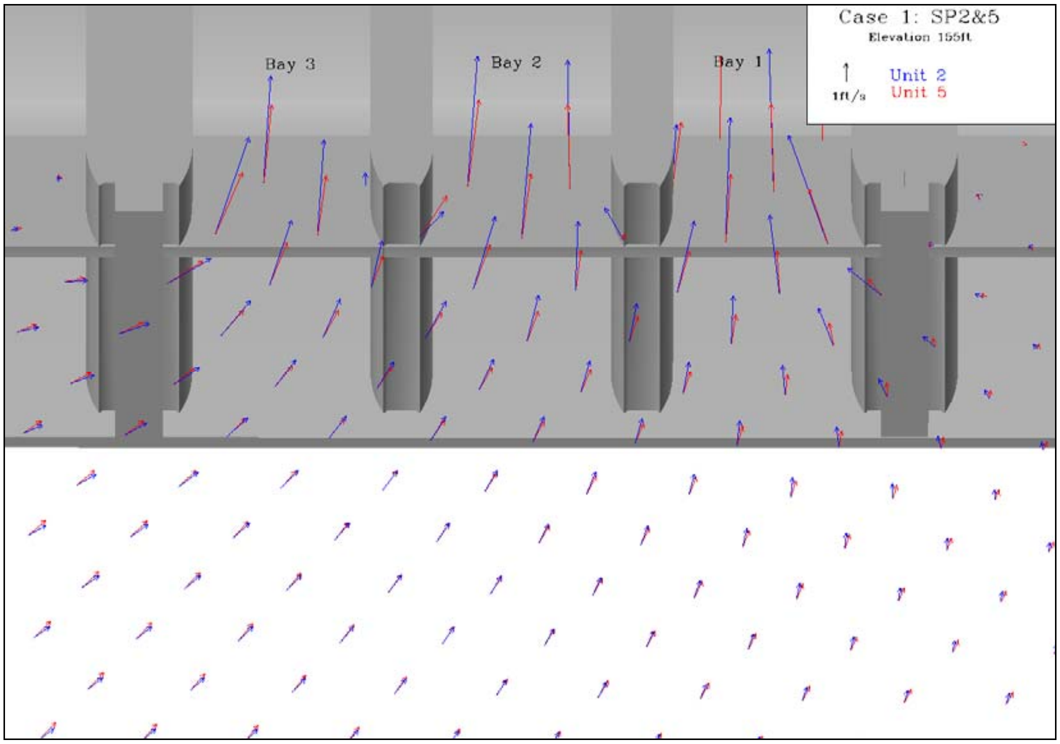

Figure 4.9. Plan View Comparing Water Velocities at SL 2 and SL 5. Data are from elevation 155 ft for Case 1 (Table 3.4).

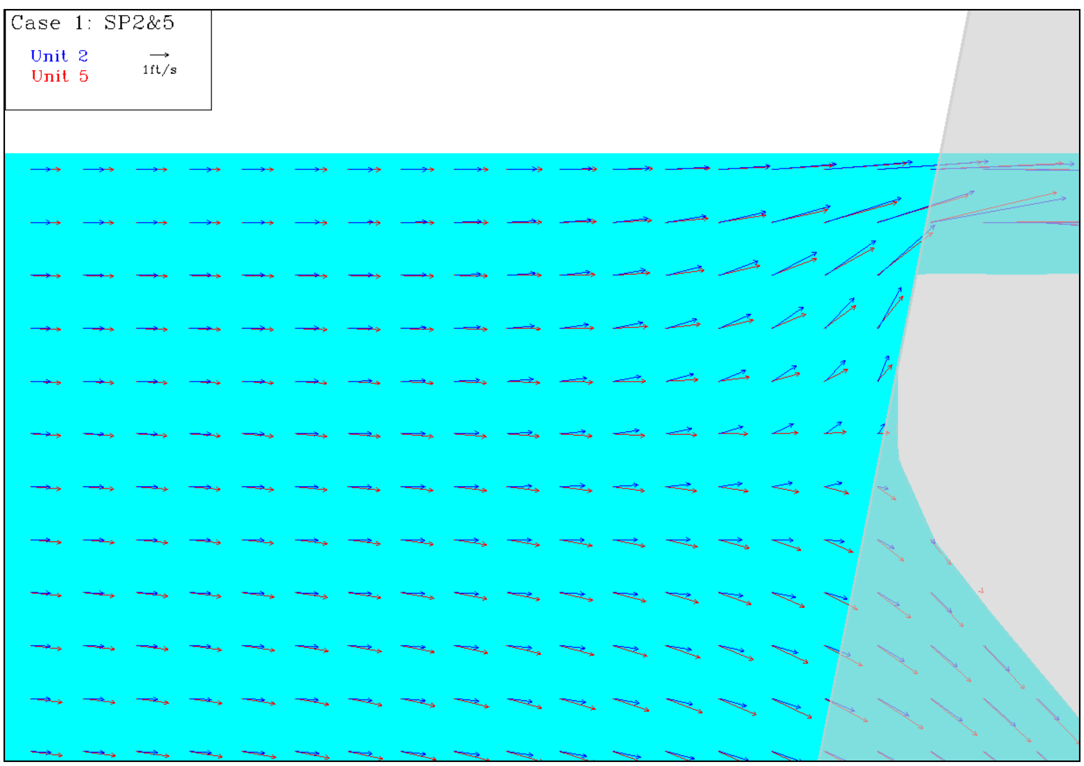

Figure 4.10. Cross-Sectional View Comparing Water Velocities at SL 2 and SL 5. Data are from the centerline of the respective locations for Case 1 (Table 3.4).

4.2 Fish Passage Evaluation

The 2005 fish passage evaluation involved data on daily fish passage and fish distributions at the powerhouse. The sluiceway evaluation is in the next section.

4.2.1 Daily Fish Passage

A comparison of the peaks in the hydroacoustic and SMP passage indices showed a reasonable match (Figure 4.11). The hydroacoustic passage index peaked ~5 days after the SMP index during spring and ~5 days before the SMP index during summer. We did not lag the data to compensate for the fact that the HA index is for The Dalles Dam and the SMP index is for John Day Dam because of the quick travel time (~1 d) from John Day to The Dalles Dam (J. Beeman, USGS-BRD, pers. comm.).

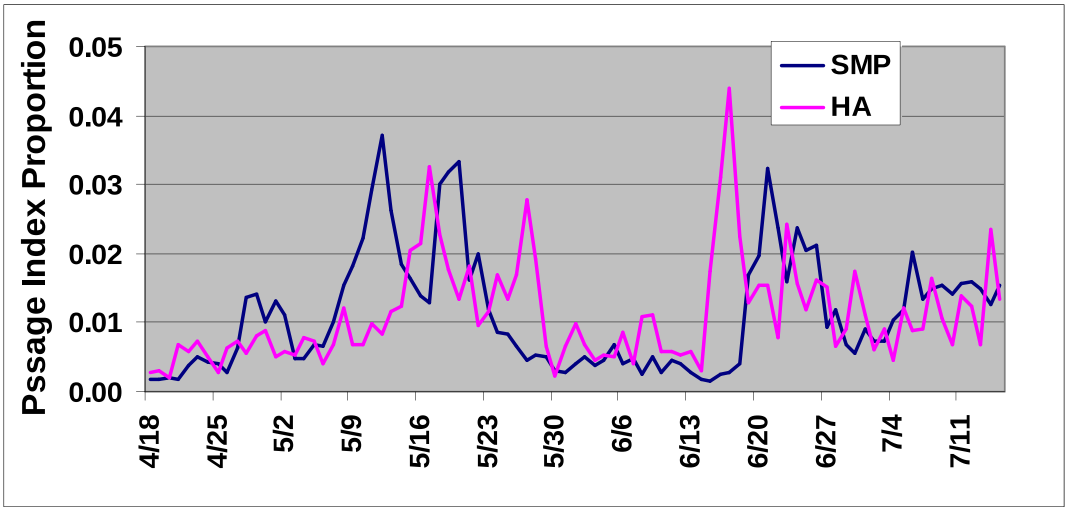

Figure 4.11. Fish Passage Indices for The Dalles Dam, 2005. Data are expressed as daily proportion of the total for the April 19 to July 17 study period. The hydroacoustic index (HA) is for the run at large as sampled at TDA. The Smolt Monitoring Program index (SMP) is for all species combined as sampled at John Day Dam.

4.2.2 Fish Distributions

Three types of fish distribution data were analyzed from the fixed location hydroacoustic data set: vertical, horizontal, and diel.

4.2.2.1 Vertical Distribution

The vertical distribution of fish in the sampled intakes of the main turbine units at The Dalles Dam was skewed to the ceiling during both spring and summer (Figure 4.12). In spring, 49% and 46% of the fish during day and night, respectively, were within 4 m of the ceiling. In summer, 53% and 45% of the fish during day and night, respectively, were within 4 m of the ceiling.

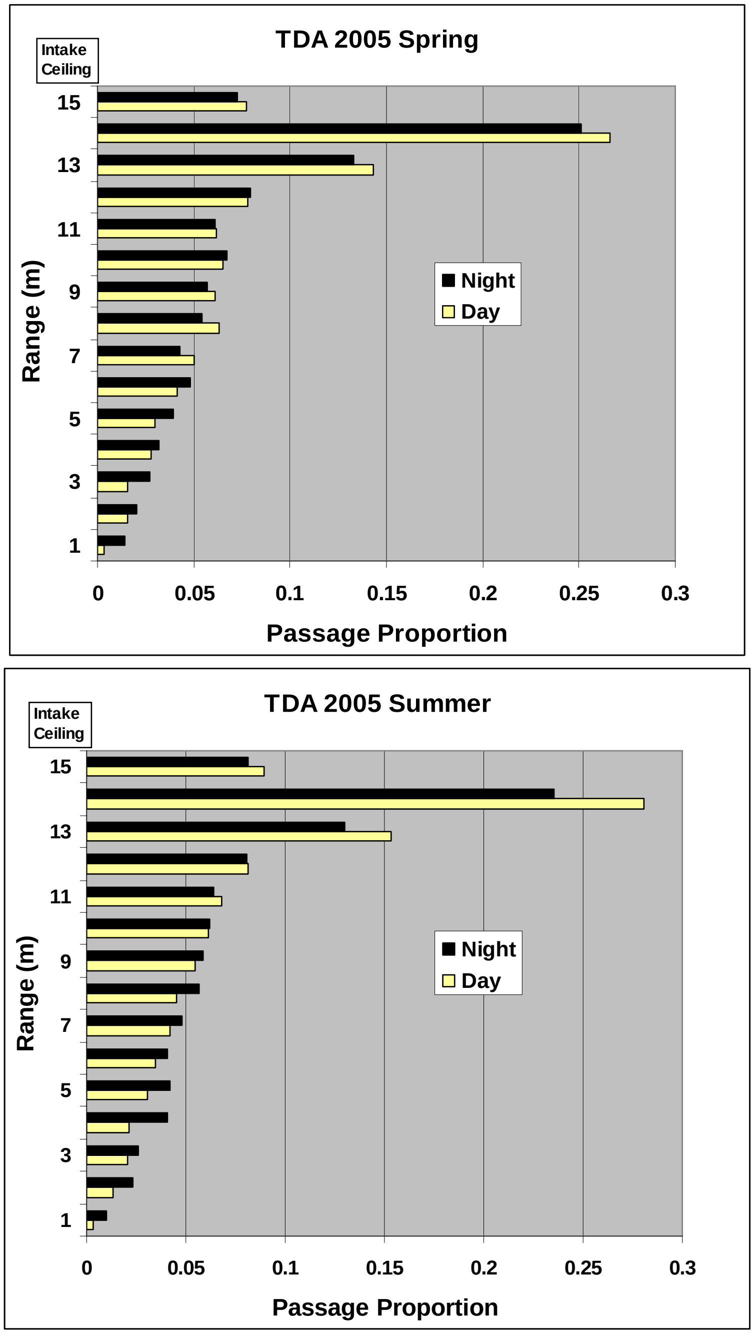

Figure 4.12. Vertical Distributions at the Powerhouse Turbine Intakes for Day and Night in Spring and Summer 2005. Data are presented as proportions of total passage in 1-m-range bins from the transducer to the intake ceiling (top of each figure).

4.2.2.2 Horizontal Distribution

At the powerhouse turbines and sluices, total fish passage was highest at SL 2 and MU 8 during spring and summer (Figure 4.13). There was little or no passage at MU 1, 3, 4, 15, and 16 because, as mentioned above, these units were off-line most or all of the study. Except for SL 2, SL 5, and MU 8, the horizontal distribution of total fish passage was reasonably uniform across the powerhouse. This distribution does not account for turbine discharge.

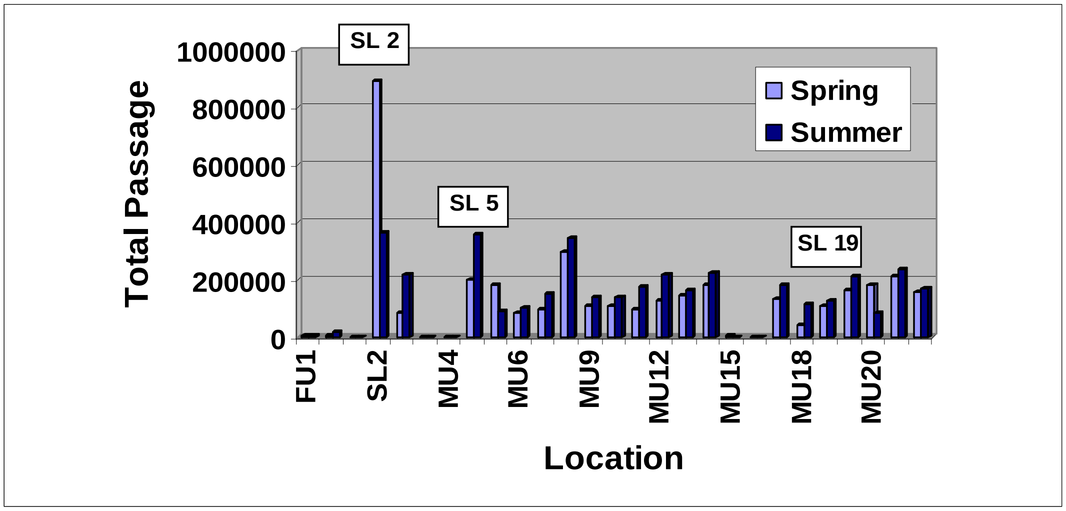

Figure 4.13. Horizontal Distributions of Total Fish Passage at the Powerhouse Turbines and Sluices in Spring and Summer in 2005

At the turbines, the horizontal distribution of fish per unit flow was higher in the eastern than western portion of the powerhouse during both spring and summer (Figure 4.14). Fish passage per unit flow into turbine intakes was higher during summer (Figure 4.14). It was highest at MU 21 during both seasons (Figure 4.14).

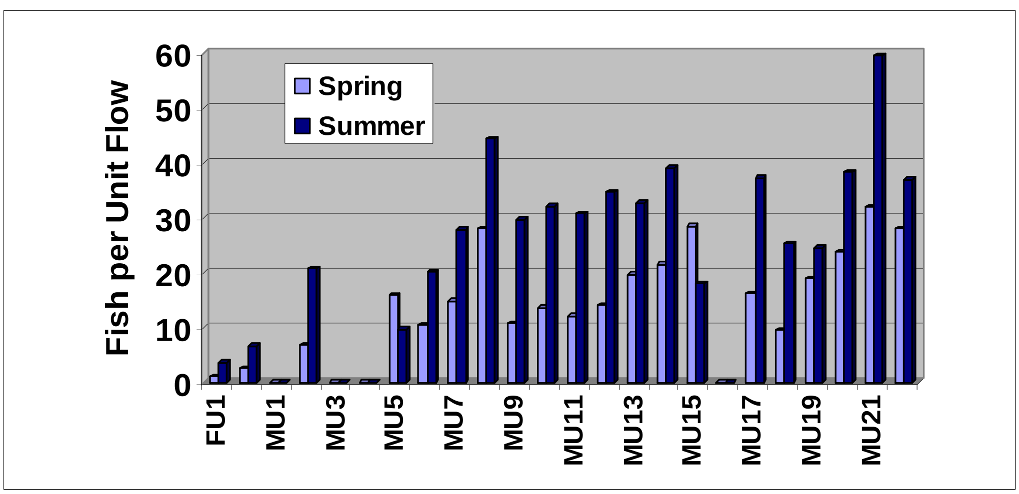

Figure 4.14. Horizontal Distributions of Fish Passage per Unit Flow (kcfs) at the Powerhouse Turbines in Spring and Summer in 2005

4.2.2.3 Diel Distribution

The diel distribution of fish passage was much more variable during spring than summer (Figures 4.15 and 4.16). During spring, passage at the powerhouse turbine intakes peaked in late afternoon and evening, while sluiceway passage peaked at mid-day with another peak at dusk (Figure 4.15). During summer, powerhouse turbine intake passage was highest during 2200-2300 h, and sluiceway passage was greatest at mid-day and evening (Figure 4.16). Turbine passage was lowest during the morning (0500-0900 h) in both spring and summer (Figures 4.15 and 4.16).

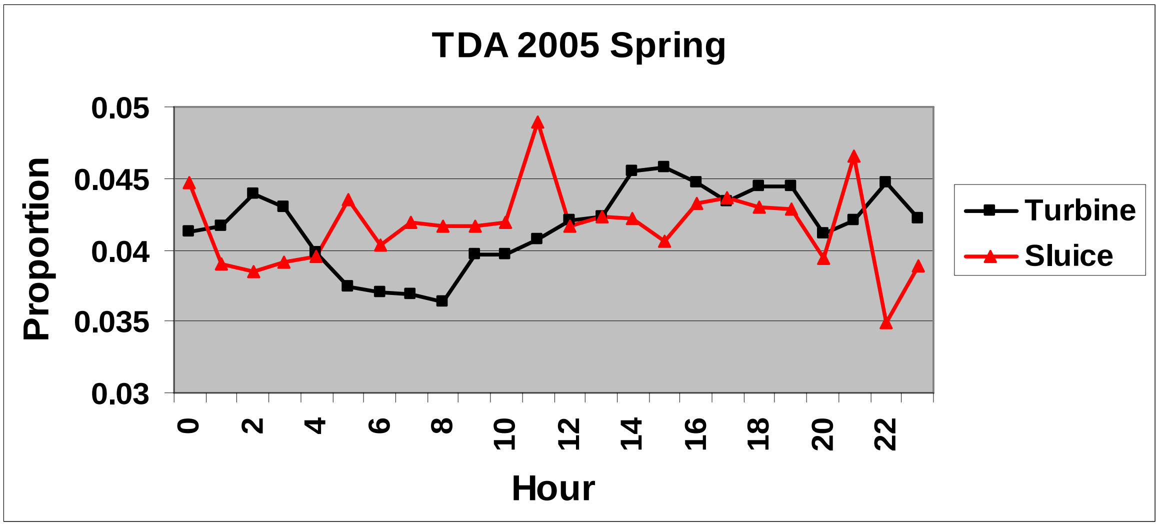

Figure 4.15. Diel Distributions at the Powerhouse Turbine Intakes and the Sluiceway during Spring 2005. Data are the hourly proportions of total passage for each route separately.

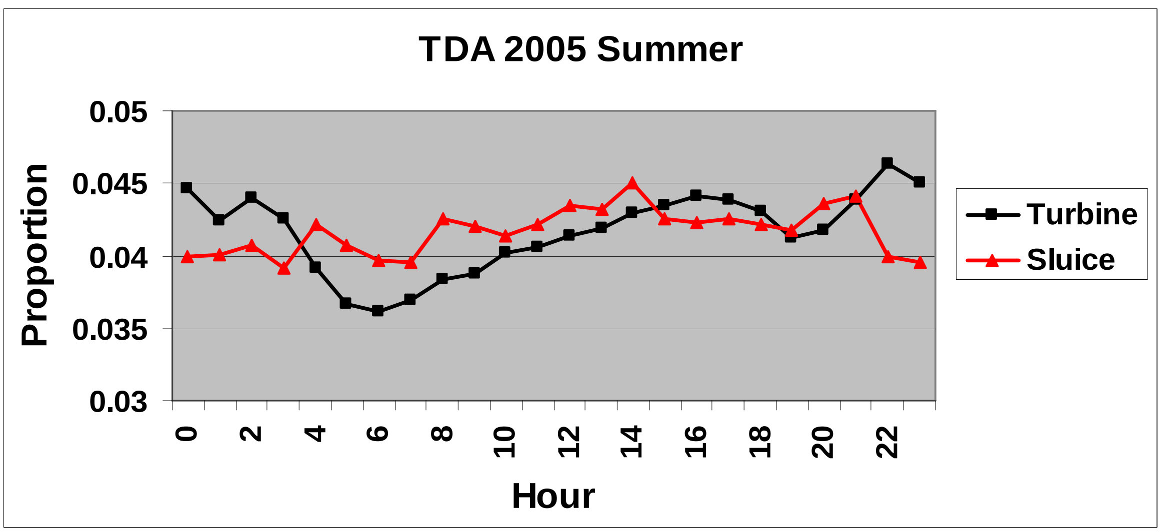

Figure 4.16. Diel Distributions at the Powerhouse Turbine Intakes and the Sluiceway during Summer 2005. Data are the hourly proportions of total passage for each route separately.

4.2.3 Load Following and Fish Passage

The exploratory analysis regressing load following and fish passage at the powerhouse rarely revealed significant relationships (Appendix B, Tables B1-B5). At $\alpha = 0.05$, results were significant in 2 of 50 cases in spring and 15 of 50 cases in summer. On face value, the results suggest load following

- is more likely to occur during summer than spring;
- is more likely to occur during non-peak electrical usage periods;

- affects powerhouse passage, not sluiceway passage;
- explains only a small fraction of the variance in fish passage.

4.3 Sluiceway Evaluation

The objectives for the sluiceway evaluation for The Dalles Dam in 2005 included 1) estimation of seasonal and daily sluiceway efficiency and effectiveness, 2) evaluation of sluice gate operations, 3) description of fish movements in the sluiceway nearfield (< 30 ft), and 4) recommendations for sluiceway operations and long-term measures to enhance sluiceway passage and reduce turbine passage. The first four objectives are addressed in this section; the later objective is addressed in Section 5.

4.3.1 Seasonal and Daily Sluiceway Efficiency and Effectiveness

Seasonal sluiceway passage metrics in 2005 were higher during spring than summer (Table 4.1). Sluiceway efficiency (re: powerhouse) was about 50% higher in spring than summer. Sluiceway effectiveness (re: powerhouse) was twice as high in spring as it was in summer.

Table 4.1. Seasonal Fish Passage Metrics for the run at large at The Dalles Dam, 2005. Data are presented separately for spring and summer. Confidence intervals are at the 95% level.

	Spring (4/18-6/4)	Summer (6/5-7/16)
Sluice Efficiency re: powerhouse	0.333 ± 0.14	0.217 ± 0.008
Sluice Effectiveness re: powerhouse	10.17 ± 0.43	5.72 ± 0.20

Daily sluiceway efficiency (re: powerhouse) was variable ranging from 0.09 to 0.72 (Figure 4.17). Sluiceway efficiencies generally decreased as the study progressed (Figure 4.17). There were sluiceway efficiency peaks on April 18 (0.72), April 27 (0.67), and June 19 (0.64).

Daily sluiceway effectiveness (re: powerhouse) was also variable, ranging from 2.26 to 21.20 (Figure 4.17). Sluiceway effectiveness was highest during the spring migration peak (May 9-20).

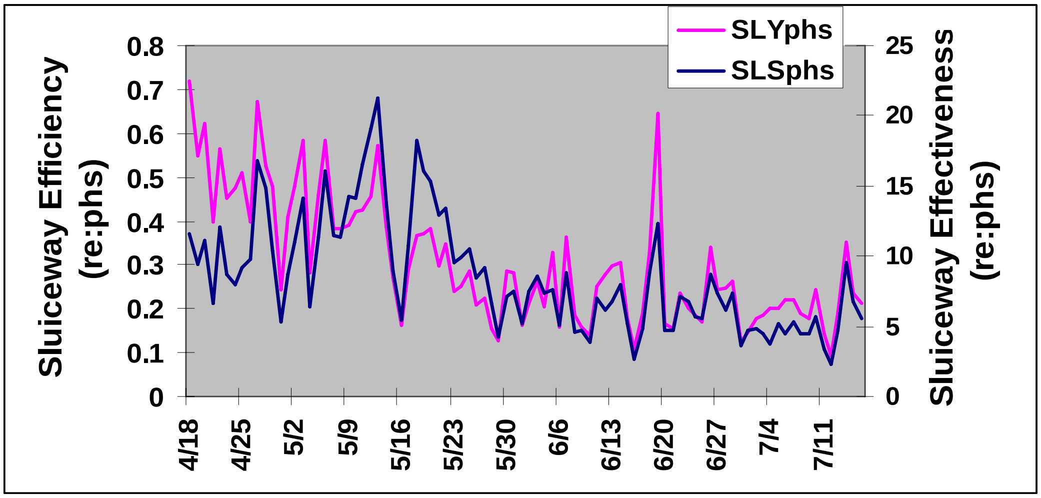

Figure 4.17. Daily Sluiceway Efficiency (SLYphs) and Effectiveness (SLSphs) Relative to the Powerhouse at The Dalles Dam**,** 2005.

4.3.2 Evaluation of Sluiceway Operations

Sluiceway efficiency (re: powerhouse) was higher for the SL 2+5 than for the SL 2+19 treatment in 7 of 8 study blocks in spring and 6 of 7 study blocks in summer (Figure 4.18). Overall sluiceway efficiency was 6.3 and 9.3 percentage points higher for the SL 2+5 than for the SL 2+19 treatment during spring and summer, respectively (Figure 4.19). The ANOVA comparison of arcsin-transformed sluiceway efficiency results for each treatment was significant during both spring ($P < 0.1$) and summer ($P < 0.05$).

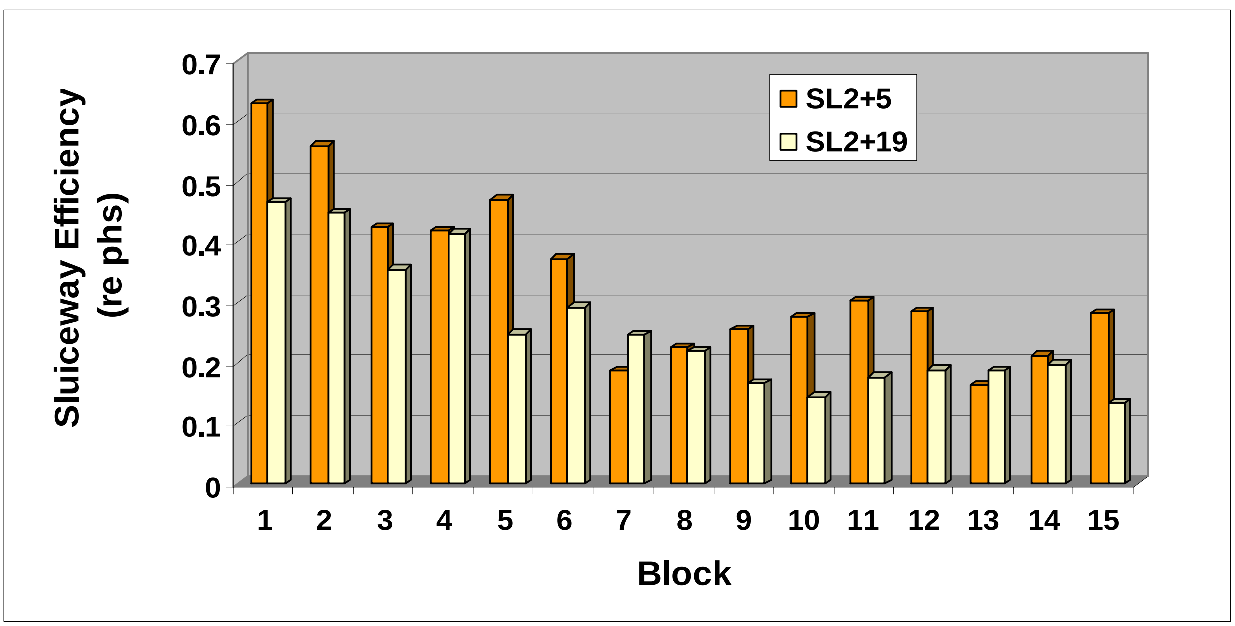

Figure 4.18. Sluiceway Efficiency for the Powerhouse by Study-Block for each Sluice Treatment (SL 2+5, SL 2+19). Blocks 1-8 cover spring and Blocks 9-15 cover summer study periods.

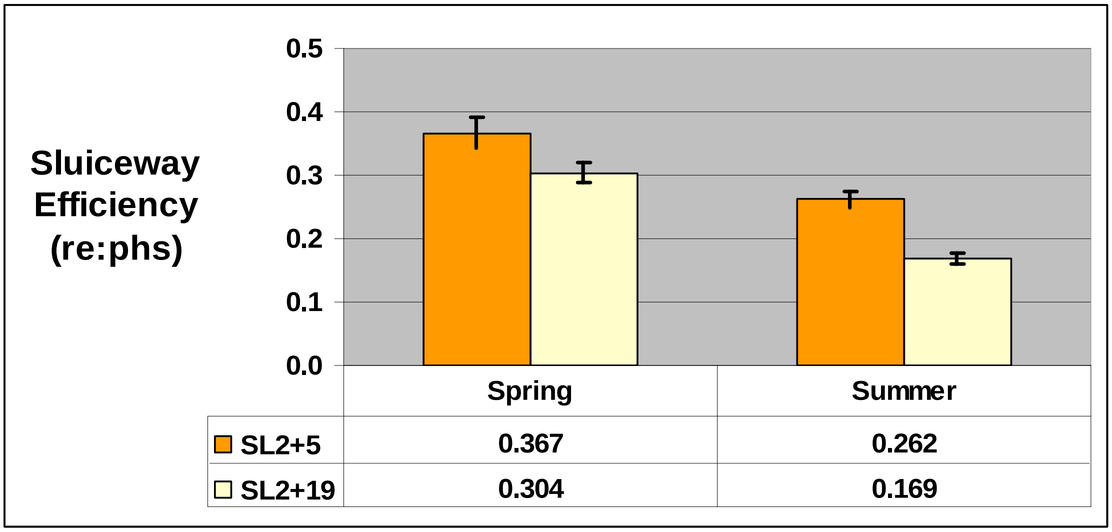

Figure 4.19. Sluiceway Efficiency for the Powerhouse by Season for each Sluice Treatment (SL 2+5, SL 2+19). Error bars represent the 95% confidence interval.

For a given sluice location, sluiceway efficiency (re: turbine unit) was higher at the western sluice locations (SL 2 and SL 5) than at the eastern location (SL 19) during both seasons (Figure 4.20). Sluiceway efficiency (re: turbine unit) was higher in spring than summer at SL 2 and SL 19; the opposite was observed for SL 5.

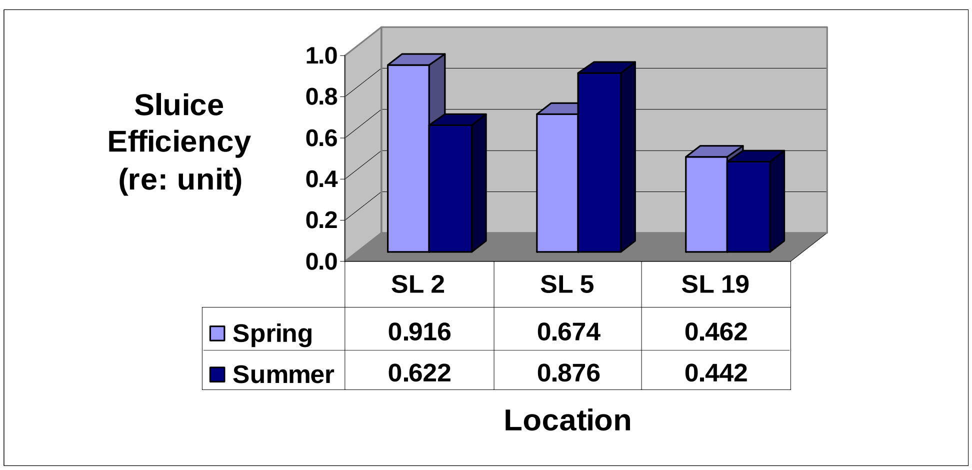

Figure 4.20. Sluiceway Efficiency Relative to the Associated Turbine Unit by Season. For example, sluiceway efficiency re: MU 2 is computed as follows: SLY_{SL2}=SL 2/(SL 2 + MU 2).

Mean hourly passage rates were 2 to 3 times higher at SL 2 than at the other sluice locations during spring 2005 (Figure 4.21). During summer, mean passage rates for the sluice locations were highest at SL 5. Sluice passage rates were lowest at SL 19, regardless of season.

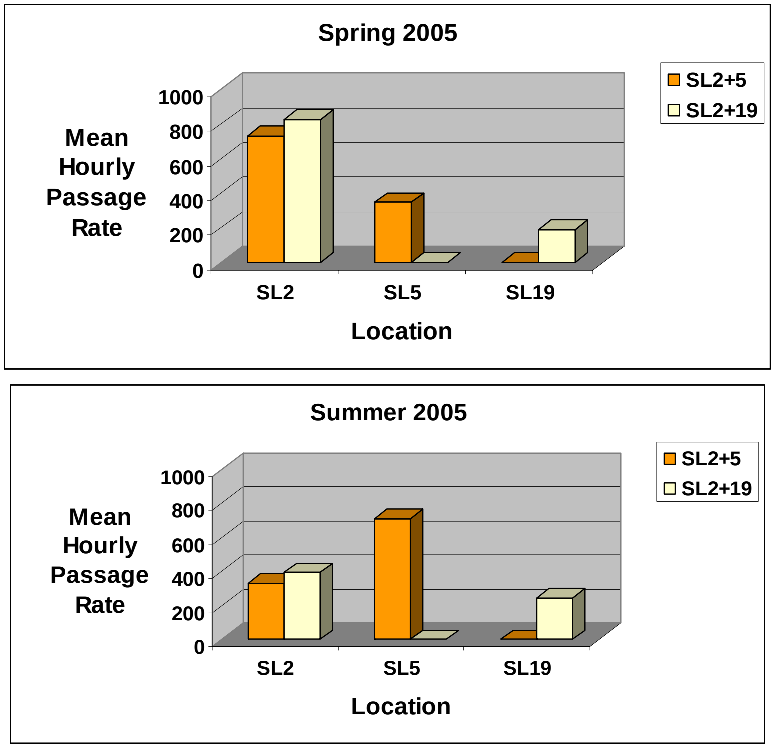

Figure 4.21. Horizontal Distribution of Passage into the Three Sluice Locations by Treatment (SL 2+5 vs. SL 2+19) during Spring (top) and Summer (bottom).

The horizontal distribution of mean hourly passage rates at the three individual sluice gates at a given location was highest at SL 2-1 during spring and SL 5-2 during summer (Figure 4.22). The lowest passage rates for individual gates were observed at SL 19-2 during spring and SL 2-3 during summer. For a given sluice location, passage was highest at the westernmost gate (the "1" gate) at SL 2 and SL 19, regardless of season; this pattern did not hold for SL 5.

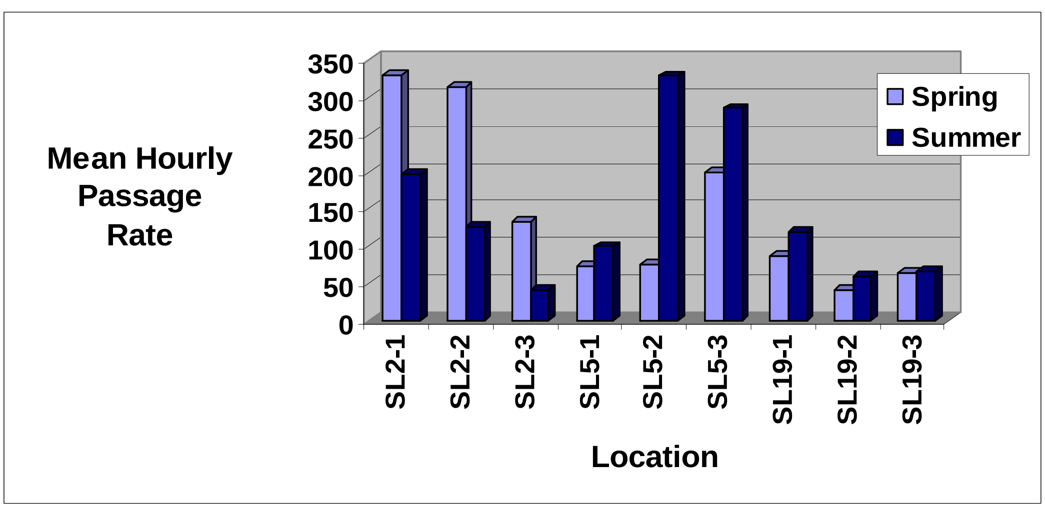

Figure 4.22. Horizontal Distribution of the Mean Hourly Sluice Passage Rate by Individual Gate by Season.

4.3.3 Fish Movements in the Sluiceway Nearfield

This section contains data on juvenile salmonid movements in the nearfield (< 30 ft) of the sluiceway entrances at SL 2 and SL 19. The sluiceway zone of influence is the region immediately upstream of a sluice entrance where juvenile salmonids have a high probability of ultimately moving into the sluiceway.

A total of 181,829 unique fish were tracked using the DIDSON at TDA in 2005 (Table 4.2). Of these 63,910 were from data collected in spring at SL 19 and were not used in Markov chain analyses because almost exclusively one 28º sector was sampled. A total of 97,356 fish tracks from the remainder fell within the sampling volumes and were used in Markov analyses (Table 4.3).

At SL 2, fish were tracked during 9 spring days and 8 summer days. The number of 0.5-s movements (spring 192,710 versus 47,635 and summer 163,255 versus 94,566) used for the Markov chain analyses was greater in day than night for both spring and summer and reflected the number of fish tracked during each period (Table 4.3). The maximum track length was 64 ft. Mean fish speed was greater in summer than spring (1.9 versus 1.6 ft/s, respectively).

At SL 19, fish were tracked during 3 spring days and 8 summer days. Only the summer data were used for Markov chain analyses. Similar to SL 2 data, the number of 0.5-s movements (99,809 versus 60,850) used for the Markov chain analyses was greater in daytime (Table 4.3). The two longest track lengths of 66.56 ft and 64.70 ft occurred at SL 19 and during the day. Fish track duration increased as fish approached the sluiceway during the summer period. Mean speed was slightly faster in day than night and in spring than summer, and averaged 1.8 ft/s. The average interval between image detections for all conditions ranged from 0.22 s to 0.27 s with an overall average of 0.25 s.

Table 4.2. Characteristics of DIDSON Tracked Fish at The Dalles Dam, 2005

Period and Location	Dates	Fish Tracks (n)	Fish Image Detection (n)	Mean Speed (ft/s)	Max Speed (ft/s)	Mean Track Length (ft)	Max Track Length (ft)	Average Images Per Track	Average Image Interval (s)
Spring Day SL 2	5/05 to 5/24	35,880	998,613	1.71	6.62	8.41	63.56	27.8	0.24
Spring Night SL 2	5/09 to 5/24	11,022	311,429	1.20	5.29	5.78	54.28	28.3	0.24
Spring Day SL 19	5/25 to 5/27	28,730	839,478	2.02	6.57	10.77	66.56	29.2	0.26
Spring Night SL 19	5/05 to 5/24	35,180	1,108,733	1.87	6.41	10.71	62.86	31.5	0.27
Summer Day SL 2	6/20 to 7/14	26,450	650,671	1.89	7.79	8.51	51.32	24.6	0.25
Summer Night SL 2	6/20 to 7/14	14,410	403,748	2.00	6.74	9.41	60.83	28.0	0.22
Summer Day SL 19	7/02 to 7/11	19,964	433,408	1.75	6.48	7.27	64.70	21.7	0.27
Summer Night SL 19	7/02 to 7/11	10,193	277,904	1.60	5.54	7.90	58.17	27.3	0.26

Table 4.3. Characteristics of the Fish Observations for Markov Chain Analyses at The Dalles Dam, 2005

Period and Location	Dates	Total Fish Tracks (N)	Used Fish Tracks (N)	Total 0.5 s Moves (N)	Used 0.5 s Moves (n)	Average Measures Per Track
Spring Day SL 2	5/05 to 5/24	35,880	27,557	311,274	192,710	7.0
Spring Night SL 2	5/09 to 5/24	11,022	6,486	94,099	47,635	7.3
Summer Day SL 2	6/20 to 7/14	26,450	24,587	208,088	163,255	6.6
Summer Night SL 2	6/20 to 7/14	14,410	13,734	177,307	94,566	6.9
Summer Day SL 19	7/02 to 7/11	19,964	16,992	143,676	99,809	5.9
Summer Night SL 19	7/02 to 7/11	10,193	8,000	87,763	60,850	7.6

Figures 4.23 to 4.27 show the sums of each spatial cell's fates (states) over the Sluiceway, West, East and Reservoir absorbing edges after 214 multiplications of the transition matrices. The largest passage probabilities were West except for at SL 2 spring night when Sluiceway passage was highest. There was little Reservoir and East passage. The largest Reservoir and East movement occurred in summer night at SL 2 (18.6% and 1%). On average, the largest probabilities were to the West (65%) and to the Sluiceway (31%) (Table 4.4). Sluiceway movement varied from 16%-64% with the lowest values occurring in summer. Sluiceway movement was largest in spring at SL 2. All movement was absorbed at the boundaries and no stagnation occurred.

Table 4.4. Relative Fates near SL 2 and SL 19 at The Dalles Dam, 2005

Period	Location	West	East	Reservoir	Sluiceway
Spring Day	SL 2	0.62	<0.001	<0.01	0.37
Spring Night	SL 2	0.35	<0.01	<0.01	0.64
Summer Day	SL 2	0.73	<0.01	<0.01	0.26
Summer Night	SL 2	0.64	<0.01	0.19	0.17
Summer Day	SL 19	0.82	<0.001	<0.01	0.17
Summer Night	SL 19	0.75	<0.001	0.01	0.24
Average		0.65	0.011	0.04	0.31

A fish entrainment zone (FEZ) may be defined as the point where 90% of fish are entrained. Using the Sluiceway Fate, shown in Figure 4.23 and Figure 4.24 as a function of distance from the dam (piernose edge at elevation 158 ft), the FEZ varied from 0 to 17 ft (0-5.2 m) (Figure 4.28). The extents of the zone of influence were similar to 2004 results that visually showed the limit of the FEZ at about 13 ft (4.0 m). The FEZ was spread more to the East than to the West, generally following water flow patterns into the sluiceways (Johnson et al. 2005). The highest Sluiceway passage in spring at SL 2 corresponded to a FEZ of 7 to 17 ft (2.1-5.2 m) and is less than the 6-8 m FEZ reported in Johnson et al. (2004) at SL 1-1. The FEZ decreased at both sluiceway entrances in summer.

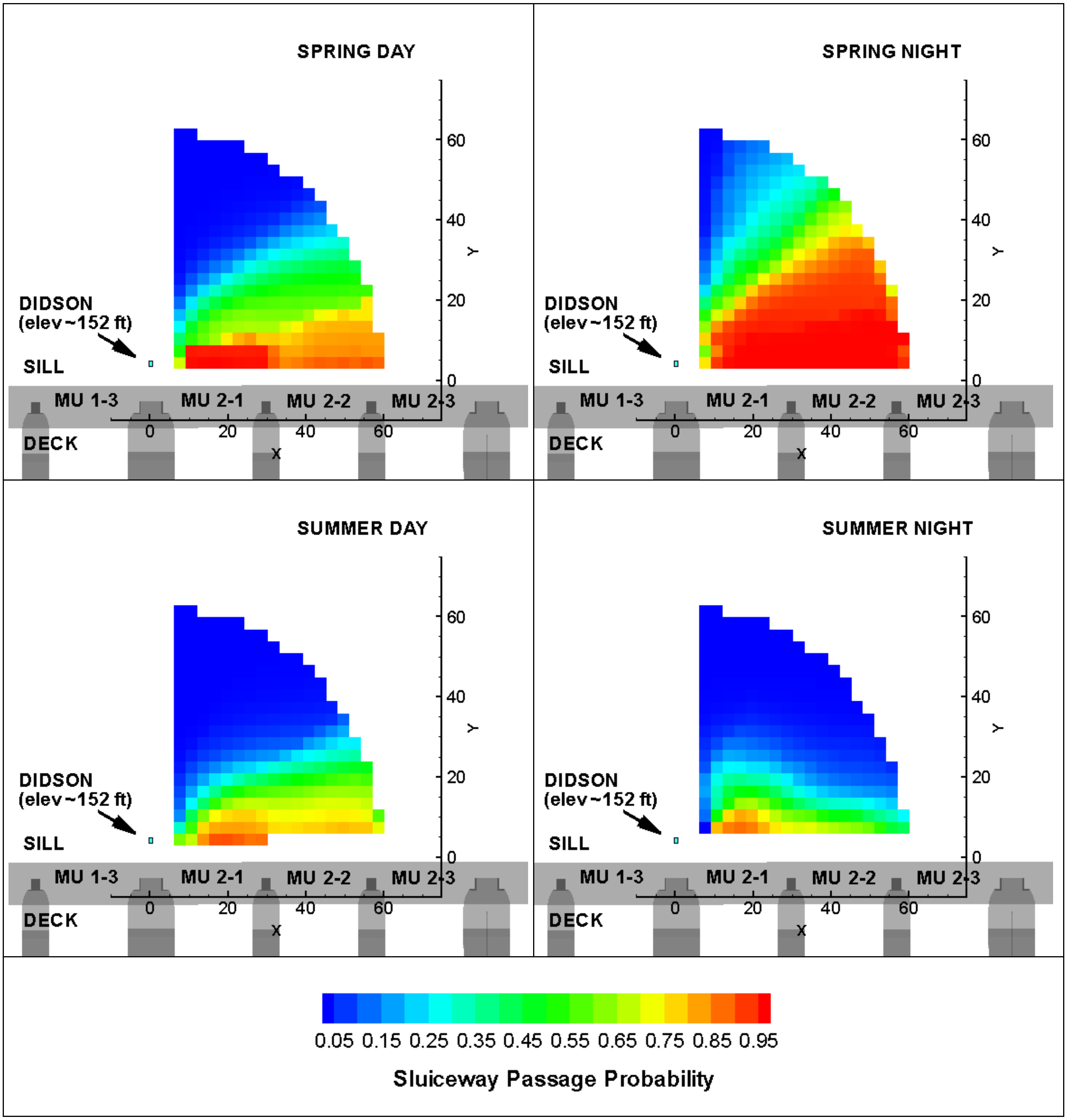

Figure 4.23. Contours of Fish Passage Probabilities at The Dalles Dam SL 2 for Spring and Summer 2005. Probabilities above are shown for the day (left panels) and night (right panels) Sluiceway passage fates. X- and Y-scales are in feet.

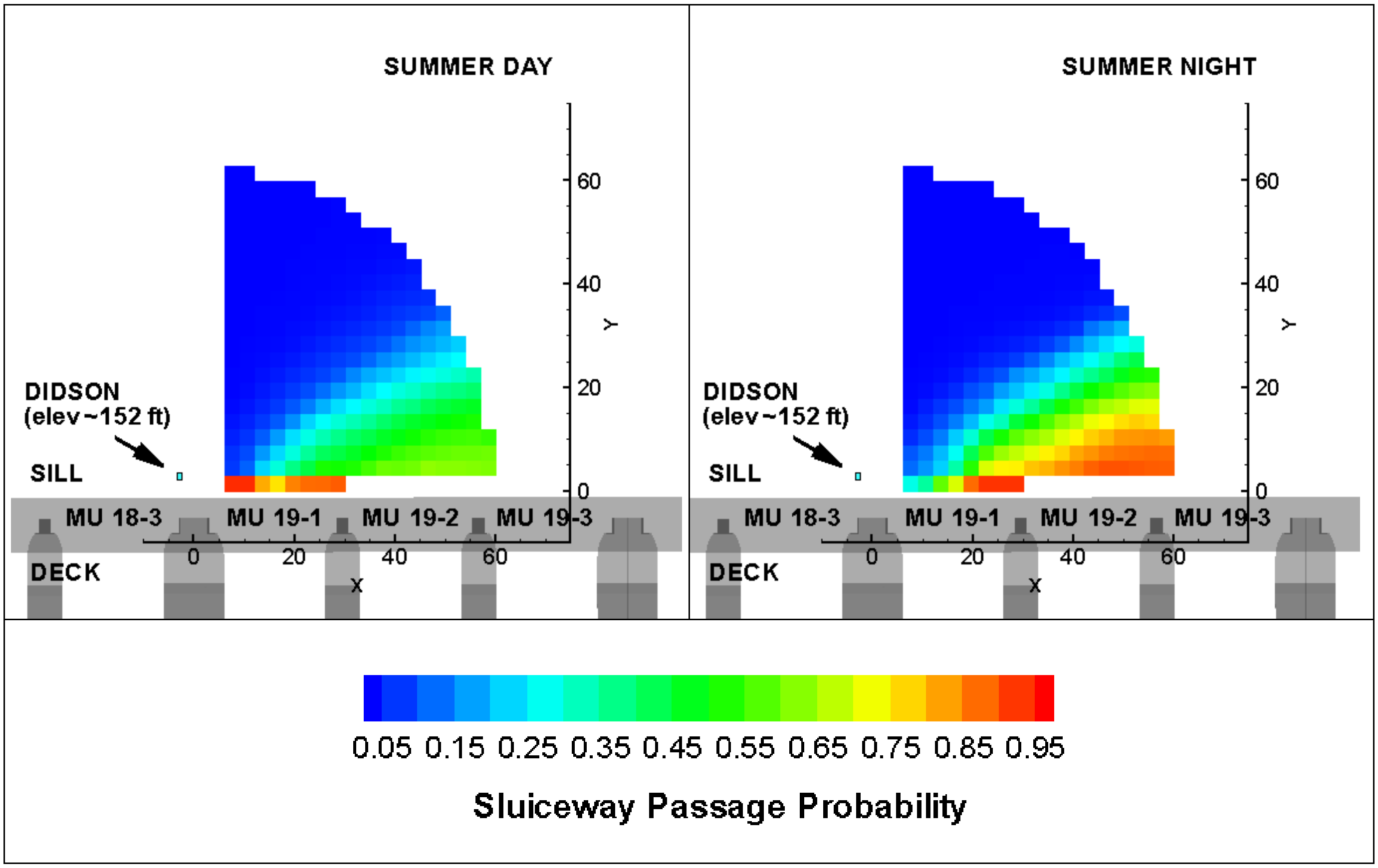

Figure 4.24. Contours of Fish Passage Probabilities at The Dalles Dam SL 19 for Summer 2005. Probabilities above are shown for the day (left panels) and night (right panels) Sluiceway passage fates. X- and Y-scales are in feet.

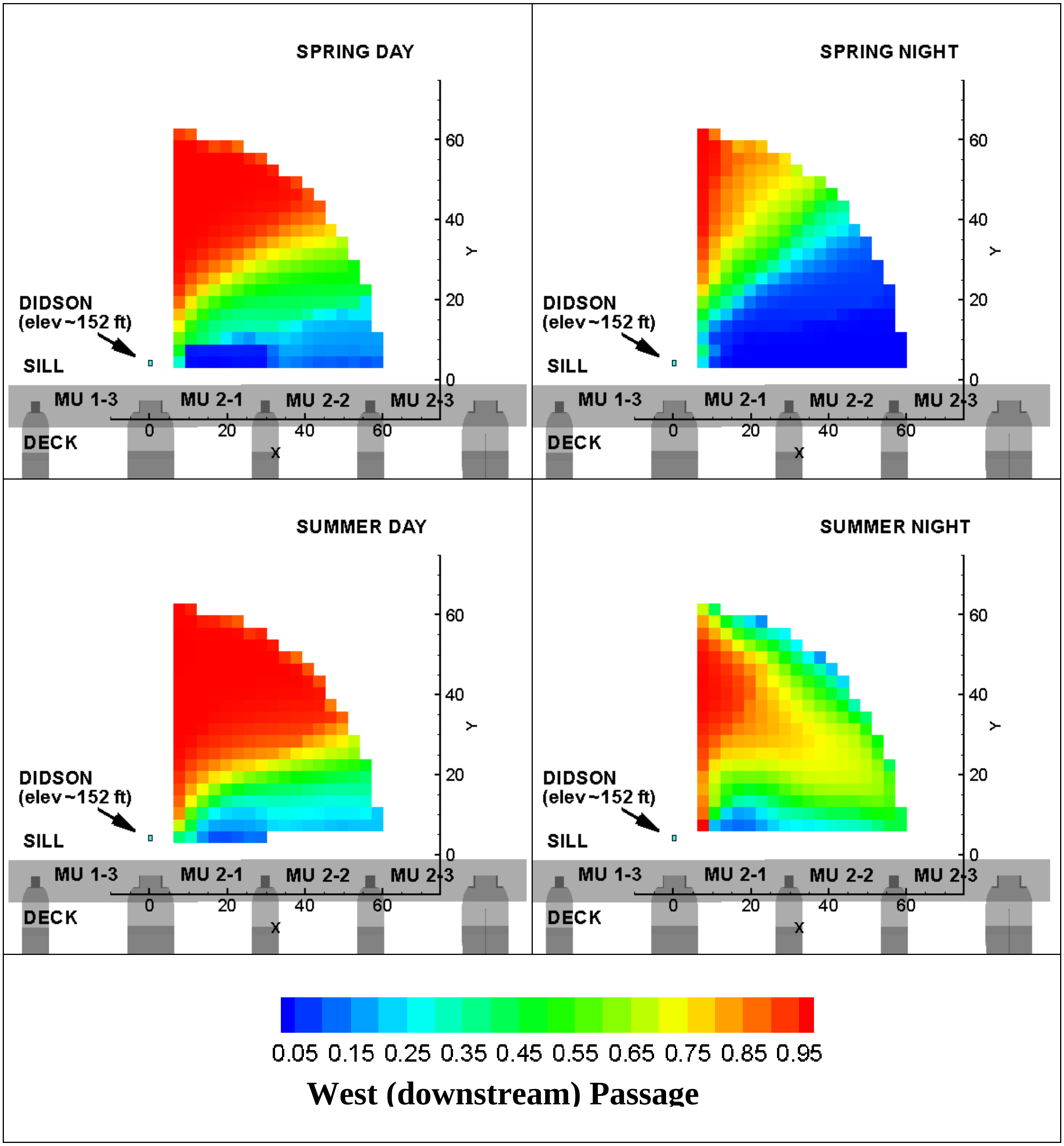

Figure 4.25. Contours of Fish Passage Probabilities at The Dalles Dam SL 2 for Spring and Summer 2005. Probabilities above are shown for the day (left panels) and night (right panels) West passage fates. X- and Y-scales are in feet.

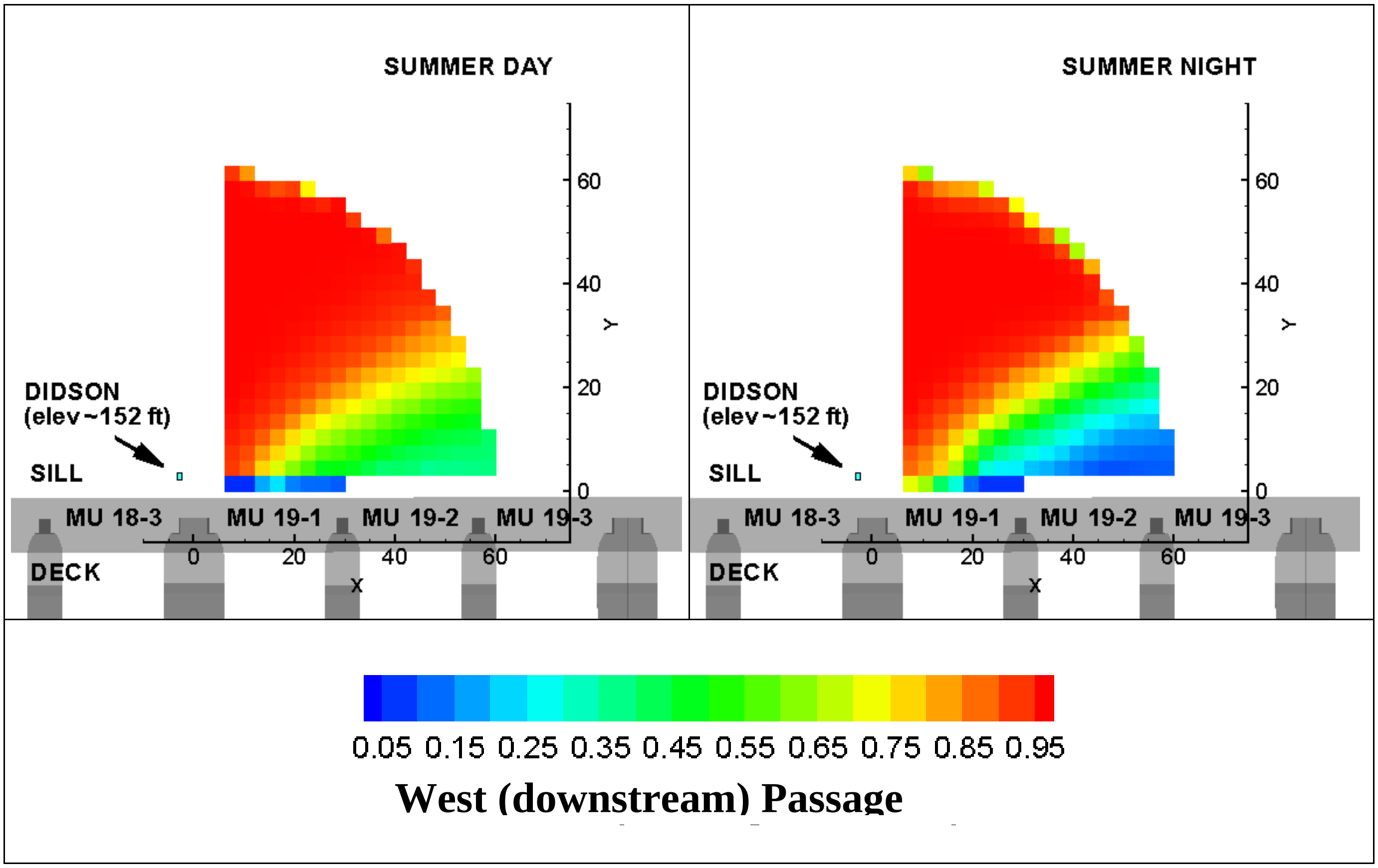

Figure 4.26. Contours of Fish Passage Probabilities at The Dalles Dam SL 19 for Summer 2005. Probabilities above are shown for the day (left panels) and night (right panels) West passage fates. X- and Y-scales are in feet.

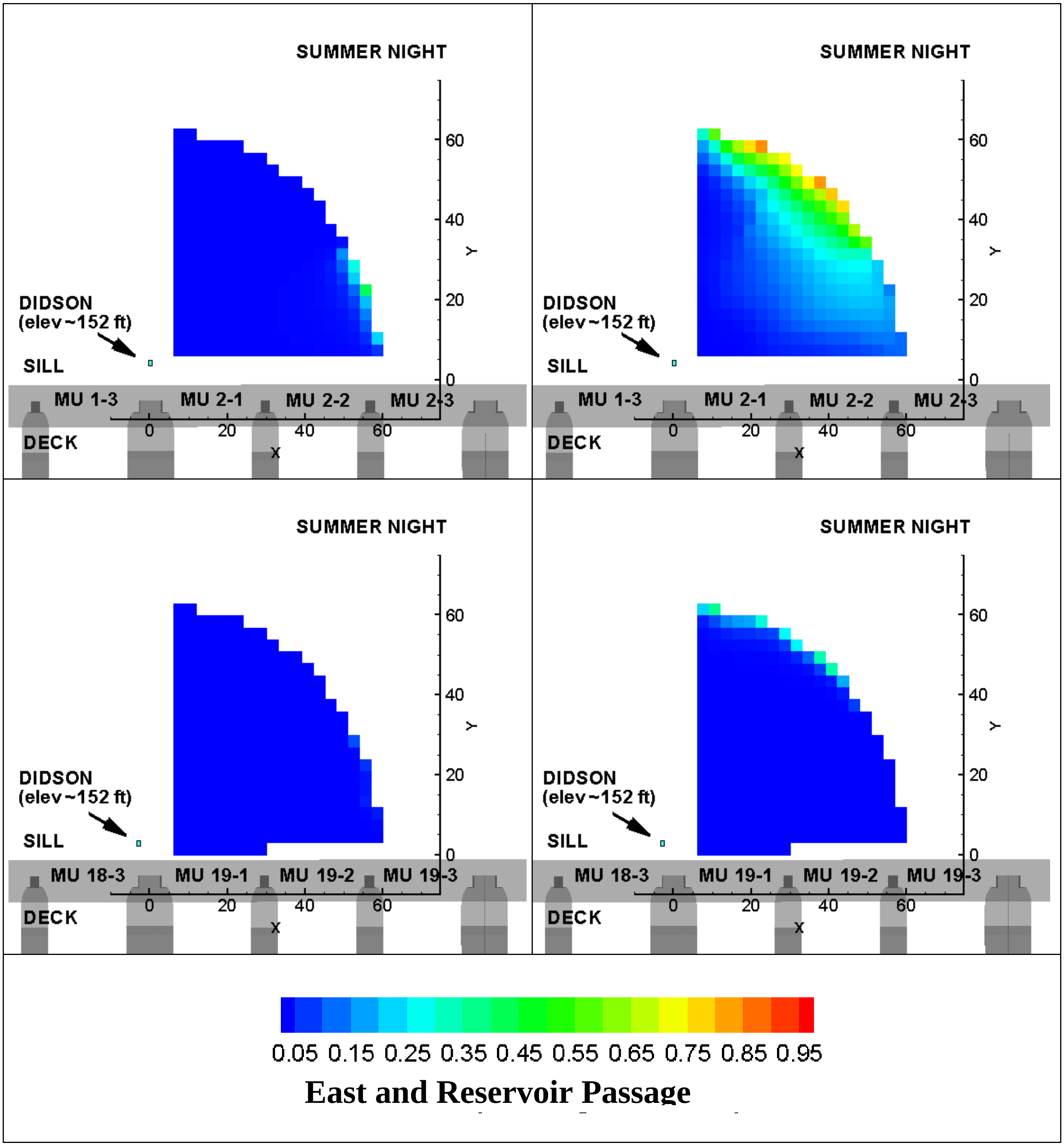

Figure 4.27. Contours of Fish Passage Probabilities at The Dalles Dam SL 2 (upper panels) and SL 19 (lower panels) for Summer 2005. Probabilities above are shown for the East (left panels) and Reservoir (right panels) passage fates. X and Y scales are in feet.

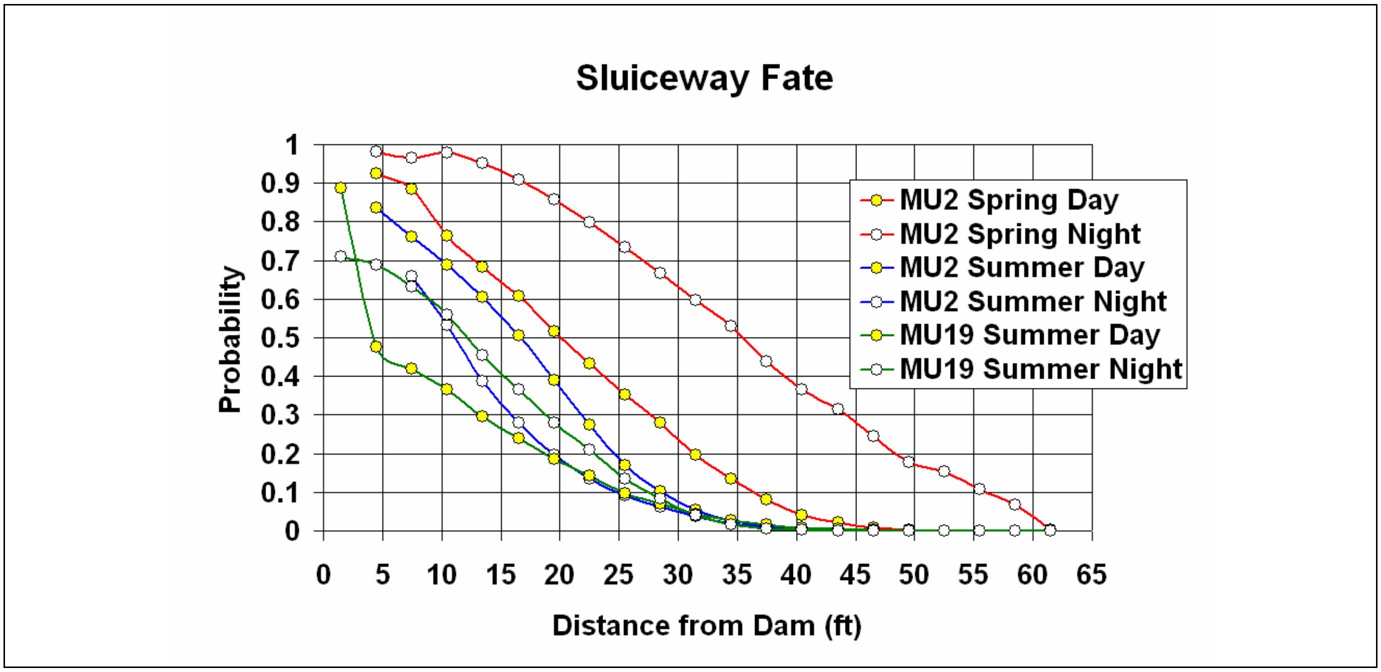

Figure 4.28. Fish Passage Probabilities at The Dalles Dam SL 2 (= MU 2) and SL 19 (= MU 19) in 2005. Expressed as a function of distance from dam (piernose edge at elevation 158 ft).

5.0 Discussion

The fish passage evaluation at The Dalles Dam powerhouse in 2005 showed 1) peaks in daily passage during spring and summer, 2) vertical distribution concentrated within 3 m of the turbine intake ceilings, 3) horizontal distribution of passage highest at MU 8 and 21, and 4) diel distribution highest during daytime at the sluiceway and during evening at the turbine intakes. These patterns from the fish passage evaluation in 2005 are consistent with previous observations (Johnson et al. 2004; 2005), as are the results from the 2005 sluiceway evaluation.

The 2005 study substantiated the importance of the sluiceway as a non-turbine passage route at The Dalles Dam. Of total powerhouse passage, about 33% in spring and 22% in summer was through the sluiceway. Furthermore, the effectiveness of the sluiceway (the ratio of sluiceway fish passage proportion to sluiceway discharge proportion) was around 10 in spring and 6 in summer, whereas spillway effectiveness is typically 1 to 2 (Ploskey et al. 2001a).

The 2004 and 2005 sluiceway evaluations examined whether east-end sluice gates would pass appreciable numbers of fish. This question was pursued because the majority of radio-tagged fish in previous studies were first detected in the forebay off the east end of the powerhouse (Sheer et al. 1997; Holmberg et al. 1997; Hensleigh et al. 1999; Hansel et al. 2000) and because passage rates estimated from hydroacoustic data were relatively high at east turbine units when they were operated, especially in summer (Ploskey et al. 2001a; Johnson et al. 2003). Indeed, fixed-location hydroacoustic and acoustic camera data showed that juvenile salmonids passed into the experimental east end sluice entrances in 2004 (SL 18) and 2005 (SL 19). The majority (> 62%) of fish passage into the sluiceway, however, occurred through the west gates in 2004 (SL 1) and in 2005 (SL 2 and 5). This was true in both spring and summer. Thus, the hypothesized effect of east-end sluice gates on total sluiceway passage, especially for subyearling migrants in summer, was equivocal for the operations we tested in 2004 and 2005, because of the relatively low inflow (~1,700 cfs) and corresponding small flow net for the sluice entrances at the east end of the dam.

The optimum location for open sluice gates remains a question, as shown by sluiceway efficiency data from 1999-2005 (Figure 5.1). No single sluiceway operation stands out as the best in terms of efficiency relative to total powerhouse passage. Extremes for spring and summer were observed in 2001, a drought year with little spill (Figure 5.1). Hydroacoustic data from 2004 for SL 1+18 did not comport with data from the radio telemetry evaluation (Beeman et al. 2004). Certainly the three gates above the western-most operating main turbine unit should be opened. Given the apparent advantage of six over three gates, we suggest opening three more gates at MU 8 where turbine passage rates are relatively high.

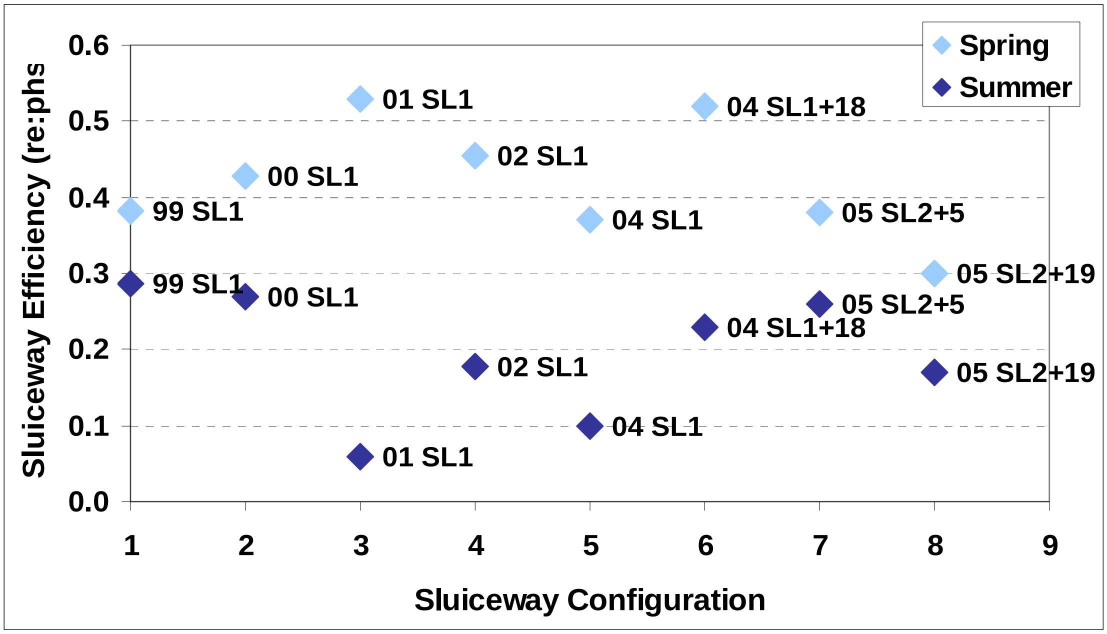

Figure 5.1. Sluiceway Efficiency (re: powerhouse) for Configuations Tested 1999-2005. Data are from hydroacoustic evaluations.

Another concern for fish operations at The Dalles Dam is whether or not to operate turbine units beneath open sluice gates as a standard procedure. In 2004, passage rates into both the west and east sluice entrance were higher with the turbine units operating below and adjacent to the open sluices (Table 5.1). This finding is consistent with sluiceway evaluations at Ice Harbor Dam in 1982 and 1983 (Johnson et al. 1983). Therefore, we believe turbine units below open sluice gates should be operated as a standard fish operations procedure.

Table 5.1. Mean Hourly Passage Rates at the West (SL1) and East (SL18) Sluice Entrances by Operation of Main Units Below and Adjacent to the Open Sluice. Data are from the 2004 sluiceway evaluation (Johnson et al. 2005).

MU1	MU2	Mean SL1	MU18	MU19	Mean SL18
On	On	99	On	On	37
On	Off	19	On	Off	34
Off	Off	36	Off	Off	21

Previous researchers studied the passage survival of juvenile salmon at the TDA sluiceway using releases of PIT-tagged fish in 1998 (Dawley et al. 2000) and 2000 (cited in Ploskey et al. 2001a). In 1998, relative survival rates for juvenile coho salmon and subyearling Chinook salmon were 96% (95% CI: 87-105%) and 89% (95% CI: 81-98%), respectively. In 2000, sluiceway survival rates were 95% (95% CI: 92-98%) for yearling coho salmon and 96% (95% CI: 88-104%) for subyearling Chinook salmon. Therefore, passage survival at the sluiceway could be high enough to warrant enhancements of the sluiceway as a non-turbine route at The Dalles Dam.

The Corps of Engineers is currently drafting a Configuration and Operations Plan for The Dalles Dam. This plan will include modeling of various operational scenarios and hypothesized effects on survival rates. This comprehensive effort will help determine if enhanced sluiceway passage is likely to result in an appreciable (>2%) increase in total project survival. A key aspect to the sluiceway's potential is that it passes fish otherwise destined for turbines. This is certainly possible because of the sluiceway's location at the powerhouse where 60% or more of total project discharge occurs. However, an enhanced sluiceway may also divert fish that otherwise would pass in spill, especially with a 40% spill level. Indeed, sluiceway enhancements may be most applicable in conjunction with reduced spill levels, 30% for example. The integrative passage and survival modeling effort for the Configuration and Operations Plan will be regarding about the benefits of sluiceway enhancements at TDA.

Sluiceway discharge is fundamental to the efficacy of sluiceway enhancements at The Dalles Dam. As a design parameter, sluiceway discharge is consistent with the considerations for surface flow bypasses identified by Johnson et al. (2004): 1) form an extensive surface flow bypass flow net (surface bypass discharge greater than ~7% of total project discharge) at the *west* and *east* ends of the dam; 2) create a gradual increase in water velocity approaching the surface flow bypass (ideally, acceleration <1 m/s/m); 3) make water velocities at an entrance high enough (> 3 m/s) to entrain the subject juvenile fishes; 4) adapt the shape and orientation of the surface entrance(s) to fit site-specific features; and 5) design a new high flow outfall(s). These elements should be considered during design of sluiceway enhancements at The Dalles Dam.

Specifically, we suggest a portable weir with specially designed shaping be constructed and evaluated at the TDA sluiceway. This structure, called the "Removable Sluiceway Weir," would allow comparison of fish response to hydraulic conditions created by entrance shaping with those at an existing, non-shaped sluice entrance at TDA. A portable structure would allow researchers to prevent any location effects from confounding the evaluation. Since many fish approach the sluiceway entrances but move away toward the west (Johnson et al. 2004), this structure also could also be used to develop immediate improvements to sluiceway efficiency, even at its existing hydraulic capacity.

In general, sluiceway enhancement could be a reliable, long-term strategy for juvenile salmonid passage at The Dalles Dam. Because of the variability among years in spill efficiency (Ploskey et al. 2001a), spillway improvements alone may not be sufficient to protect juvenile salmonids across the entire dam during every annual emigration. Surface flow bypasses are being designed, installed, and operated as long-term juvenile salmonid passage routes at a growing number of mainstem dams. Examples include the "Removable Spillway Weirs" at Lower Granite and Ice Harbor dams and the "Corner Collectors" at Bonneville and Rocky Reach dams. Therefore, a diverse, multi-faceted approach that includes sluiceway enhancements as a surface flow bypass at the powerhouse is in order. Data have repeatedly shown that The Dalles Dam sluiceway has the potential to be highly efficient and effective at passing juvenile salmonids, especially when assessed relative to powerhouse passage. This potential could be tapped with hydraulic and entrance enhancements to the sluiceway.

6.0 Conclusions and Recommendations

The overall goal of this study was to provide information on smolt passage at The Dalles Dam to support decisions on long-term measures and operations to increase sluiceway passage and reduce turbine passage to improve smolt survival at the dam. In 2005, the hydroacoustic evaluation of juvenile salmonid passage at The Dalles Dam involved fixed-location hydroacoustic methods at the powerhouse turbines and sluiceway. Sampling was especially intensive at the sluiceway where multiple split-beam transducers to sample fish passage were complemented by an acoustic camera to track fish in the sluiceway nearfield. The fish data were interpreted and integrated with hydraulic data from a CFD model. An "experiment" was conducted to compare two sluiceway operations: SL 2+5 vs. SL 2+19. We concluded that:

- SL 2+5 had significantly higher sluiceway efficiency than SL 2+19 in both spring and summer.
- Sluiceway efficiency was higher at SL 2 and SL 5 than at SL 19.
- Fish passage per unit flow in turbines was higher in summer than spring.
- Fish passage per unit flow in turbines was higher at the middle and eastern areas than at the western areas of the powerhouse in 2005.

To enhance sluiceway and spillway passage and reduce turbine passage at The Dalles Dam, our recommendations for sluiceway operations and long-term measures are as follows:

- Operate the sluice 24 h/d from April until November.
- Open six rather than three sluice gates to take advantage of the maximum hydraulic capacity of the sluiceway.
- Open the three gates above the western-most operating main turbine unit and the three gates at MU 8 where turbine passage rates are relatively high.
- Operate the turbine units below open sluice gates as a standard fish operations procedure.
- Develop hydraulic and entrance enhancements to the sluiceway to tap the potential of The Dalles Dam sluiceway to be highly efficient and effective at passing juvenile salmonids, including:
    - form an extensive surface flow bypass flow net (surface bypass discharge greater than ~7% of total project discharge) at both the west and east ends of the dam;
    - create a gradual increase in water velocity approaching the surface flow bypass (ideally, acceleration < 1 m/s per meter);
    - make water velocities at an entrance high enough (> 3 m/s) to entrain the subject juvenile fishes;
    - adapt the shape and orientation of the surface entrance(s) to fit site-specific features, i.e., test a Removable Sluiceway Weir;
    - design a new high flow outfall(s).

The Dalles Dam sluiceway has the potential to be highly efficient and effective at passing juvenile salmonids. We recommend tapping this potential with enhancements to the sluiceway.

7.0 Literature Cited

Beeman, J., H. Hansel, P. Haner, and K. Daniel. 2004. *Estimate Fish, Spill, and Sluiceway Passage Efficiencies of Radio-Tagged Juvenile Steelhead and Yearling Chinook Salmon at The Dalles Dam, 2001.* Draft final report of research submitted to the U.S. Army Corps of Engineers – Portland District, October 10, 2002, by the USGS Biological Resources Division.

Carlson, T. J., W. C. Acker, and D. M. Gaudet. 1981. *Hydroacoustic Assessment of Downstream Migrant Salmon and Steelhead at Priest Rapids Dam in 1980.* APL-UW 8016, Applied Physics Laboratory, University of Washington, Seattle, Washington.

Cash, K. and 13 co-authors. 2005. *Three-Dimensional Behavior and Passage of Juvenile Salmonids at The Dalles Dam, 2004.* Draft final report submitted to the U.S. Army Corps of Engineers, Portland District, February 2005, by the USGS Biological Resources Division and PNNL.

Dawley, E. M., L. G. Gilbreath, R. F. Absolon, B. P. Sandford, and J. W. Ferguson. 2000. *Relative Survival of Juvenile Salmon Passing through the Spillway and the Ice and Trash Sluiceway of The Dalles Dam, 1998.* Final report submitted to the U.S. Army Corps of Engineers, Portland District, by the National Marine Fisheries Service.

Faber, D. M,. M. E. Hanks, S. A. Zimmerman, J. R. Skalski, and P. W. Dillingham. 2005. *The Distribution and Flux of Fish in the Forebay of The Dalles Dam in 2003*. PNNL-14628, Final report submitted to the U.S. Army Corps of Engineers, Portland District, by Pacific Northwest National Laboratory, Richland, Washington.

Hansel, H. C., and six co-authors. 2000. *Estimates of Fish-, Spill-, and Sluiceway Passage Efficiencies of Radio-Tagged Juvenile Steelhead and Yearling Chinook Salmon at The Dalles Dam, 1999.* Annual report of research, 1999, submitted to the U.S. Army Corps of Engineers, Portland District, by the USGS Biological Resources Division.

Hansel, H. C., and six co-authors. 2005. *Estimates of Fish-, Spill-, and Sluiceway Passage Efficiencies of Radio-Tagged Juvenile Chinook Salmon at The Dalles Dam in 2004.* Draft final report of research during 2004 submitted to the U.S. Army Corps of Engineers, Portland District, April 21, 2005, by the USGS Columbia River Research Laboratory.

Hausmann, B., J. Beeman, H. Hansel, S. Juhnke, and P. Haner. 2004. *Estimates of Fish, Spill, and Sluiceway Passage Efficiencies of Radio-Tagged Juvenile Salmonids Relative to the Sluiceway Guidance Improvement Device at The Dalles Dam in 2002.* Final report of research prepared for the U.S. Army Corps of Engineers, Portland District, by the USGS Biological Resources Division.

Hedgepeth, J. B., G. E. Johnson, A. E. Giorgi, and J. R. Skalski. 2002a. *Sonar Tracker Evaluation of Fish Movements Relative to J-Occlusions at The Dalles Dam in 2001.* Final report submitted to U.S. Army Corps of Engineers, Portland District, March 8, 2002, by Battelle Pacific Northwest Division, Richland, Washington.

Hedgepeth, J., G. Johnson, J. Skalski, and J. Burczynski. 2002b. *Active fish tracking sonar (AFTS) for assessing fish behavior.* Acta Acustica 88:739-742.

Hensleigh, J. E. and nine co-authors. 1999. *Movement, Distribution, and Behavior of Radio-Tagged Juvenile Chinook Salmon and Steelhead in John Day, The Dalles and Bonneville Dam Forebays, 1997.* Annual Report of Research, 1997, submitted to the U.S. Army Corps of Engineer, Portland District, by the U.S. Geological Survey.

Holmberg, G. S. and eight co-authors. 1997. *Movement, Distribution, and Behavior of Radio-Tagged Juvenile Chinook Salmon in John Day, The Dalles, and Bonneville Dam Forebays, 1996.* Annual Report of Research, 1996, submitted to the U.S. Army Corps of Engineers, Portland District, by the U.S. Geological Survey.

Johnson, G. E., M. E. Hanks, F. Khan, J. B. Hedgepeth, R. P. Mueller, C. L. Rakowski, M. C. Richmond, S. L. Sargeant, J. A. Serkowski, and J. R. Skalski. 2005. *Hydroacoustic Evaluation of Juvenile Salmonid Passage at The Dalles Dam in 2004.* PNNL-15180, Final report submitted to the Corps of Engineers, Portland District by Pacific Northwest National Laboratory, Richland, Washington.

Johnson, G.E., J.B. Hedgepeth, J.R. Skalski, and A.E. Giorgi. 2004. A Markov Chain Analysis of Fish Movement to Determine Entrainment Zones. *Fisheries Research* 69:349-358.

Johnson, G.E., R.A. Moursund, and R.P. Mueller. 2003. *Hydroacoustic Evaluation of the J-Occlusion Plates at the Dalles Dam in 2002*, PNWD-3226, prepared for the US Army Corps of Engineers, Portland District by Battelle, Pacific Northwest Division, Richland, Washington.

Johnson, G.E., J.B. Hedgepeth, A.E. Giorgi, and J.R. Skalski. 2001. *Evaluation of Smolt Movements Using an Active Fish Tracking Sonar at the Sluiceway Surface Bypass, The Dalles Dam, 2000.* Final report submitted to the U.S. Army Corps of Engineers – Portland District. September 30, 2001, by BioAnalysts, Inc.

Johnson, G. E., A. E. Giorgi, and M. W. Erho. 1997. *Critical Assessment of Surface Flow Bypass Development in the Lower Columbia and Snake Rivers.* PNNL-15265, Completion report submitted to the U.S. Army Corps of Engineers, Walla Walla District, by Pacific Northwest National Laboratory, Richland, Washington.

Johnson, L., Noyes, C., and McClure, R. 1983. *Hydroacoustic Evaluation of the Efficiencies of the Ice and Trash Sluiceway and Spillway at Ice Harbor Dam for Passing Downstream Migrating Juvenile Salmon and Steelhead,1983.* Volume I. Draft report submitted to the U.S. Army Corps of Engineers, Walla Walla District, by BioSonics, Inc.

Karlin, S., 1968. *A First Course in Stochastic Processe*s. Academic Press, New York.

Kemeny, J. G. and J. L. Snell. 1960. *Finite Markov Chains.* D. Van Nostrand Company, Inc., Princeton, New Jersey.

MacLennan, D.N. and E. J. Simmonds. 1992. *Fisheries Acoustics.* Chapman and Hall, London.

Michimoto, R. 1971. *Bonneville and The Dalles Dams Ice-Trash Sluiceway Studies, 1971.* Fisheries Engineering Research Program, Report #20, submitted to the U.S. Army Corps of Engineers – Portland District, by the Oregon Department of Fish and Wildlife.

Moursund, R. A., K. D. Ham, P. S. Titzler, R. P. Mueller, G. E. Johnson, J. Hedgepeth, and J. R. Skalski. 2002. *Hydroacoustic Evaluation of Fish Passage at The Dalles Dam in 2001.* Report by Battelle's Pacific Northwest Division to the U.S. Army Corps of Engineers – Portland District.

Moursund, R.A., K.D. Ham, B.D. McFadden, and G.E. Johnson. 2001. *Hydroacoustic evaluation of downstream fish passage at The Dalles Dam in 2000.* PNWD-3226, Report to the U.S. Army Corps of Engineers, Portland District, by Battelle Pacific Northwest Division, Richland, Washington.

National Marine Fisheries Service. 2000. *Re-initiation of Consultation on Operation of the Federal Columbia River Power System, including the Juvenile Fish Transportation Program, and 19 Bureau of Reclamation Projects in the Columbia Basin. Biological Opinion.* December 21, 2000, National Marine Fisheries Service, Northwest Region, Seattle, Washington.

Nichols, D. W. 1979. *Passage Efficiency and Mortality Studies of Downstream Migrant Salmonids Using The Dales Ice-Trash Sluiceway During 1978.* Oregon Department of Fish and Wildlife.

Nichols, D. W. 1980. *Development of Criteria for Operating the Trash Sluiceway at The Dalles Dam as a Bypass System for Juvenile Salmonids, 1979.* Report submitted to the U.S. Army Corps of Engineers, Portland District, by the Oregon Department of Fish and Wildlife.

Nichols, D. W., and B. H. Ransom. 1981. *Development of The Dalles Dam Trash Sluiceway as a Down-Stream Migrant Bypass System, 1980.* Report submitted to the U.S. Army Corps of Engineers, Portland District, by the Oregon Department of Fish and Wildlife.

Nichols, D. W., and B. H. Ransom. 1982. *Development of The Dalles Trash Sluiceway as a Downstream Migrant Bypass System, 1981.* Annual Progress Report, submitted to the U.S. Army Corps of Engineers, Portland District, by the Fish Research Project Oregon, Fish Division, Oregon Department of Fish and Wildlife.

Ploskey G., T. Poe, A. Giorgi, and G. Johnson. 2001a. *Synthesis of Radio Telemetry, Hydroacoustic, and Survival Studies of Juvenile Salmon at The Dalles Dam (1982-2000).* PNWD-3131, Final report submitted to the U.S. Army Corps of Engineers, Portland District, by Battelle Pacific Northwest Division, Richland, Washington.

Ploskey, G. R., W. T. Nagy, L. R. Lawrence, M. E. Hanks, C. R. Schilt, P. N. Johnson, G. E. Johnson, D. S. Patterson, and J. R. Skalski. 2001b. *Hydroacoustic Evaluation of Juvenile Salmon Passage at The Dalles Dam: 1999.* ERDC/EL TR-01-11, U.S. Army Engineer Research and Development Center, Vicksburg, Mississippi.

Sheer, M. B., G. S. Holmberg, R. S. Shively, H. C. Hansel, T. L. Martinelli, T. P. King, C. N. Frost, T. P. Poe, J. C. Snelling, and C. B. Shreck. 1997. *Movement and Behavior of Radio-Tagged Juvenile Spring and Fall Chinook Salmon in The Dalles and John Day Dam Forebays, 1995.* Annual Report to the U.S. Army Corps of Engineers – Portland District.

Taylor, H. and S. Karlin. 1998. *An Introduction to Stochastic Modeling*. Academic Press, San Diego, California.

Thorne, R. and G. Johnson. 1993. *A Review of Hydroacoustic Studies for Estimation of Salmonid Downriver Migration Past Hydroelectric Facilities on the Columbia and Snake Rivers in the 1980s.* Reviews in Fisheries Science 1:27-56.

Appendix A

Statistical Synopsis for the 2005 Fixed-Location Hydroacoustic Investigations at The Dalles Dam

Prepared for:
Gary Johnson
Pacific Northwest National Laboratory
620 SW Fifth Avenue, Suite 810
Portland, Oregon 97204

Prepared by:
John R. Skalski
Columbia Basin Research
School of Aquatic and Fishery Sciences
University of Washington
1325 Fourth Avenue, Suite 1820
Seattle, Washington 98101

July 19, 2005

(Formatted, updated, and acronyms edited by G. Johnson on November 3, 2005)

Appendix A

Statistical Synopsis for the 2005 Fixed-Location Hydroacoustic Investigations at The Dalles Dam

Introduction

The purpose of this synopsis is to describe the statistical methods to be used in the analysis of the 2005 hydroacoustic study at The Dalles Dam. The study will estimate fish passage through the powerhouse (i.e., turbines), fish units, and sluiceway during the spring and summer smolt outmigrations. These estimates of fish passage will be used to estimate various measures of sluiceway passage performance at The Dalles Dam. Sluiceway performance measures will be used to test the effect of two alternative sluiceway operations on smolt passage at The Dalles Dam.

Transducer Deployment and Sampling Scheme

This section describes the hydroacoustic sampling schemes that were used to estimate smolt passage at the powerhouse, spillway, sluiceway, and fish units at The Dalles Dam.

Sampling at Main Units and Fish Units at Powerhouse

The Dalles powerhouse has 22 main turbine units, each with three turbine intake slots and two fish units, each with two intake slots. Table 1 summarizes the transducer deployment and the *post hoc* grouping of the turbine units into statistical strata.

The selected intake slots were sampled 24 hours daily throughout the study period. Within an hour at an intake slot, fish passage was systematically sampled over time. The sampling effort within an hour at the various intake slots is summarized below:

Turbine Units	Sampling Effort
2, 5–22	8 1-min samples/hr
F1, F2	8 1-min samples/hr

Table A.0.1. Summary of Transducer Deployment at the Main Turbine Units 1–22 and Fish Unit F1–F2 at The Dalles Dam in 2005. Number of intakes sampled per unit is given along with the *post hoc* grouping of units into statistical strata and the number of intakes sampled per stratum.

	Fish Units		Main Units																		
	F1	F2	1	2	3	4	5	6	7	8	9	10	11	12	13	14	15	16	17	18	19
Transducer/Unit	1	1	Off	1	Off	Off	1	1	1	1	1	1	1	1	1	1	1	1	1	1	1
Strata	1				2			3		4		5		6		7		8		9	
Transducers/Stratum	3/4				2/6			2/6		2/6		2/6		2/6		2/6		2/6		2/6	

* Off-line during study

	Main Units		
	20	21	22
Transducer/Unit	1	1	1
Strata		10	
Transducers/Stratum		3/9	

Sampling at Spillway

In 2005, spillway passage was not sampled. Therefore, inferences to spillway passage will not be performed.

Sampling at Sluiceway

In 2005, the three sluice gates at each of Main Units 2, 5, and 19 were used to pass fish. At one gate per sluiceway, two horizontal hydroacoustic arrays were used to monitor fish passage. Fish were enumerated at only the wide (i.e., distal) half of each opposing array. At the other two gates per sluiceway, only one horizontal array was used. Hydroacoustic monitoring was conducted 24 hours daily through the study. Within an hour, fish passage was systematically sampled over time. The within-hour sampling effort was 15 1-min samples/hr at each transducer.

Estimating Fish Passage

The following sections describe how the estimates of smolt passage will be calculated at the various locations at The Dalles Dam.

Powerhouse Passage

The sampling at The Dalles powerhouse turbines can be envisioned as a stratified two-stage sampling program. Constructing spatial strata by combining adjacent turbine units, the first step was the random sampling of turbine intake slots within adjacent turbine units. Table 1 summarizes the 10 spatial strata constructed and the numbers of intake slots sampled per stratum. The second step was envisioned as stratified random sampling of within intake-hours.

The estimator of total turbine passage over the course of *D* days can be expressed as follows:

$$\hat{T} = \sum_{i=1}^{D} \sum_{j=1}^{24} \sum_{k=1}^{K} \left[\frac{A_k}{a_k} \left[\sum_{l=1}^{a_k} \hat{T}_{ijkl} \right] \right] \tag{1}$$

where

$\hat{T}_{ijkl}$ = estimated fish passage in the *l*th intake slot $(l = 1, \ldots, a_k)$ within the *k*th turbine stratum $(k = 1, \ldots, K)$ during the *j*th hour $(j = 1, \ldots, 24)$ on the *i*th day $(i = 1, \ldots, D)$;

a_k = number of intake slots sampled in the *k*th turbine stratum $(k = 1, \ldots, K)$;

A_k = total number of intake slots within the *k*th turbine stratum $(k = 1, \ldots, K)$;

K = number of turbine strata created (nominally $K = 8$).

The estimator of $\hat{T}_{ijkl}$ is based on the assumption of simple random sampling within a slot-hour, in which case

$$\hat{T}_{ijkl} = \frac{B_{kl}}{b_{kl}} \sum_{g=1}^{b_{kl}} w_{ijklg} \tag{2}$$

where

w_{ijklg} = expanded fish passage in the *g*th sampling unit $(g = 1, \ldots, b_{ijkl})$ in the *l*th intake slot $(l = 1, \ldots, a_k)$ within the *k*th turbine stratum $(k = 1, \ldots, K)$ during the *j*th hour $(j = 1, \ldots, 24)$ on the *i*th day $(i = 1, \ldots, D)$;

b_{kl} = number of sampling units per hour actually observed in the *l*th intake slot $(l = 1, \quad , a_k)$ within the *k*th turbine stratum $(k = 1, \quad K)$;

B_{kl} = total number of possible sampling units per hour within the *l*th intake slot $(l = 1, \quad , a_k)$ within the *k*th turbine stratum $(k = 1, \quad K)$.

Nominally, $B_{kl} = 60$ for all k and l, and $b_{kl} = 8$.

Combining Equations (1) and (2), the estimator for total powerhouse passage can be written as

$$\hat{T} = \sum_{i=1}^{D} \sum_{j=1}^{24} \sum_{k=1}^{K} \left[\frac{A_k}{a_k} \sum_{l=1}^{a_k} \frac{B_{kl}}{b_{kl}} \sum_{g=1}^{b_{kl}} w_{ijk\,lg} \right] \tag{3}$$

The variance of $\hat{T}$ can then be estimated by the formula

$$\mathrm{Var}\left(\hat{T}\right) = \sum_{i=1}^{D} \sum_{j=1}^{24} \sum_{k=1}^{K} \left[\frac{A_k^2 \left(1 - \frac{a_k}{A_k}\right) s_{\hat{T}_{ijk}}^2}{a_k} + \frac{A_k \sum_{l=1}^{a_k} \mathrm{Var}\left(\hat{T}_{ijkl}\right)}{a_k} \right] \tag{4}$$

where

$$s_{\hat{T}_{ijk}}^2 = \frac{\sum_{l=1}^{a_k} \left(\hat{T}_{ijkl} - \bar{\hat{T}}_{ijk}\right)^2}{\left(a_k - 1\right)},$$

$$\bar{\hat{T}}_{ijk} = \frac{1}{a_k} \sum_{l=1}^{a_k} \hat{T}_{ijkl},$$

and where

$$\mathrm{Var}\left(\hat{T}_{ijkl}\right) = \frac{B_{kl}^2 \left(1 - \frac{b_{kl}}{B_{kl}}\right) s_{w_{ijkl}}^2}{b_{kl}}, \tag{5}$$

$$s_{w_{ijkl}}^2 = \frac{\sum_{g=1}^{b_{kl}} \left(w_{ijklg} - \bar{w}_{ijkl}\right)}{\left(b_{kl} - 1\right)},$$

$$\bar{w}_{ijkl} = \frac{1}{b_{kl}} \sum_{g=1}^{b_{kl}} w_{ijklg}.$$

Sluiceway Passage

Sluiceway passage must be estimated as a combination of traditional SRS formula and ratio estimation because only half of the intake width was sampled at 2 of the 3 gates per sluiceway. The horizontal distribution at the two-array gate will be used to extrapolate to the unsampled halves of the one-array gates. For the half gates ensonified, the estimate of passage is estimated as follows

$$\hat{L}_{ghi} = \sum_{j=1}^{d} \sum_{k=1}^{24} \left[\frac{N_{ghijk}}{n_{ghijk}} \sum_{l=1}^{n_{ghijk}} y_{ghijkl} \right] \tag{6}$$

where

$\hat{L}_{ghi}$ = passage of the *i*th horizontal stratum $(i = 1, 2)$ of the *h*th gate $(h = 1, \quad ,3)$ of the *g*th sluiceway $(g = 1, \quad ,3)$;

and where

y_{ghijkl} = expanded fish count in the *l*th sampling unit $(l = 1, \quad , n_{ghijk})$ in the *k*th hour $(k = 1, \quad ,24)$ in the *j*th day $(j = 1, \quad ,D)$ at the *i*th horizontal stratum $(i = 1, 2)$ at the *h*th gate $(h = 1, \quad ,3)$ of the *g*th sluiceway $(g = 1, \quad ,3)$;

N_{ghijk} = total number of sampling units in the *k*th hour $(k = 1, \quad ,24)$ in of the *j*th day $(j = 1, \quad ,D)$ at the *i*th horizontal stratum $(i = 1, 2)$ at the *h*th gate $(h = 1, \quad ,3)$ of the *g*th sluiceway $(g = 1, \quad ,3)$;

n_{ghijk} = number of sampling units actually observed in the *k*th hour $(k = 1, \quad ,24)$ in of the *j*th day $(j = 1, \quad ,D)$ at the *i*th horizontal stratum $(i = 1, 2)$ at the *h*th gate $(h = 1, \quad ,3)$ of the *g*th sluiceway $(g = 1, \quad ,3)$.

At sluiceway gates $h = 1$, both horizontal strata were directly estimated $(i = 1, 2)$. At sluiceway gates $h = 2$ and 3, only the first horizontal stratum was directly estimated $(i = 1)$. Total passage through the gth sluiceway can therefore be estimated as

$$\begin{aligned} \hat{L}_g &= \left(\hat{L}_{g_{11}} + \hat{L}_{g_{12}} \right) + \left(\hat{L}_{g_{21}} + \hat{L}_{g_{31}} \right) + \frac{\hat{L}_{g_{12}} \left(\hat{L}_{g_{21}} + \hat{L}_{g_{31}} \right)}{\hat{L}_{g_{11}}} \\ &= \left(\hat{L}_{g_{11}} + \hat{L}_{g_{12}} \right) + \left(\hat{L}_{g_{21}} + \hat{L}_{g_{31}} \right) \cdot \left(1 + \frac{\hat{L}_{g_{21}}}{\hat{L}_{g_{11}}} \right). \end{aligned} \tag{7}$$

Passage through all gates is then estimated by

$$\hat{L} = \sum_{g=1}^{3} \hat{L}_g \tag{8}$$

The variance of $\hat{L}$ is the sum of the sluiceway-specific variance estimates, where

$$\operatorname{Var}\left(\hat{L}\right) = \sum_{g=1}^{3} \operatorname{Var}\left(\hat{L}_g\right). \tag{9}$$

In turn, the individual estimates of $\hat{L}_g$ have the approximate variance estimator

$$
\begin{aligned}
\operatorname{Var}\left(\hat{L}_g\right) = {} & \operatorname{Var}\left(\hat{L}_{g_{11}}\right)\left(1-\frac{\hat{L}_{g_{21}}+\hat{L}_{g_{31}}}{\hat{L}_{g_{11}}{}^{2}}\right)^2 + \operatorname{Var}\left(\hat{L}_{g_{12}}\right)\left(1+\frac{\hat{L}_{g_{21}}+\hat{L}_{g_{31}}}{\hat{L}_{g_{11}}}\right)^2 \\
& + \operatorname{Var}\left(\hat{L}_{g_{21}}\right)\left(1+\frac{\hat{L}_{g_{12}}}{\hat{L}_{g_{11}}}\right)^2 + \operatorname{Var}\left(\hat{L}_{g_{31}}\right)\left(1+\frac{\hat{L}_{g_{12}}}{\hat{L}_{g_{11}}}\right)^2 \\
& + 2\operatorname{Cov}\left(\hat{L}_{g_{11}},\hat{L}_{g_{12}}\right)\left(1-\frac{\hat{L}_{g_{21}}+\hat{L}_{g_{31}}}{\hat{L}_{g_{11}}{}^{2}}\right)\left(1+\frac{\hat{L}_{g_{21}}+\hat{L}_{g_{31}}}{\hat{L}_{g_{11}}}\right) \\
& + 2\operatorname{Cov}\left(\hat{L}_{g_{11}},\hat{L}_{g_{21}}\right)\left(1-\frac{\hat{L}_{g_{21}}+\hat{L}_{g_{31}}}{\hat{L}_{g_{11}}{}^{2}}\right)\left(1+\frac{\hat{L}_{g_{12}}}{\hat{L}_{g_{11}}}\right) \\
& + 2\operatorname{Cov}\left(\hat{L}_{g_{11}},\hat{L}_{g_{31}}\right)\left(1-\frac{\hat{L}_{g_{21}}+\hat{L}_{g_{31}}}{\hat{L}_{g_{11}}{}^{2}}\right)\left(1+\frac{\hat{L}_{g_{12}}}{\hat{L}_{g_{11}}}\right) \\
& + 2\operatorname{Cov}\left(\hat{L}_{g_{12}},\hat{L}_{g_{21}}\right)\left(1-\frac{\hat{L}_{g_{21}}+\hat{L}_{g_{31}}}{\hat{L}_{g_{11}}}\right)\left(1+\frac{\hat{L}_{g_{12}}}{\hat{L}_{g_{11}}}\right) \\
& + 2\operatorname{Cov}\left(\hat{L}_{g_{12}},\hat{L}_{g_{31}}\right)\left(1+\frac{\hat{L}_{g_{21}}+\hat{L}_{g_{31}}}{\hat{L}_{g_{11}}}\right)^2,
\end{aligned} \tag{10}
$$

where

$$\operatorname{Var}\left(\hat{L}_{ghi}\right)=\sum_{j=1}^{D}\sum_{k=1}^{24}\left[N_{ghijk}^2\left(1-\frac{n_{ghijk}}{N_{ghijk}}\right)\frac{s_{y_{ghijk}}^2}{n_{ghijk}}\right],$$

and where

$$s_{y_{ghijk}}^2=\frac{\sum_{l=1}^{n_{ghijk}}\left(y_{ghijkl}-\overline{y_{ghijk}}\right)^2}{\left(n_{ghijk}-1\right)},$$

for

$$\overline{y_{ghijk}}=\frac{\sum_{l=1}^{n_{ghijk}}y_{ghijkl}}{n_{ghijk}},$$

and where

$$\operatorname{Cov}\left(\hat{L}_{ghi},\hat{L}_{gh'i'}\right)=\sum_{j=1}^{D}\sum_{k=1}^{24}\left[N_{ghi}^2\left(1-\frac{n_{ghi}}{N_{ghi}}\right)\frac{\operatorname{Cov}\left(y_{ghijkl},y_{gh'i'jkl}\right)}{n_{ghi}}\right],$$

where

$$\left.\begin{aligned} N_{ghi} &= N_{ghikjk} = N_{gh'i'jk} \\ n_{ghi} &= n_{ghijk} = n_{gh'i'jk} \end{aligned}\right\}$$ (i.e., equal sampling effort within hour for sluice gate strata compared),

and where

$$\mathrm{Cov}\left(y_{ghijkl}, y_{gh'i'jkl}\right) = \frac{\sum_{l=1}^{n_{ghi}} \left(y_{ghijkl} - \overline{y_{ghijk}}\right)\left(y_{gh'i'jkl} - \overline{y_{gh'i'jk}}\right)}{\left(n_{ghi} - 1\right)} .$$

Estimating Passage Performance

Sluiceway Efficiency at the Powerhouse (CLY)

The conditional probability of a smolt going through the sluiceway given it is passing through the powerhouse can be estimated by the quotient

$$CLY = \frac{\hat{L}}{\hat{L} + T} . \tag{11}$$

The variance of CLY can then be expressed as follows

$$\mathrm{Var}\left(CLY\right) = CLY^2 \left(1 - CLY\right)^2 \left[\frac{\mathrm{Var}\left(\hat{L}\right)}{\hat{L}^2} + \frac{\mathrm{Var}\left(\hat{T}\right)}{\hat{T}^2}\right] . \tag{12}$$

Sluiceway-to-Turbine Passage

Another localized measure of sluiceway efficiency is relative to fish passage through a particular turbine unit, where

$$LY_g = \frac{\hat{L}_g}{\hat{L}_g + \hat{T}_g} , \tag{13}$$

where

$\hat{L}_g$ = estimated fish passage through the *g*th sluiceway (*g* = 2, 5, or 19),

$\hat{T}_g$ = estimated fish passage through the *g*th turbine units (*g* = 2, 5, or 19).

The variance of LY_g can be estimated by

$$\mathrm{Var}\left(LY_g\right) = LY_g^2 \left(1 - LY_g\right)^2 \left[\frac{\mathrm{Var}\left(\hat{L}_g\right)}{\hat{L}_g^2} + \frac{\mathrm{Var}\left(\hat{T}_g\right)}{\hat{T}_g^2}\right]. \tag{14}$$

Sluiceway Effectiveness at the Powerhouse (CLN)

Conditional sluiceway effectiveness (CLN) will be estimated by the quantity

$$CLN = \frac{\left(\dfrac{\hat{L}}{f_L}\right)}{\left(\dfrac{\hat{L}+\hat{T}}{f_L+f_T}\right)} = \left(\frac{f_L+f_T}{f_L}\right)\cdot CLY. \tag{15}$$

The variance of CLN can then be expressed as

$$\mathrm{Var}\left(CLN\right) = \left(\frac{f_L+f_T}{f_L}\right)^2 \cdot \mathrm{Var}\left(CLY\right), \tag{16}$$

where f_L = total flow through sluiceway,

f_T = total flow through turbines.

Relative Effectiveness of Sluiceway-to-Turbine Passage

The relative effectiveness of the sluiceway-to-turbine effectiveness can be estimated by the quantity

$$LN_k = \frac{\left(\dfrac{\hat{L}_k}{f_{L_k}}\right)}{\left(\dfrac{\hat{L}_k+\hat{T}_k}{f_{L_k}+f_{T_k}}\right)} = \left(\frac{f_{L_k}+f_{T_k}}{f_{L_k}}\right)\cdot LY_k \tag{17}$$

with associated variance estimator

$$\mathrm{Var}\left(LN_k\right) = \left(\frac{f_{L_k}+f_{T_k}}{f_{L_k}}\right)^2 \cdot \mathrm{Var}\left(LY_k\right) \tag{18}$$

where

f_{T_k} = flow volume through turbine unit *k*,

f_{L_k} = flow volume through sluiceway *k*.

Sluiceway Passage across Select Units

Corresponding to the two sluiceway treatment conditions of Units 2 and 5 or Units 2 and 19 operational, total sluiceway passage can be estimated as

$$\hat{L} = \sum_{g=1}^{2} \hat{L}_g \ , \tag{19}$$

i.e., $\hat{L} = \hat{L}_2 + \hat{L}_5$ or $\hat{L} = \hat{L}_2 + \hat{L}_{19}$, as specific cases of Eq. (8), where $\hat{L}_g$ = estimated total passage through the *g*th sluiceway for the period of interest. The variance of $\hat{L}$ can, in turn, be expressed as

$$\mathrm{Var}\left(\hat{L}\right) = \sum_{g=1}^{2} \mathrm{Var}\left(\hat{L}_g\right), \tag{20}$$

as special cases of Eq. (9).

Test of Sluiceway Treatments

During spring and summer, a randomized block experimental design will be performed to compare passage performance measures under two different treatment conditions. The two treatment conditions are as follows:

a. Sluices 2 and 5 operating.

b. Sluices 2 and 19 operating.

The summer study will consist of approximately 7 blocks, the spring study will consist of approximately 8 blocks. Each block will be six days in duration, three days under each sluiceway test condition.

The test of the effect of sluiceway treatments will be performed using a two-way ANOVA for a randomized block experimental design. The ANOVA table will be of the form depicted below.

Source	df	SS	MS	*F*
Total	2B			
Mean	1			
$\text{Total}_{\text{Cor}}$	2B-1	SSTOT		
Blocks	B-1	SSB		
Treatment	1	SST	MST	$F_{B-1} = \dfrac{\text{MST}}{\text{MSE}}$
Error	B-1	SSE	MSE	

The *F*-test from the ANOVA is a two-tailed test of no treatment effect. In 2005, all statistical comparisons are two-tailed. It is recommended that all response variables be ln-transformed before the ANOVA.

Separate analyses will be performed to assess the following response variables and hypotheses:

1. CLY
$$\begin{aligned} &H_o: \mu_{2,5} = \mu_{2,19} \\ &H_a: \mu_{2,5} \neq \mu_{2,19} \end{aligned}$$

2. LY_k
$$\begin{aligned} &H_o: \mu_{2,5} = \mu_{2,19} \\ &H_a: \mu_{2,5} \neq \mu_{2,19} \end{aligned}$$

3. CLN
$$\begin{aligned} &H_o: \mu_{2,5} = \mu_{2,19} \\ &H_a: \mu_{2,5} \neq \mu_{2,19} \end{aligned}$$

4. LN_k
$$\begin{aligned} &H_o: \mu_{2,5} = \mu_{2,19} \\ &H_a: \mu_{2,5} \neq \mu_{2,19} \end{aligned}$$

5. $\hat{L}$
$$\begin{aligned} &H_o: \mu_{2,5} = \mu_{2,19} \\ &H_a: \mu_{2,5} \neq \mu_{2,19} \end{aligned}$$

where $\mu_{2,5}$ is the mean when Sluiceways 2 and 5 are operating, and $\mu_{2,19}$ is the mean when Sluiceways 2 and 19 are operating.

Appendix B

Analysis of Relationships between Load Following and Fish Passage at The Dalles Dam, 2005

Prepared for:
Gary Johnson
Pacific Northwest National Laboratory
620 SW Fifth Avenue, Suite 810
Portland, Oregon 97204

Prepared by:
John R. Skalski
Columbia Basin Research
School of Aquatic and Fishery Sciences
University of Washington
1325 Fourth Avenue, Suite 1820
Seattle, Washington 98101

January 3, 2006
(Formatted, updated, and edited by G. Johnson on May 8, 2006)

Appendix B

Analysis of Relationships between Load Following and Fish Passage at The Dalles Dam, 2005

Introduction

The purpose of this analysis is to explore the relationships between load following (flow) and fish passage at The Dalles Dam in spring and summer 2005. There are large hour-to-hour changes in flow past the project in response to the demand for electricity, a pattern called load following or power peaking. Fisheries maangers and project operators are interested in possible effects of load following on juvenile salmonid passage at The Dalles Dam.

Methods

We examined five different fish movement—flow relationships. Preliminary analysis suggested that changes in fish movements versus changes in flow would be best characterized by analyzing the change (Δ) in fish movements on an hourly basis versus change (Δ) in flow that same hour (i.e. Δ 1 hour, no time log). The five different dependent-independent variable relationships examined were as follows:

Dependent variable (Δ fish)	Independent variable (Δ flow)	Table of Results
1. $MU + FU + SL$	$MU + FU + SL + SP$	Tables B.1a, b
2. $MU + FU + SL$	$MU + FU + SL$	Tables B.2a, b
3. $MU + FU$	$MU + FU$	Tables B.3a, b
4. SL	SL	Tables B.4a, b
5. $\frac{SL}{MU + FU + SL}$	$\frac{SL}{MU + FU + SL}$	Tables B.5a, b

where MU = main unit,
FU = fish unit,
SL = sluiceway, and
SP = spillway.

The symbols refer to either fish counts or flow volume, depending on context. For example, the results in Table B.4a,b were based on the regression

$$Fish(SL_{i+1} - SL_i) = \alpha + \beta \; Flow(SL_{i+1} - SL_i)$$

where SL_{i+1} = fish count or flow in hour $i + 1$ at sluiceway, and
SL_i = fish count or flow in hour i at sluiceway.

Analogous regression relationships were formed for each model. Separate analyses were performed for spring (19 April – 6 June) and summer periods (7 June – 18 July). Analyses were also separated by time of day (i.e., 0-4 hours, 5-9 hours, 10-17 hours, 18-21 hours, and 22-23 hours). Only Sunday and Thursday diel patterns were analyzed. These days had the most dramatic and consistent diel patterns of load use.

Results

Tables B.1-B.5 summarize the regression results. Regression relationships were rarely significant during the spring periods (2 of 50 tests at $\alpha = 0.05$), but occasionally significant during the summer (13 of 50 tests at $\alpha = 0.05$). One might hope that a significant relationship detected on "Sundays" would also be observed on "Thursdays". This only occurred for the first three regression relationships (Tables B.1-B.3) involving passage through the powerhouse. No such consistency was observed for sluiceway related variables.

Another observation relates to time of day. A priori, it was expected a load following relationship would be most likely to occur during the hours of 5-9 or 18-21, when people prepare to go to work or come home from work. However, significant relationships never occurred during these time periods (0 of 100 tests).

Conclusions

Overall, load following relationships with fish passage were not observed in the results from this analysis. On face value, the results suggest load following:

1. is more likely to occur during summer, rather than spring,
2. is more likely to occur during non-peak electrical usage periods,
3. affects powerhouse passage, not sluiceway passage, and
4. explains only a small fraction of the variance in fish passage.

Table B.1a. Sunday All Routes

	Spring				Summer				Slopes different?	
	R-squared	slope	s.e.	t p-value	R-squared	slope	s.e.	t p-value	Z	p-value
0 to 4	0.003	5.9	19.2	0.761	0.184	92.0	36.6	**0.018**	2.085	**0.019**
5 to 9	0.034	28.0	26.2	0.292	0.080	61.5	39.4	0.130	0.708	0.239
10 to 17	0.000	3.2	32.8	0.923	0.040	51.8	37.5	0.174	0.976	0.165
18 to 21	0.045	42.9	38.8	0.279	0.001	4.1	28.3	0.887	0.809	0.209
22 to 23	0.172	16.1	10.2	0.140	0.261	90.2	48.0	0.090	1.511	0.065

Table B.1b. Thursday All Routes

	Spring				Summer				Slopes different?	
hours	R-squared	slope	s.e.	t p-value	R-squared	slope	s.e.	t p-value	Z	p-value
0 to 4	0.333	60.7	15.0	0.566	0.001	-1.7	12.7	**0.894**	3.184	**0.001**
5 to 9	0.004	10.2	26.8	0.706	0.071	20.6	14.0	0.154	0.344	0.366
10 to 17	0.069	44.8	22.4	0.051	0.339	60.4	12.4	0.000	0.608	0.272
18 to 21	0.014	17.4	28.6	0.548	0.064	33.8	27.5	0.232	0.413	0.340
22 to 23	0.261	67.0	32.5	0.062	0.468	39.2	13.2	0.014	0.792	0.214

Table B.2a. Sunday Powerhouse

	Spring				Summer				Slopes different?	
	R-squared	slope	s.e.	t p-value	R-squared	slope	s.e.	t p-value	Z	p-value
0 to 4	0.005	9.7	23.0	0.676	0.187	142.0	56.0	**0.017**	2.186	**0.014**
5 to 9	0.026	24.9	26.6	0.356	0.076	79.1	52.1	0.140	0.926	0.177
10 to 17	0.000	-5.0	34.2	0.884	0.020	37.8	38.5	0.332	0.831	0.203
18 to 21	0.046	42.9	38.5	0.275	0.000	2.2	29.7	0.941	0.837	0.201
22 to 23	0.164	15.5	10.1	0.152	0.421	126.0	46.6	0.022	2.316	0.010

Table B.2b. Thursday Powerhouse

	Spring				Summer				Slopes different?	
hours	R-squared	slope	s.e.	t p-value	R-squared	slope	s.e.	t p-value	Z	p-value
0 to 4	0.337	62.9	15.3	0.000	0.002	3.5	14.7	**0.815**	2.792	**0.003**
5 to 9	0.003	11.2	34.5	0.748	0.062	25.8	18.9	0.185	0.371	0.355
10 to 17	0.090	59.1	25.5	0.024	0.340	65.6	13.5	0.000	0.225	0.411
18 to 21	0.019	22.9	32.4	0.705	0.066	35.9	28.8	0.226	0.300	0.382
22 to 23	0.172	58.1	36.9	0.141	0.516	57.1	17.5	0.008	0.024	0.491

Table B.3a. Sunday Turbine

	Spring				Summer				Slopes different?	
hours	R-squared	slope	s.e.	t p-value	R-squared	slope	s.e.	t p-value	Z	p-value
0 to 4	0.007	-10.5	21.9	0.635	0.236	131.0	44.5	**0.006**	2.854	**0.002**
5 to 9	0.043	27.1	22.3	0.233	0.088	78.7	47.9	0.111	0.977	0.164
10 to 17	0.008	-20.0	29.6	0.501	0.015	27.5	32.4	0.401	1.083	0.139
18 to 21	0.102	22.7	13.2	0.097	0.010	-15.8	33.2	0.638	1.078	0.140
22 to 23	0.082	10.5	10.1	0.321	0.439	124.0	44.5	0.019	2.489	0.006

Table B.3b. Thursday Turbine

	Spring				Summer				Slopes different?	
hours	**R-squared**	**slope**	**s.e.**	**t p-value**	**R-squared**	**slope**	**s.e.**	**t p-value**	**Z**	**p-value**
0 to 4	0.279	45.7	12.8	0.001	0.000	-0.2	13.3	**0.989**	2.487	**0.006**
5 to 9	0.008	13.1	26.0	0.618	0.030	16.5	17.6	0.357	0.108	0.457
10 to 17	0.104	51.9	20.8	0.016	0.277	55.1	13.1	0.000	0.130	0.448
18 to 21	0.000	1.7	16.9	0.923	0.011	11.8	24.1	0.630	0.344	0.365
22 to 23	0.042	19.0	26.0	0.481	0.483	61.3	20.1	0.012	1.287	0.099

Table B.4a. Sunday Sluiceway

	Spring				Summer				Slopes different?	
hours	**R-squared**	**slope**	**s.e.**	**t p-value**	**R-squared**	**slope**	**s.e.**	**t p-value**	**Z**	**p-value**
0 to 4	0.009	-1139.0	2110.9	0.593	0.080	-3450.0	2211.6	**0.130**	0.756	**0.225**
5 to 9	0.001	147.0	1147.2	0.899	0.007	577.0	1270.1	0.653	0.251	0.401
10 to 17	0.014	1177.0	1339.3	0.383	0.000	-103.0	1981.5	0.959	0.535	0.296
18 to 21	0.021	-4333.0	5779.1	0.460	0.015	-1161.0	1991.0	0.566	0.519	0.302
22 to 23	0.016	-334.0	758.4	0.668	0.073	-1112.0	1257.6	0.397	0.530	0.298

Table B.4b. Thursday Sluiceway

	Spring				Summer				Slopes different?	
hours	**R-squared**	**slope**	**s.e.**	**t p-value**	**R-squared**	**slope**	**s.e.**	**t p-value**	**Z**	**p-value**
0 to 4	0.035	-1213.0	1116.8	0.210	0.004	366.0	1030.3	**0.725**	1.039	**0.149**
5 to 9	0.023	2281.0	2564.9	0.380	0.114	-974.0	514.4	0.069	1.244	0.107
10 to 17	0.007	280.0	1432.7	0.846	0.352	-2345.0	469.4	0.000	1.741	0.041
18 to 21	0.063	-4481.0	3395.9	0.198	0.047	-2741.0	2646.5	0.312	0.404	0.343
22 to 23	0.231	-13747.0	7236.0	0.082	0.000	96.5	1536.8	0.951	1.871	0.031

Table B.5a. Sunday Sluiceway Efficiency

	Spring				Summer				Slopes different?	
hours	**R-squared**	**slope**	**s.e.**	**t p-value**	**R-squared**	**slope**	**s.e.**	**t p-value**	**Z**	**p-value**
0 to 4	0.099	-29.0	15.2	0.065	0.073	10.9	7.3	**0.149**	2.361	**0.009**
5 to 9	0.083	9.7	5.6	0.093	0.026	6.8	7.9	0.395	0.299	0.382
10 to 17	0.000	1.3	16.5	0.938	0.000	0.7	4.6	0.882	0.034	0.486
18 to 21	0.049	16.5	14.2	0.256	0.122	-17.2	9.9	0.095	1.949	0.026
22 to 23	0.005	-2.0	7.7	0.803	0.022	3.5	7.3	0.647	0.510	0.305

Table B.5b. Thursday Sluiceway Efficiency

	Spring				Summer				Slopes different?	
hours	**R-squared**	**slope**	**s.e.**	**t p-value**	**R-squared**	**slope**	**s.e.**	**t p-value**	**Z**	**p-value**
0 to 4	0.099	-13.8	7.2	0.066	0.003	-1.4	5.0	**0.786**	1.414	**0.079**
5 to 9	0.078	13.0	7.8	0.105	0.046	-11.2	9.6	0.253	1.954	0.025
10 to 17	0.000	-1.5	14.0	0.915	0.004	1.2	2.8	0.686	0.185	0.427
18 to 21	0.022	-8.6	11.1	0.448	0.035	-7.3	8.1	0.379	0.093	0.463
22 to 23	0.022	8.2	15.7	0.610	0.513	14.2	4.4	0.009	0.366	0.357